TECHNISCHE UNIVERSITÄT MÜNCHEN

Lehrstuhl für Biotechnologie

Aggregation propensities of the yeast Sup35p and mouse prion protein domains in the cytosol of mammalian cells

Dipl.-Biol. (Univ.) Carmen Krammer

Scio me nihil scire

(Sokrates)

Dedicated to Hildegard and Johann Krammer

TABLE OF CONTENTS

iii

I.   SUMMARY

I.A ENGLISH VERSION

Prion diseases are fatal neurodegenerative diseases that affect both humans and animals. They are characterized by the accumulation of an abnormal isoform (PrP^{Sc}) of the cellular prion protein (PrP^{C}). PrP^{Sc} is closely associated with infectivity and has been proposed as the protein-only agent responsible for prion diseases. A nucleated polymerization model has been suggested for mammalian prion propagation. In this model, the normal isoform PrP^{C} binds to a PrP^{Sc} oligomer, which catalyzes the conformational change to the β-sheet rich isoform. A similar prion-like phenomenon has been reported for the *Saccharomyces cerevisiae* translation termination factor Sup35p that can adopt an epigenetic self-propagating conformation. Fibrillar aggregates of Sup35p share several features with PrP^{Sc} aggregates, like high β-sheet content, SDS insolubility and partial protease resistance. The striking similarities in the conformational conversion of both proteins make the yeast prion system an interesting model for the study of mammalian prion diseases. The exact mechanism of prion replication, the domains in PrP mediating prion assembly and potential co-factors remain elusive. Aim of this study was a comparative analysis of the aggregation propensities of PrP and Sup35p in the cytosol of mammalian cells.

        In the first part of this work aggregation propensities of chimeric proteins derived from the Sup35p prion domain NM and PrP were examined. Mouse neuroblastoma cells (N2a) were transiently transfected with vectors coding for NM, cytosolic PrP, or chimera thereof. Sup35p-NM and PrP displayed strikingly different aggregation behaviours when expressed in mammalian cells, with NM remaining soluble and cytosolic PrP spontaneously aggregating due to the globular domain of PrP. When fused to PrP_{90-230}, Sup35p-M inhibited nucleation, but increased aggregate growth, probably by enhancing the recruitment of newly synthesized proteins into the growing aggregates. Fusion of the prion forming region Sup35p-N to M-PrP counter-acted this effect, thereby increasing aggregate frequency. Interestingly, a lowered nucleation rate was also observed in the presence of the amino-terminal region of PrP, indicating that Sup35p-M and PrP_{23-90} have a similar biological function in prion protein assembly. These results demonstrate the impact of dynamic interactions between prion

domains and further suggest that aggregation of yeast and mammalian prion proteins is strongly influenced by the cellular environment.

In the second part of the present work NM was stably expressed in N2a cells by use of a lentiviral vector system. Similar to results with transient transfection, stably, ectopically expressed NM remained soluble in the cytosol of N2a cells. Surprisingly, addition of *in vitro* generated Sup35p-NM fibrils to the cell culture medium resulted in endogenous NM aggregation. Furthermore, NM aggregates were heritable and infectious, indicating that the mammalian cytosol promotes prion propagation. Aggregate types differed in individual cells, and established single cell clones showed dramatic differences in aggregate types, ranging from spindle-shaped aggregates to small, punctuate aggregates. Thus, although several different types of aggregates were induced in bulk cells, an individual phenotpye was faithfully propagated by a single cell clone, indicating that cellular factors might determine phenotypical variant selection. As the Sup35p prion domain aggregates appeared to propagate as prion variants in the absence of any Hsp104 orthologs, other cellular mechanisms must enable prion propagation in the mammalian cytosol.

I.B Deutsche Version

Prionkrankheiten sind fatale neurodegenerative Erkrankungen von Mensch und Tier. Allen gemeinsam ist die charakteristische Ablagerung einer abnormalen Isoform (PrP^{Sc}) des zellulären Prionproteins (PrP^C). PrP^{Sc} ist eng mit dem infektiösen Agens assoziiert und stellt nach heutigen Erkenntnissen den ausschließlich aus Protein bestehenden Erreger der Prionerkrankungen dar. Die Vermehrung von Säugerprionen scheint nach einer keimabhängigen Polymerisation zu verlaufen. Nach diesem Modell bindet die normale Isoform PrP^C an ein PrP^{Sc} Oligomer, welches dessen Umfaltung zur β-Faltblatt-reichen Struktur katalysiert. Ein Prion-ähnliches epigenetisches Phänomen wurde für den Translationsterminationsfaktor Sup35p in der Hefe *Saccharomyces cerevisiae* beschrieben, welcher ebenfalls eine autokatalytische Konformation annehmen kann. Fibrilläre Aggregate von Sup35p besitzen ähnliche Eigenschaften wie PrP Aggregate, wie etwa ein hoher β-Faltblatt Anteil, SDS-Unlöslichkeit oder partielle Proteaseresistenz. Bemerkenswerte Ähnlichkeiten im Umfaltungsprozess beider Proteine machen das Hefepriorsystem zu einem interessanten Modell für Prionkrankheiten von Säugetieren. Der Mechanismus der Prionvermehrung in Säugern, Domänen in PrP, die zur Prionaggregation beitragen und potentielle Kofaktoren sind derzeit noch ungeklärt. Ziel dieser Arbeit war eine vergleichende Analyse des Aggregationsverhaltens von PrP und Sup35p im Zytosol von Säugerzellen.

Im ersten Teil dieser Arbeit wurde das Aggregationsverhalten chimärer Proteine, abgeleitet aus der Priondomäne NM von Sup35p und PrP, untersucht. Maus Neuroblastomzellen (N2a) wurden transient mit Vektoren transfiziert, die für NM, zytosolisches PrP oder Chimären aus beiden kodieren. In Säugerzellen exprimiert zeigten Sup35p-NM und PrP ein bemerkenswert unterschiedliches Aggregationsverhalten. Während NM löslich blieb, kam es zur spontanen Aggregation von zytosolischem PrP aufgrund seiner globulären Domäne PrP_{90-230}. Nach Fusion von Sup35p-M mit PrP_{90-230}, wirkte M inhibierend auf die Nukleation und erhöhte gleichzeitig das Aggregatwachstum, vermutlich indem es den Einbau von neu synthetisiertem Protein in das wachsende Aggregat erleichterte. Eine Fusion der Prionbildungsregion Sup35p-N mit M-PrP konnte diesem Effekt entgegenwirken, wobei es zu einem Anstieg der Aggregationshäufikeit kam. Interessanterweise wurde eine reduzierte Nukleationsrate auch in Gegenwart der aminoterminalen Region von PrP beobachtet, was darauf hindeutet, dass Sup35p-M und PrP_{23-90} eine ähnliche biologische Funktion bei der

Prionproteinaggregation innehaben könnten. Diese Ergebnisse veranschaulichen den Einfluss von dynamischen Interaktionen zwischen Priondomänen und weisen darauf hin, dass die Aggregation von Hefe- und Säugerprionproteinen durch das zelluläre Umfeld stark beeinflusst wird.

Im zweiten Teil der vorliegenden Arbeit wurden N2a Zellen mit NM mithilfe eines lentivirales Vektorsystems transduziert. Wie auch bei der transienten Transfektion blieb das nun stabil exprimierte NM im Zytosol von N2as löslich. Überraschenderweise konnte jedoch die Zugabe von *in vitro* hergestellten Fibrillen aus bakteriell exprimiertem Sup35p-NM in das Zellkulturmedium eine endogene Aggregation von NM auslösen. Desweiteren waren diese Aggregate von NM vererbbar und infektiös, was zeigt, dass Säugerzellen die Vermehrung von artifiziellen Prionen im Zytosol ermöglichen. Das Aussehen der Aggregate, von spindelförmigen bis zu kleinen punktförmigen, unterschied sich in einzelnen Zellen wie auch in den daraus etablierten Einzelzellklonen. Somit wurde nur ein Aggregattyp von einem einzelnen Zellklon wirklich weiter gegeben, obwohl viele verschiedene Arten von Aggregaten in den unklonierten Zellen induziert wurden. Dies deutet darauf hin, dass zelluläre Faktoren die Selektion der phänotypischen Variante bestimmen. Da sich die Sup35p Priondomänaggregate als Prionvarianten, anders als in Hefen, offensichtlich trotz des Fehlens eines Hsp104 Orthologs vermehren können, scheinen andere zelluläre Mechanismen die Prionvermehrung im Säugerzytosol zu ermöglichen.

II. INTRODUCTION

II.A PRION DISEASES

Prion diseases or transmissible spongiform encephalopathies (TSEs) are infectious neurodegenerative disorders that affect both humans and animals. They feature a rapidly progressing clinical course that inevitably leads to death, usually within a few months. Typically, this is preceded by a long incubation time completely free of symptoms, lasting for years to decades. Thus, a ´slow virus` was first proposed to be the causative agent of this disease (Sigurdsson 1954). The failure to isolate a virus and the lack of an immune response typical for viral infections argued against this theory. Furthermore, the infectious agent could not be inactivated by methods destroying nucleic acids like UV-radiation, but rather was sensitive to treatments with substances which hydrolyze or modify proteins like urea or sodium hydroxide, indicated that the infectious agent might be a protein (Alper *et al.* 1966; Alper *et al.* 1967; Griffith 1967).

Fifteen years later S. Prusiner and coworkers successfully isolated a protease resistant glycoprotein from diseased hamster brains which constituted the main component of the infectious fraction (Prusiner 1982). According to the protein-only hypothesis subsequently proposed and elaborated by S. Prusiner, these diseases are caused by prions, ***pr**oteinaceous **in**fectious* particles devoid of encoding nucleic acid (Prusiner 1982; Prusiner 1998a). Further analysis revealed that prions consist mainly, if not entirely, of an abnormally folded isoform (PrP^{Sc}, for scrapie-associated prion protein) of the normal, host encoded prion protein (PrP^{C}, for cellular prion protein) (Cohen *et al.* 1994; Prusiner 1998a; Collinge 2001; Aguzzi & Polymenidou 2004; Weissmann 2004). Recently, this controversially discussed hypothesis was strongly supported by studies showing the *in vitro* generation of prion infectivity (Legname *et al.* 2004; Castilla *et al.* 2005).

A severe loss of neurons is characteristic of all prion diseases, which is accompanied by strong astrogliosis and mild microglia activation (**Figure 1**). This results in a severe progressive spongiform vacuolation and degeneration of the central nervous system (CNS) which manifests itself particularly in ataxia, behavioral changes and, in humans, a highly progressive loss of intellectual abilities (i.e., rapidly proceeding dementia) (DeArmond & Prusiner 1995; Prusiner 1998a; Weissmann 2004; Aguzzi & Polymenidou 2004; Collinge

2005). Amyloid plaques, consisting of ordered proteinaceous deposits with high β-sheet, are characteristic traits of TSEs. (Clinton *et al.* 1992; Bessen *et al.* 1997). However, there are cases where no amyloid plaques were found (Tateishi *et al.* 1995; Collinge *et al.* 1995). To date, neither pre-clinical diagnostic tests nor therapeutic or prophylactic treatments are available.
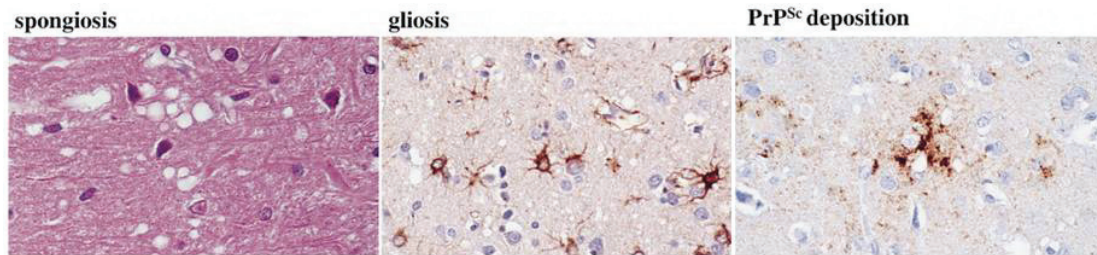
Figure 1. Neuropathologic characteristics of TSEs. The left panel displays spongiform vacuolation of the brain of a CJD patient stained with hematoxylin-eosin (HE). Activated astrocytes (brown) are visualized by staining with antibodies against glial fibrillary acidic protein (GFAP, middle). The right picture depicts an immunohistochemical staining of PrP[Sc] deposits (brown). From (Glatzel & Aguzzi 2001).

The pathogenic agent has self-propagating capacities in that it is able to catalyze a profound conformational switch of PrP[C] into an aggregated structure eventually resulting in the accumulation of misfolded and aggregated PrP[Sc] in the brain. Therefore, the prion pathology shares several profound similarities with other protein misfolding and neurodegenerative diseases like Alzheimer's, Huntington's and Parkinson's disease (Aguzzi & Haass 2003; Chiti & Dobson 2006). Nevertheless, prions are unique as they are not only able to replicate their conformation but are also naturally and experimentally transmissible within and to some extend between species (Weissmann *et al.* 1996; Prusiner 1998a).

II.A.1 HUMAN PRION DISEASES

Human prion diseases encompass Creutzfeldt-Jakob disease (CJD), Gerstmann-Sträussler-Scheinker (GSS) syndrome, fatal familial insomnia (FFI), kuru, and the new variants of CJD (vCJD and secondary vCJD). A hallmark of human TSEs is the existence of three distinct manifestations (Prusiner 1998b; Collinge 2001) (**Table 1**). The disease can occur either due to genetic mutations (i.e., mutations or insertions in the PrP open reading frame), as in the case of genetic CJD, GSS, and FFI, or can arise sporadically (idiopathic) with an incidence of ~1 in 1.000.000. The underlying mechanism of sporadic prion formation is still unknown.

Furthermore, they can be acquired by infection through prion-contaminated food or medically used human-derived materials as is the case for kuru, vCJD, or iatrogenic CJD, respectively.

Table 1. Etiologies of human prion diseases. Published in (Gilch *et al.* 2008).

Etiology	Disease and Frequency	Mechanism
Acquired	Kuru (pandemic in the 1950s, nowadays virtually extinct); iatrogenic Creutzfeldt-Jakob disease (CJD) (< 5 %), variant CJD (vCJD) (total so far > 200 cases)	infection through environmental exposure to prions; exogenous
Genetic	familiar or genetic CJD (~ 10 %); Gerstmann-Sträussler-Scheinker (GSS) syndrome; fatal familiar insomnia (FFI)	mutation in the *PRNP* gene (more than 30 different mutations are known); endogenous
Sporadic	sporadic CJD (~ 1 case per million per year worldwide, ~ 90 %)	apparently spontaneous formation of PrP^{Sc}; endogenous

Kuru reached pandemic proportions amongst the Fore people in Papua New Guinea, where it was transferred by a certain form of ritualistic cannibalism, in which the brains of the deceased were consumed as a sign of late person-worship (Gajdusek 1977). The introduction of Christianity and subsequent prohibition of such ancient customs resulted in virtual elimination of kuru, albeit some cases are still reported (Collinge 2001).

Although in particular the etiology of kuru was widely appreciated, both scientifically and within the general population, it was not until the the emergence of a new variant of Creutzfeldt-Jakob disease in the 1990s that people's awareness of the transmissibility of prion diseases was significantly raised (Collinge & Rossor 1996; Anderson *et al.* 1996; Bruce *et al.* 1997; Hill *et al.* 1997). vCJD first appeared in 1995 in the UK, but later also in several other countries (Will *et al.* 1996; Collinge & Rossor 1996) and affected mainly younger people. Interestingly, all clinical vCJD patients exhibited a homozygousity for methionine at *PRNP* codon 129, indicating a well known genetic predisposition for vCJD (Collinge *et al.* 1996), although recent evidence revealed that also people being heterozygous (methionine/valine) at

codon 129 can be infected (Peden *et al.* 2004). Regional and chronological coincidence of vCJD with bovine spongiform encephalopathy (BSE) was the first hint that they might have the same causative agent. Histopathologic analysis (Wadsworth *et al.* 2007), as well as transmission studies (Bruce *et al.* 1994; Lasmezas *et al.* 1996; Hill *et al.* 1997) and molecular strain typing (Collinge *et al.* 1996), confirmed the hypothesis that vCJD arose in humans who apparently have consumed BSE contaminated food. To date, more than 210 cases of vCJD are reported. Future predictions of cases are hard to achieve, partially because of the expected prolonged incubation time for heterozygous population. The number of potential patients may range from hundreds to thousands (Ghani *et al.* 2002; Ghani *et al.* 2003). In vCJD, the infectious agent is abundant in the lymphoreticular system and many other organs beside the CNS (Wadsworth *et al.* 2001; Sigurdson & Miller 2003), which dramatically increases the risk of horizontal spread. Indeed, vCJD transmission via blood transfusion was reported (secondary vCJD) and appears to be very effective (Peden *et al.* 2004; Llewelyn *et al.* 2004; Wroe *et al.* 2006; Hewitt *et al.* 2006).

II.A.2 ANIMAL PRION DISEASES

Animal prion diseases comprise scrapie in goat and sheep, bovine spongiform encephalopathy (BSE) in cattle, chronic wasting disease (CWD) in elk and deer, feline spongiform encephalopathy (FSE) in domestic and wild cats, transmissible mink encephalopathy (TME) , and exotic ungulate encephalopathy (EUE) in zoo animals (**Table 2**). Scrapie was first described in 1732 (Mc Gowan 1914; Mc Gowan 1922). As the name implies, excessive scratching is symptomatic for affected animals (Brotherston *et al.* 1968; Dickinson *et al.* 1974). In 1936, scrapie was experimentally transmitted to goats, providing prove for the infectious nature of the agent according to the Koch's postulates (Cuille & Chelle 1939). Because of its cross species transmissibility, especially as a zoonosis to humans, BSE or ´mad cow disease` is probably the best appreciated prion disease. First described in 1986 (Wells *et al.* 1987), it reached epidemic dimensions in the 1990s in the UK (Anderson *et al.* 1996; Hörnlimann *et al.* 2001). However, BSE cases were also reported in other European countries leading to mandatory BSE testing for any slaughtered cattle older than 30 (European Union) or 24 months (Germany), respectively, in 2000/2001. Whether BSE originated from scrapie-infected sheep (Wilesmith & Wells 1991; Prusiner *et al.* 1991) or whether it occurred sporadically in cattle (Fraser 2000) is yet unclear, but both theories

implicate that the infectious agent was distributed by feeding contaminated meat and bone meal (´neo-cannibalism`). Indeed, the sterilization method for fabrication of meat and bone meal was significantly changed in England in the late 1970s due to economy measures resulting in a completely insufficient inactivation of prions (Wilesmith & Wells 1991).

Table 2. Animal prion diseases.

Disease	Species	Mechanism
Scrapie	Sheep and goat	Vertical and horizontal transmission; oral transmission; sporadic
BSE (bovine spongiform encephalopathy)	Cattle	Ingestion of contaminated bone meal; sporadic?
TME (transmissible mink encephalopathy)	Mink	Apparently ingestion of contaminated food (produced from sheep and cow)
FSE (feline spongiform encephalopathy)	Cat and big cat	Ingestion of BSE contaminated food
CWD (chronic wasting disease)	Deer and elk	Vertical and horizontal transmission; oral transmission; sporadic?
EUE (exotic ungulate encephalopathy)	Exotic hoofed animals	Ingestion of BSE contaminated food

II.B THE PRION PROTEIN

II.B.1 THE *PRNP* GENE

The prion protein gene *prnp* is located on the short arm of the human chromosome 20 and on the homologous region of chromosome 2 in mice, respectively (Robakis *et al.* 1986; Sparkes *et al.* 1986). It is highly conserved during the course of evolution, from fish to amphibia to birds and mammals (Schatzl *et al.* 1995; Wopfner *et al.* 1999; Strumbo *et al.* 2001; Suzuki *et al.* 2002; Rivera-Milla *et al.* 2003), indicating an important function. Exon 2 or 3 at the 3'-end of the gene encodes the entire open reading frame (ORF) of the prion protein, excluding a possible formation of different proteins through alternative splicing (Basler *et al.* 1986;

Westaway *et al.* 1994). Human *PRNP* exhibits one, mouse *prnp* two short non coding exons at the 5'-end of the gene. The transcribed mRNA is 2,1 to 4 kb in length and is translated into a protein of approx. 250 amino acids (aa), depending on the species. The *prnp* promoter contains no TATA-box, it is rather composed of GC-rich regions, a typical feature for so-called ´house-keeping` genes (Basler *et al.* 1986).

II.B.2 STRUCTURAL AND BIOCHEMICAL CHARACTERISTICS OF PRP^C AND PRP^{Sc}

For a long time it was accepted that a single amino acid sequence allows only one biological active conformation (Anfinsen 1973). However, the prion protein can acquire at least two structural isoforms, which share the same primary amino acid sequences and apparently also covalent modifications (Pan *et al.* 1993). Several studies revealed that the structure of PrP^C contains a high content of α-helices (~ 42 %) and very few β-sheets (~ 3 %) whereas PrP^{Sc} is rich in β-sheet regions (~ 45 %) and exhibits a decreased amount of α-helices (~ 30 %) (Pan *et al.* 1993; Gasset *et al.* 1993; Pergami *et al.* 1996). Nuclear magnetic resonance (NMR) analysis of recombinant PRP$_{23-231}$ further revealed that the amino-terminal domain of cellular PrP (aa 23-120) is highly flexible with no defined structure whereas the carboxyl-terminus (aa 121-231) adopts a globular structure with three α-helices and two short antiparallel β-sheets (Zahn *et al.* 2000) (**Figure 2**).
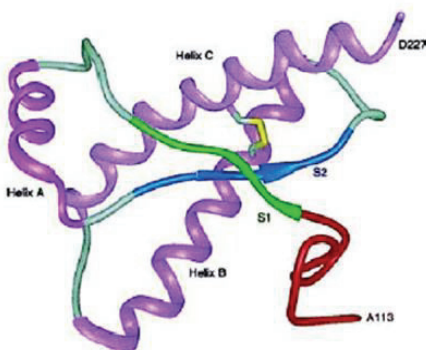
Figure 2. NMR structure of recombinant Syrian hamster PrP^C (aa 90-231). PrP^C contains 3 α-helices (purple) and two β-sheets (blue and green). The C-terminal part of the flexible amino-terminus (aa 90-120) is depicted in red. The intramolecular disulfide bond is shown in yellow. From (Prusiner 1998a).

Due to its insolubility NMR spectroscopy can not be performed from PrP^{Sc}. Thus, information on the structure of PrP^{Sc} was obtained by analysis of 2D-crystals in electron

microscopy and subsequent molecular modeling (Wille *et al.* 2002; Govaerts *et al.* 2004). According to this, PrP^{Sc} aggregates are assemblies of trimers with left-handed β-helices, conserved disulfide bonds and carboxyl-terminal α-helices. Recent findings obtained by site-directed spin labeling (SDSL) coupled with electron paramagnetic resonance (EPR) spectroscopy using recombinant human PrP$_{90-231}$ favor a model where the amyloid core of PrP^{Sc} corresponds to the carboxyl-terminal part of the protein forming a parallel, in-register β-sheet structure (Cobb *et al.* 2007) (**Figure 3**).
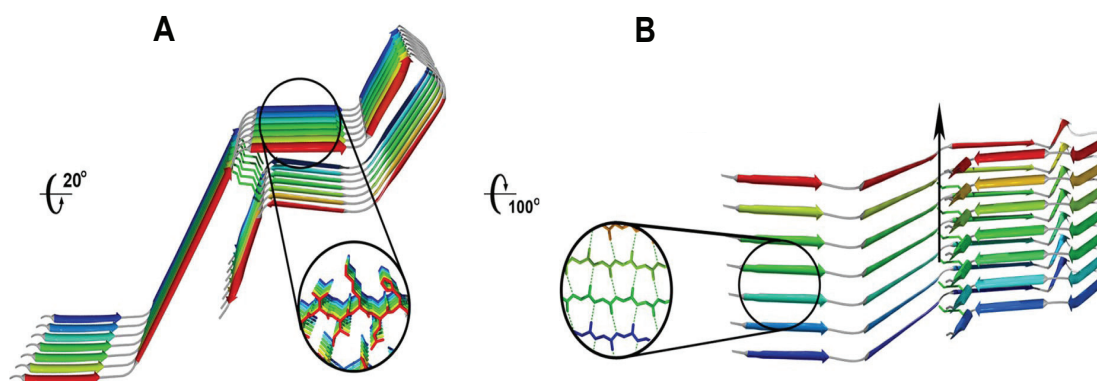
Figure 3. Model of recombinant PrP amyloid structure. A: PrP monomers form single, parallel layers that stack on top of each other with an in-register stacking of β-strands. **B**: The rotated structure demonstrates hydrogen bonds between aligned molecules. The long axis of the fibril is indicated by an arrow. From (Cobb *et al.* 2007).

The enormous structural differences between PrP^{C} and PrP^{Sc} are reflected by several distinct biochemical characteristics which are summarized in **Table 3**. The partial resistance of PrP^{Sc} to hydrolysis by proteinase K (PK) (Prusiner *et al.* 1984; Oesch *et al.* 1985) generating a aminoterminally truncated PrP^{Sc} moiety (PrP27-30) compared to a complete degradation of PrP^{C} upon proteolytic digestion is utilized to experimentally and diagnostically discriminate between the two isoforms.

Table 3. Structural and biochemical properties of PrP^C and PrP^{Sc}.

Cellular prion protein (PrP^C)	Pathogenic isoform of PrP (PrP^{Sc})
Non-infectious	Infectious
Mainly α-helical structure	β-sheet rich structure
Detergent soluble	Detergent insoluble
Proteinase K (PK) sensitive	Partially PK resistant (PrP27-30)

II.B.3 CELL BIOLOGY OF PRP^C

As a glycoprotein, the normal host-encoded prion protein PrP^C transits the secretory pathway. After synthesis, it is co-translationally translocated into the lumen of the endoplasmic reticulum (ER), where the aminoterminal signal sequence is removed (**Figure 4**).
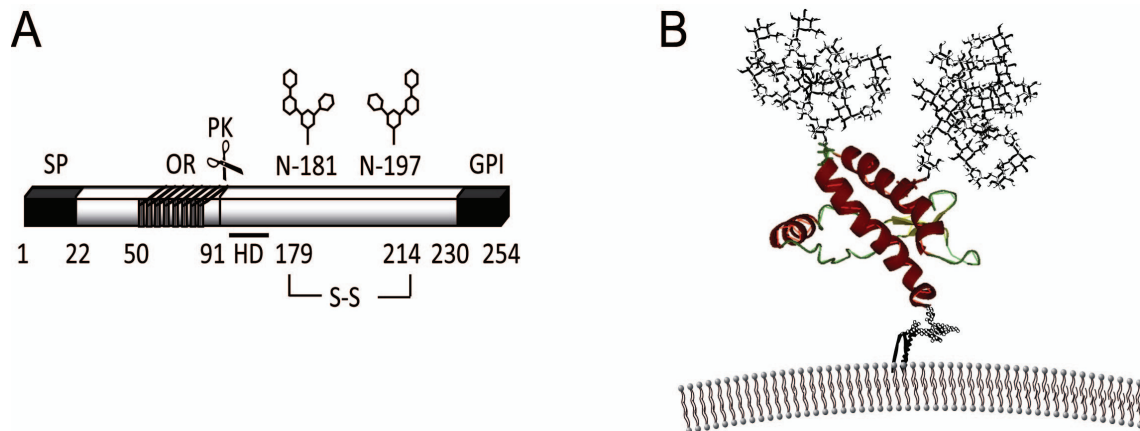
Figure 4. Primary structure, post-translational modifications and localization of the cellular prion protein. A: Schematic representation of cellular prion protein PrP^C, including primary structure and post-translational modifications. The signal peptide (SP) is removed during translocation into the ER lumen. The octapeptide region (OR) comprises residues 51-90; the proteinase K (PK) resistant portion of PrP^{Sc} is denoted by a scissors symbol. The hydrophobic domain (HD) encompasses residues 110-135, the disulfide bond and the two asparagine-glycosylation sites are arranged in the C-terminal part. For the addition of the GPI anchor residues 231-254 are co-translationally removed. **B**: Model of PrP^C as it is attached to the outer leaflet of the membrane via its GPI achor. Published in (Krammer *et al.* 2009b).

Further post-translational modifications include the addition of carbohydrate chains at two asparagine-glycosylation sites, the formation of an intramolecular disulphide bond, and the attachment of a glycosyl-phosphatidyl-inositol (GPI) anchor promoted by a C-terminal signal peptide which is cleaved off. Properly folded PrP^C further post-translationally matures,

exits the Golgi apparatus, and finally incorporates into the outer leaflet of the plasma membrane via its GPI anchor moiety. PrP^C mainly resides within lipid rafts, specific cholesterol and glycosphingolipid-rich micro-domains of the plasma membranes and important sites for signal transduction. This suggests that PrP^C might play a physiological role in such a process. Additionally, it is anticipated that PrP^C has antioxidant properties and it was shown to bind copper (Westergard *et al.* 2007). The true function of PrP^C remains enigmatic, allowing room for different presumptions (Aguzzi & Miele 2004; Caughey & Baron 2006; Westergard *et al.* 2007). There is now growing evidence that PrP^C has a neuroprotective function (Kuwahara *et al.* 1999; Chiarini *et al.* 2002; McLennan *et al.* 2004; Weise *et al.* 2004; Spudich *et al.* 2005; Lee *et al.* 2006b). The 37-kDa/67-kDa laminin receptor (LRP/LR) (Hundt *et al.* 2001; Leucht *et al.* 2003) or glycosaminoglycans (Priola & Caughey 1994) are promising candidates for potential receptors for PrP^C. The internalization mechanism of PrP^C is controversially discussed, it may either be endocytosed via lipid rafts (Taraboulos *et al.* 1995), or depend on clathrin- (Sunyach *et al.* 2003), or caveolin-mediated pathways (Prado *et al.* 2004), potentially in concert with LRP/LR or the lipoprotein receptor-related protein 1 (LRP1) (Taylor & Hooper 2007; Parkyn *et al.* 2008). PrP^C containing endosomes can recycle back to the plasma membrane (Vey *et al.* 1996) or fuse with lysosomes for degradation.

II.B.4 THE PRION CONVERSION PROCESS

The conformational change of PrP^C into PrP^{Sc} is thought to occur at the cell surface, either in lipid rafts or caveolae-like domains (CLDs), and/or along the early endocytotic pathway (Caughey *et al.* 1991; Borchelt *et al.* 1992), involving a direct contact between PrP^C and PrP^{Sc} isoforms (**Figure 5**). Potential co-factors for prion generation are the laminin receptor or its precursor (Leucht *et al.* 2003) or glycosaminoglycans (Priola & Caughey 1994). PrP^{Sc} is mainly located in secondary endosomes and lysosomes (McKinley *et al.* 1991; Arnold *et al.* 1995; Mironov, Jr. *et al.* 2003), only a small fraction was found at or near the plasma membrane (Borchelt *et al.* 1990; Caughey & Raymond 1991; Vey *et al.* 1996). Additionally, a small portion of PrP^{Sc} was shown to accumulate in cytosolic aggresomes under certain experimental conditions (Kristiansen *et al.* 2005) where it appears to impair proteasomal function (Kristiansen *et al.* 2007). The spread of prions from cell to cell could be imparted through exosomes (Vella *et al.* 2007) or via cell-to-cell contact (Kanu *et al.* 2002).
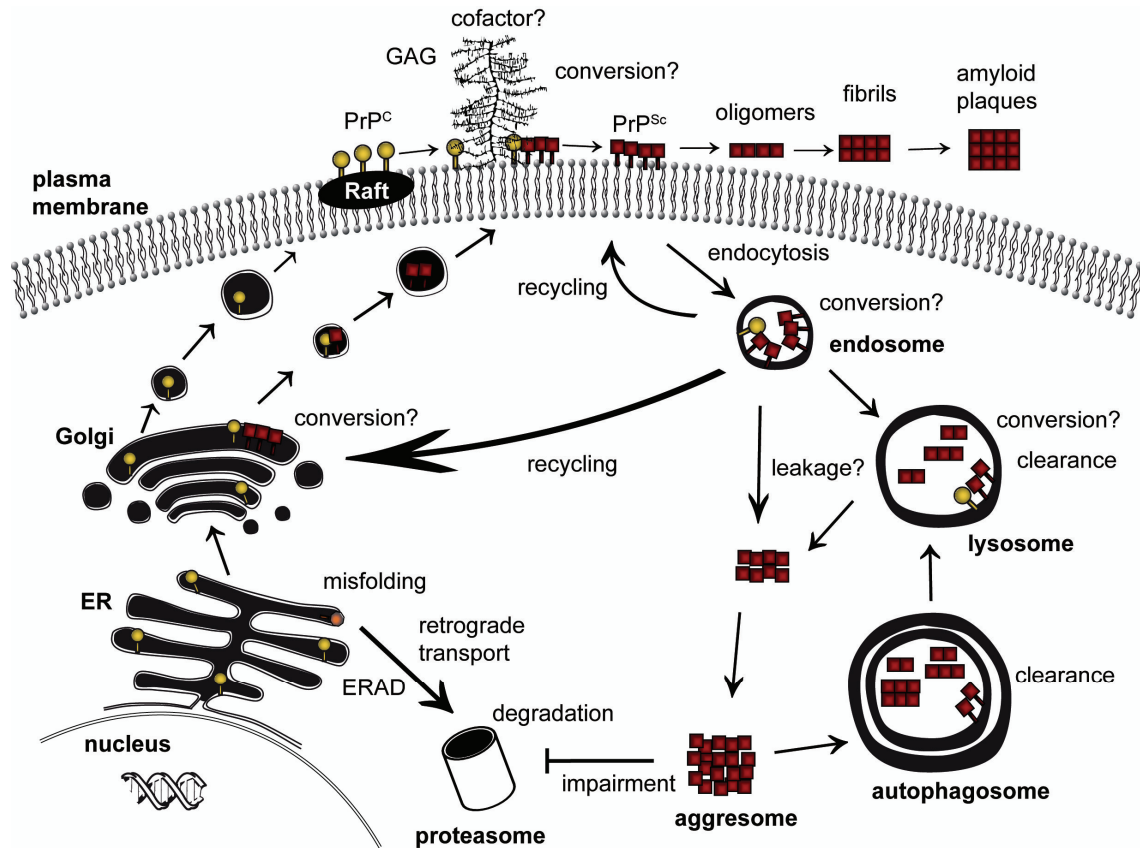
Figure 5. Cell biology of PrP^C and PrP^Sc with potential sites of conversion. As a membrane protein PrP^C migrates through the ER and Golgi compartments to the cell surface where it resides within lipid rafts via its GPI anchor. A direct contact between PrP^C and PrP^Sc isoforms is indispensable. The conformational refolding of PrP^C into PrP^Sc is thought to take place at the cell surface and/or along the endocytic pathway, probably involving co-factors, e. g., glycosaminoglycans (GAGs). PrP^Sc has been localized mainly in the lysosomes of persistently infected cell cultures, some PrP^Sc was also found on the cell surface or in the Golgi apparatus. A small portion of PrP^Sc has also been reported to aggregate in the cytosol. Published in (Krammer *et al.* 2009b).

The exact molecular mechanism of conversion is still subject to intensive research, but several lines of evidence suggest a general amyloid formation model in which PrP^Sc aggregates are formed by a crystallization-like process, known as nucleated polymerization (Serio *et al.* 2000; Caughey 2003; Soto *et al.* 2006) (**Figure 6**).
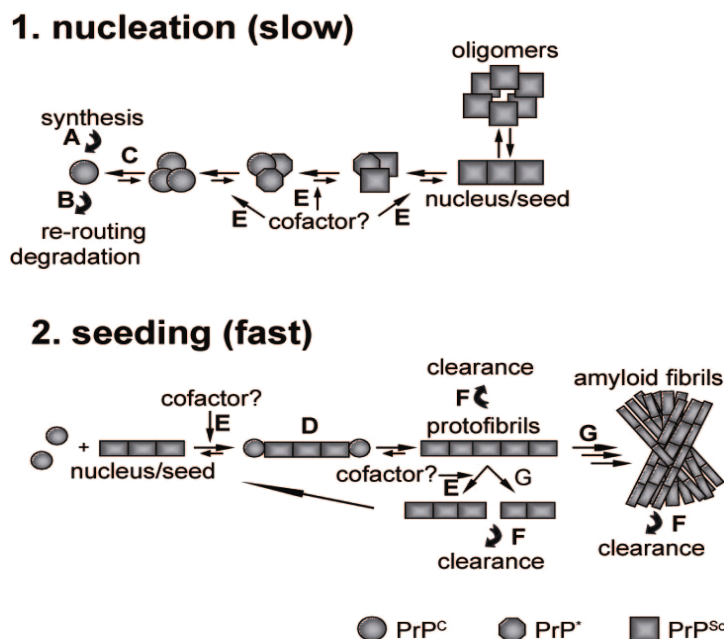
Figure 6. Prion replication according to the nucleated polymerization model. PrP^{Sc} formation may be a two-step event. The initial and pivotal step is formation of 'nuclei' which involves at least partially unfolding and misfolding of the PrP protein leading to small oligomers. This rare and slow process is followed by a much faster elongation phase in which the nuclei act as seeds that recruit native proteins into the growing aggregate. During this process a breakage of the elongated fibrils may be necessary to generate new seeds resulting in an exponential rise in amyloid formation. Spontaneous formation of PrP^{Sc} from normal PrP^{C} is a very rare event leading to sporadic forms, whereas mutations in the *prnp* gene apparently render the protein more aggregation prone (genetic prion disease). In acquired prion diseases the exogenous addition of PrP^{Sc} seeds induces conversion of the host-encoded protein. Published in (Gilch *et al.* 2008).

II.B.5 PRION STRAINS AND THE SPECIES BARRIER

The phenomenon that prions can be experimentally transmitted very efficiently within species but less efficient between species, is referred to as the 'species barrier'. In most cases incubation times of the disease are prolonged upon the first transmission to a new host compared to the incubation times upon subsequent passages within the same host (Pattison 1965). It has been proposed that the species barrier is mainly determined by aa differences in the *prnp* gene. Consequently, the degree of homology of the primary amino acid sequence between donor and host PrP, as well as the position of a possible amino acid exchange seem to play an important role for disease transmission (Scott *et al.* 1989; Scott *et al.* 1992; Scott *et al.* 1993; Telling *et al.* 1994; Priola *et al.* 2001; Schatzl *et al.* 1995). As mentioned above, in humans a polymorphism at residue 129 is critical for the susceptibility to vCJD (Parchi *et al.* 1999).

A challenge for the protein-only hypothesis was the observation that prions from a given species can cause relatively distinct disease patterns such as different incubation times

and lesion profiles within the brain upon passaging in the same species (Bessen & Marsh 1992). In order to explain this observation on the basis of a protein-only agent the term 'prion strain' was introduced. Prion strains are associated with several distinct characteristics of PrP^{Sc}, like relative resistance to PK digestion, glycoform profile and disease phenotypes such as incubation time, clinical symptoms and neuropathological changes (Bessen & Marsh 1992; Collinge *et al.* 1996; Telling *et al.* 1996; Safar *et al.* 1998). Prion strains appear to represent different three-dimensional conformations of PrP^{Sc} and the different properties are likely encoded in different folds of PrP^{Sc} (Telling *et al.* 1996; Scott *et al.* 1997). They can be faithfully propagated in inbred mouse lines and in the case of BSE even across a variety of species (Will *et al.* 1996; Collinge & Rossor 1996). In humans, for example, different prion strains are responsible for the various phenotypes of CJD (Bruce 2003).

While the aforementioned studies clearly demonstrate the importance of PrP primary amino acid sequence for prion transmission, a number of experiments have doubted this hypothesis. Early analysis revealed that the species barrier varies with different strains in spite of their origin from the same donor species, indicating that the type of prion strain markedly influences the outcome of interspecies transmission (Bruce *et al.* 1994; Bruce *et al.* 1997). The transmission of prions from different species to transgenic mice expressing PrP with a single amino acid mutation in the amino-terminus resulted in an increase or decrease in the incubation time compared to wild-type mice which cannot be explained simply by sequence differences (Barron *et al.* 2001). Moreover, transgenic mice expressing bovine PrP propagated vCJD prions but were resistant to sporadic, familiar, or iatrogenic forms of CJD, which prompted S. Prusiner and colleagues to introduce the denotation ´strain barrier` for this phenomenon (Scott *et al.* 2005). Surprisingly, wild-type mice are more susceptible to vCJD than transgenic mice over-expressing human PrP (Hill *et al.* 1997), providing evidence that factors other than PrP sequence similarity of host and donor PrP may play a role in TSE transmission and suggesting that the term ´transmission barrier` might be more appropriate than species barrier. Recent work showed that some Creutzfeldt-Jakob disease isolates could be primarily transmitted to bank voles in the absence of any obvious species barrier, although the sequence of man and vole shows various aa exchanges (Nonno *et al.* 2006). In conclusion, compelling evidence now suggests that the three-dimensional structures of host PrP^{C} and donor PrP^{Sc}, rather than exact primary amino acid sequence similarity, is the major susceptibility determinant of a species to a certain strain (**Figure 7**).
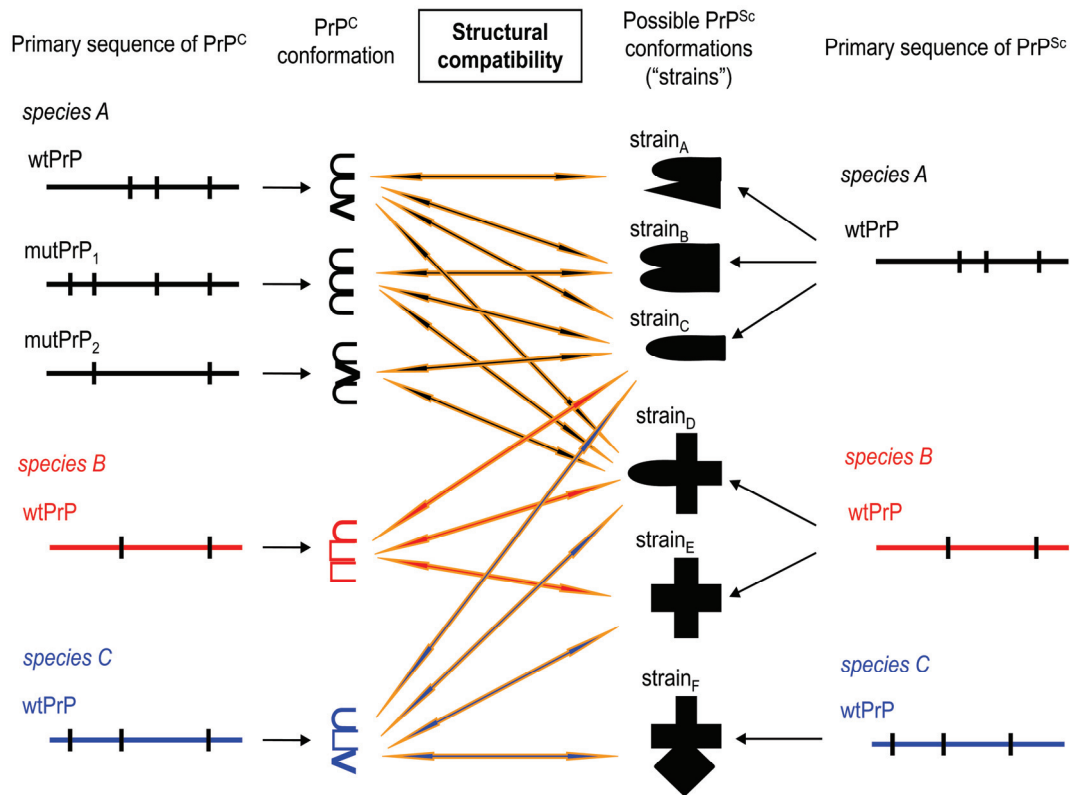
Figure 7. The structural compatibility of PrP^C and PrP^{Sc} determines the transmission barrier. The primary sequence of wild-type (wt) PrP^C influences its tertiary structure, therefore mutations (in mutant PrP, mutPrP) lead to a modified conformation (left side). On the other hand, a certain PrP primary structure is able to form a restricted variety of possible PrP^{Sc} conformers (right side). Conformations of both PrP^C and PrP^{Sc} have to be compatible, so that a certain donor PrP^{Sc} is able to interact with and convert host PrP^C. Structural differences are depicted as vertical bars. Arrows indicate structural compatibility. Modified version published in (Gaedtke *et al.* 2009).

The influence of the primary structure is obvious, albeit indirect, as it determines the secondary and tertiary structure of a protein. According to the conformational selection model (Collinge 1999) the host PrP^C amino acid sequence allows only a subset of possible PrP^{Sc} conformations and influences which PrP^{Sc} is thermodynamically preferentially propagated. In line with this, a lack of overlap in possible PrP^{Sc} conformers of different species may be the basis of the transmission barrier (Collinge & Clarke 2007). On the basis of this model a further phenomenon, the prion strain mutation, can be explained (**Figure 8**). Some strains like BSE are highly transmissible across a wide variety of species maintaining its strain characteristics. In this case the conformation of a certain strain is compatible with a range of different PrP^C conformers. Other strains do not ´breed true` upon transmission into a new host, resulting in the occurrence of a new strain in the infected species (Collinge & Clarke 2007). Strains may constitute an ensemble of PrP^{Sc} molecules and the new host

preferentially propagates a non prevalent conformer. Alternatively, when strains are composed of a single PrP^{Sc} conformer, only a direct conformational mutation enables its successful transmission to a host due to a previous PrP sequence incompatibility for this certain strain. Of note, some studies revealed that background genes other than the *prnp* gene may also influence strain selection (Asante *et al.* 2002; Lloyd *et al.* 2004).
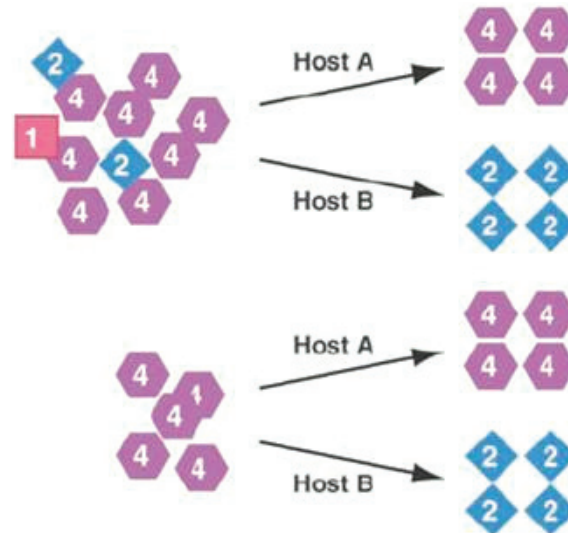
Figure 8. Prion strain mutation. If strains consist of a mixture of different PrP^{Sc} molecules, a certain host cell can either preferentially propagate the prevalent conformer (upper panel, Host A) or select a non prevalent conformer leading to the occurrence of a new strain in the foreign host (upper panel, Host B). On the other hand, strain may be based on a single PrP^{Sc} conformer which is able to ´breed true` upon transmission to one host (lower panel, Host A) but during infection of another host (lower panel, Host B) it has to change its conformation in order to propagate. From (Collinge & Clarke 2007).

II.C PRP AND ITS ROLE IN NEURODEGENERATION IN PRION DISEASES

Although *prnp*$^{0/0}$ mice were rapidly made available for research (Bueler *et al.* 1992), the function of PrP^C is far from being thoroughly understood. Mice lacking PrP^C do not show a precise phenotype. They are generally viable (Bueler *et al.* 1992) and suffer only from subtle defects, like altered circadian activity rhythms and sleep (Tobler *et al.* 1996), an abnormal synaptic function (Collinge *et al.* 1994), or a disturbance of the intracellular Ca^{2+} homoeostasis (Colling *et al.* 1996). On the other hand, compelling evidence now suggests that PrP^C has neuroprotective properties. It is up-regulated upon ischemic brain damage (McLennan *et al.* 2004; Weise *et al.* 2004), and in PrP-deficient mice the infarct size is

drastically increased (Spudich *et al.* 2005). In addition, PrP^C is able to protect against several pro-apoptotic stimuli (Kuwahara *et al.* 1999; Chiarini *et al.* 2002; Lee *et al.* 2006a). Neuronal PrP^C expression is absolutely necessary for disease development, as *prnp$^{0/0}$* mice are totally resistant to prion infection (Bueler *et al.* 1993). The fundamental role of neuronal PrP^C expression in prion disease was elegantly demonstrated in follow-up studies using either grafting approaches (Brandner *et al.* 1996), inducible transgenic knock-down approaches (Mallucci *et al.* 2002; Mallucci *et al.* 2003; Mallucci *et al.* 2007), or transgenic studies involving a secreted (GPI-minus) version of PrP^C (Chesebro *et al.* 2005). Taken together, it is possible that a certain loss of function phenotype related to PrP^C plays a major role in prion disease pathogenesis. Another scenario is that PrP^{Sc} could impair important signaling mechanisms of the cell, thereby gaining a toxic function. Indeed, a recent study demonstrated that PrP^{Sc} is able to impair the neuroprotective signaling of PrP^C (Rambold *et al.* 2008).

Additionally, PrP^C can be found in three distinct topological forms (Hay *et al.* 1987; Hegde *et al.* 1998). While the vast majority constitutes the normal post-translationally modified form that is attached on the outer leaflet of the plasma membrane via a GPI anchor, two transmembrane forms are known that differ in their membrane topology. The carboxylterminal-trans transmembrane form (^{Ctm}PrP) has been experimentally linked to neurotoxicity, especially in some heritable prion diseases. For example, in GSS involving the mutation A117V, the formation of the pathogenic ^{Ctm}PrP form is increased (Hegde *et al.* 1998). Whether the topological PrP isoforms play a more general role in prion pathogenesis is still not completely resolved.

The artificial expression of an entirely cytosolic form of PrP in a transgenic mouse model resulted in severe ataxia with cerebellar degeneration and gliosis (Ma *et al.* 2002). Good evidence exists that cytosolic accumulation of PrP may actually have a more general relevance in prion diseases (Ma & Lindquist 2002; Heller *et al.* 2003; Rane *et al.* 2004). In addition, truncated pathogenic GSS-related PrP mutations (W145Stop or Q160Stop) are associated with mislocated cytosolic PrP (Zanusso *et al.* 1999; Heske *et al.* 2004). Work of J. Collinge's laboratory demonstrated that cytosolic PrP^{Sc} aggregates might exist that cluster in aggresome-like forms, thereby activating caspase-3 and inhibiting the 26S proteasome (Kristiansen *et al.* 2005; Kristiansen *et al.* 2007). These facts argue that cytosolic PrP species might be a common toxic denominator in various prion-linked diseases.

PrP^{Sc} is thought to be the causative agent responsible for prion diseases, hence, exerting both neurotoxicity AND prion infectivity. This hypothesis has been challenged by several observations during the last decade. First, the amount of PrP^{Sc} detectable by standard methods does not always correlate with the severity of neurodegeneration. In fact, it is known for long that there are natural and experimental prion diseases without almost any PrP^{Sc} accumulation in the brain (Collinge *et al.* 1995). Second, injection of brain homogenate of terminally-ill mice into *prnp$^{0/0}$* mice does not lead to disease symptoms (Bueler *et al.* 1993; Brandner *et al.* 1996). Third, small oligomeric molecules, apparently not PK-resistant, were shown to be more toxic to various cell types than mature amyloid fibrils of the same protein (Novitskaya *et al.* 2006; Simoneau *et al.* 2007). Additionally, the group of B. Caughey provided experimental evidence that such low molecular weight species are in fact the most infectious units (Silveira *et al.* 2005). In line with this, it was shown that prion-infected transgenic mice that express a secreted form of PrP^{C} that lacks the GPI anchor exhibited hardly any clinical signs, although they had tremendous amounts of amyloid plaques in their brains (Chesebro *et al.* 2005). Several important conclusions can be drawn from these results. First, the mature amyloid fibrils appear to represent end- or by-products in prion diseases. Second, infectivity and neurotoxicity are not necessarily linked and could originate from different molecules and/or mechanisms. Third, PrP^{Sc} accumulation and deposition in the brain is not or not necessarily toxic. Hence, the identity of the toxic agent remains a conundrum. Nevertheless, it appears that prion infectivity and toxicity can be uncoupled favoring the hypothesis that the toxic agent (in this model referred to as PrP^{L}, the lethal form of PrP) is rather an intermediate or by-product of prion replication than aggregated high molecular PrP^{Sc} itself (Collinge & Clarke 2007) (**Figure 9**).
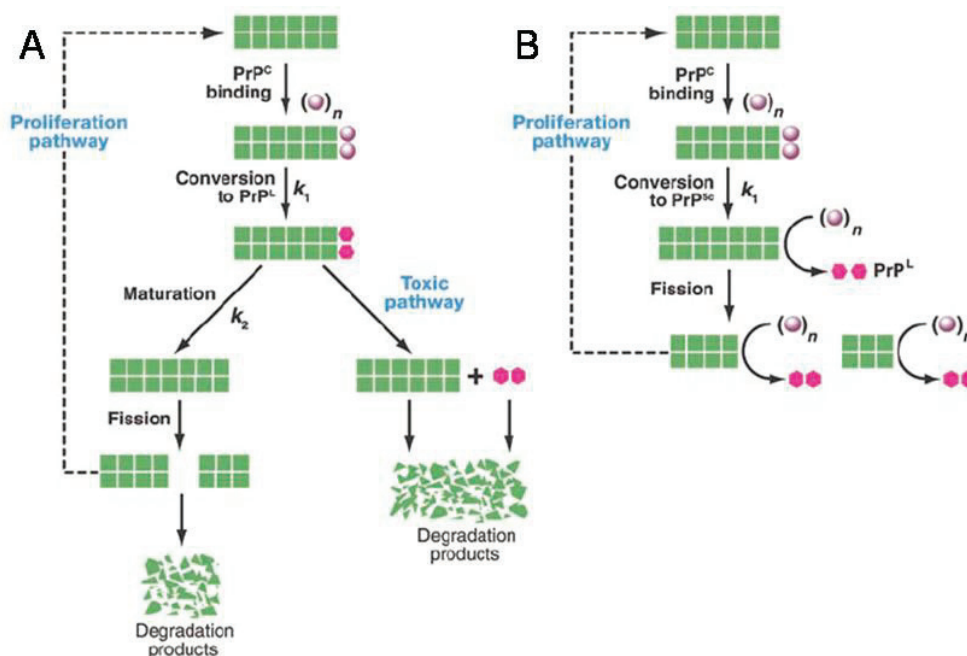
Figure 9. Possible pathways for the production of the ´lethal´ form of PrP (PrP^L). A: PrP^L could be generated during the conversion process by dissociating as a toxic intermediate from the growing PrP^{Sc} molecule. **B**: As a side product of the PrP^{Sc} synthesis PrP^L could be generated from PrP^C by using PrP^{Sc} as surface catalyst. From (Collinge & Clarke 2007).

II.D YEAST PRIONS

Initially, the term prion was exclusively used to describe the proteinaceous infectious agent responsible for TSEs. In 1994, R. Wickner extended the prion concept to explain two unusual non-chromosomal genetic elements [PSI$^+$] (Cox 1965) and [URE3] (Lacroute F 1971) in yeast (Wickner 1994), that were inherited from cell to cell in a non-Mendelian manner by cytoplasmic mixing. He proposed that these mysterious traits were determined by the prion form of the endogenous proteins Sup35p and Ure2p, respectively (Wickner 1994). Evidence accumulates that this is in fact the case. Unlike mammalian prions, yeast prions are not generally lethal but can rather be beneficial under certain environmental conditions (Eaglestone *et al.* 1999; True & Lindquist 2000). However, the search for [PSI$^+$] in wild-type strains was unsuccessful, arguing that these prions might be disadvantageous to yeast (Chernoff *et al.* 1993; Resende *et al.* 2003).

Prions are now more generally defined as self-propagating, infectious aggregates of misfolded proteins. To date, three amyloid prions were identified in yeast *Saccharomyces cerevisiae* and one in the fungus *Podospora anserina* (Maddelein *et al.* 2002; Tanaka *et al.*

2004; King & Diaz-Avalos 2004; Brachmann *et al.* 2005; Patel & Liebman 2007) (**Figure 10**). Recently, the chromatin-remodeling factor Swi1 was reported to be able to covert into a prion, [SWI$^+$], in *Saccharomyces cerevisiae* (Du *et al.* 2008). Initially, it was found during a screen for proteins acting as [PSI$^+$] inducible factors [PIN$^+$] (Derkatch *et al.* 2001). Still, a potential amyloid-like structure has to be formally demonstrated.
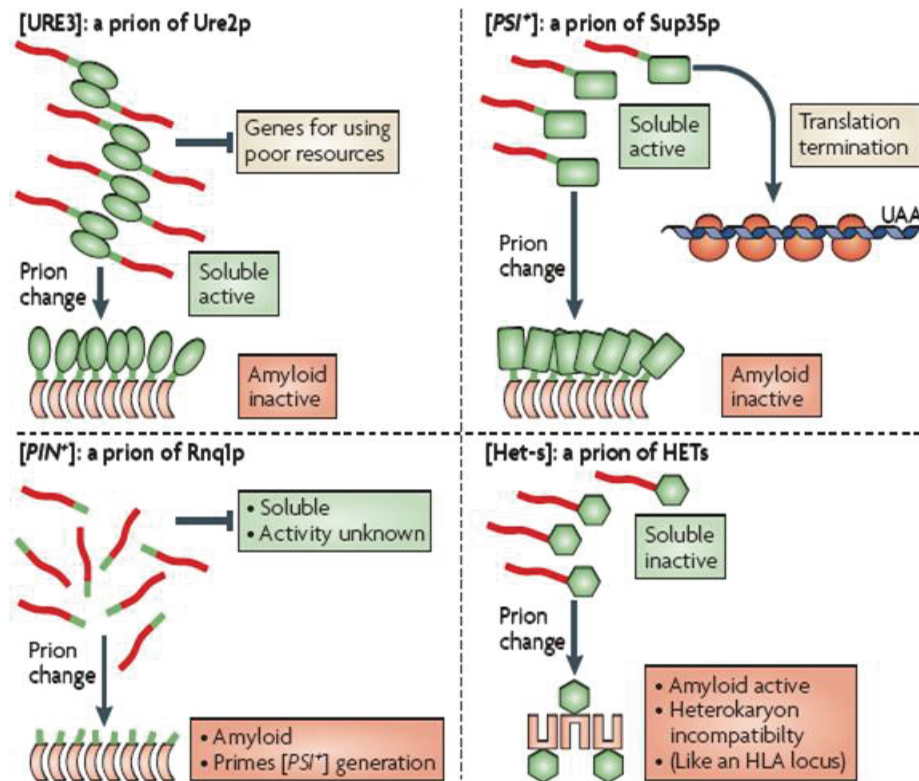
Figure 10. Amyloid prions of yeast and fungi. The amyloid forms of Ure2p and Sup35p have no function whereas their soluble forms are involved in nitrogen regulation and termination of transcription, respectively. The true function of both, the soluble or aggregated form of Rnq1p is not known, but in its prion form Rnq1p acts as a heterologous seed for the induction of [URE3] or [PSI$^+$]. The amyloid form of the HETs protein is necessary for heterokaryon incompatibility; its soluble form is non-functional. Natively structured domains are depicted in green. Unstructured domains that become amyloid during conversion into the prion form are highlighted in red. From (Wickner *et al.* 2007).

Yeast prions fulfill three genetic criteria (Wickner *et al.* 1999). First, the prion form has to be reversible curable, meaning it should be able to arise again spontaneously in a cured strain. Second, transient overproduction of the respective protein should increase the frequency of spontaneous induction of the prion form, simply because the probability of a prion conversion rises with the amount of the molecules. Third, the gene encoding the normal form of the prion protein has to be essential for prion propagation as it can only propagate by

converting the normal isoform into the prion form. However, infectivity is the most important attribute that clearly sets prions apart from other amyloids. Indeed, formal proof of the protein-only hypothesis was provided by induction of the yeast prion phenotype by *in vitro* generated amyloid fibrils from the corresponding recombinant protein (Maddelein *et al.* 2002; Tanaka *et al.* 2004; King & Diaz-Avalos 2004; Brachmann *et al.* 2005; Patel & Liebman 2007).

II.D.1 FUNCTION OF SUP35P

In 1965, Cox discovered the yeast prion [PSI+] phenotype during a screen for nonsense suppressor mutants (Cox 1965). The examined yeast strains exhibited enhanced suppression of nonsense mutations by the weak transfer-RNA (tRNA) suppressor SUP16 (SUQ5) and rendered strong tRNA suppressors (e.g., SUP4) lethal (Cox 1965; Cox 1971). Therefore, the [PSI+] determinant can be visualized by the suppression of the *ochre* mutation ade2-1 encoding an enzyme involved in the adenine biosynthesis pathway by SUQ5 (**Figure 11**). The ade2-1 mutant allele is not suppressed in [psi-] cells leading to an accumulation of a red pigment, a metabolic by-product of the adenine biosynthesis pathway. In [PSI+] cells ade2-1 is suppressed giving rise to normal white colonies. A SUQ5 independent suppression of the ade1-14 allele by [PSI+] results in a similar phenotype.

Figure 11. Discrimination of [PSI+] and [psi-] cells by the use of mutant yeast strains. Yeast strains containing either the ade2-1 or the ade1-14 nonsense alleles appear red on normal rich growth medium composed of yeast extract, bactopeptone and glucose (YEPD). In [PSI+] cells enhanced nonsense suppression of these alleles results in normal white colonies that are even able to grow in the absence of adenine. From (Tuite & Cox 2003).

It was eventually discovered that the yeast protein Sup35p plays a pivotal role in conferring the [PSI⁺] phenotype. Sup35p is the yeast homolog of the eukaryotic release factor (eRF3) and constitutes, along with Sup45p, the homolog of the eRF1 translation termination factor (Frolova *et al.* 1994; Stansfield *et al.* 1995). At a nonsense codon it terminates the polypeptide synthesis. The fact that [PSI⁺] cells and recessive mutants of Sup35p exhibited similar phenotypes and that the gene coding for Sup35p was essential for propagation of [PSI⁺] eventually linked the phenotype to its causative protein (Doel *et al.* 1994; Ter Avanesyan *et al.* 1994). In [psi⁻] cells Sup35p is soluble and functional, thus ensuring a correct termination of protein synthesis at a stop codon whereas in [PSI⁺] cells it enables the suppression of nonsense codons due to its aggregated non-functional prion form (**Figure 12**).
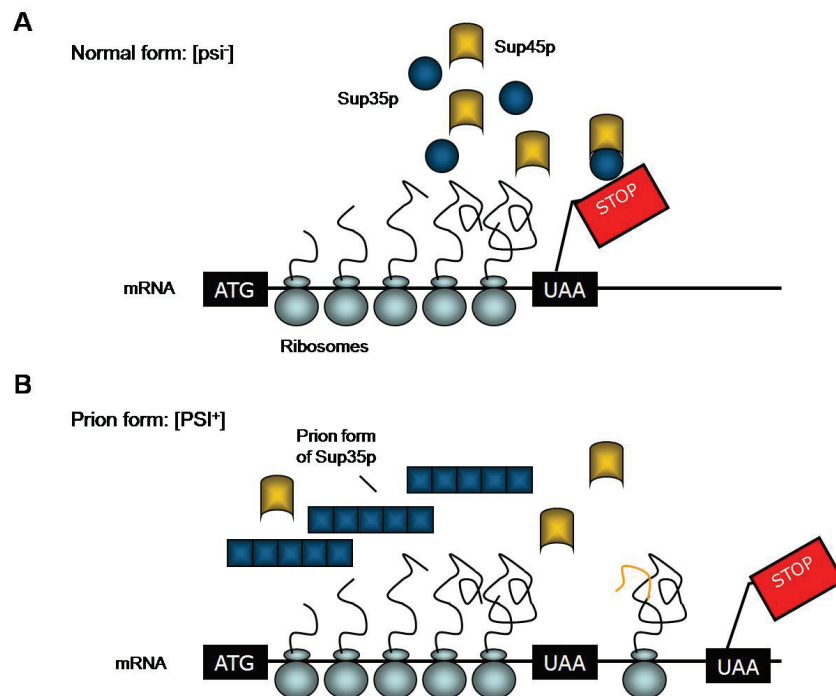
Figure 12. The function of Sup35p. A: Soluble Sup35p along with Sup45p is responsible for correct translation termination at a nonsense codon ensuring an accurate protein sequence. **B**: The aggregated form of Sup35p has a reduced ability to interact with Sup45p enabling the ribosome to read through a stop codon and to generate longer proteins with sometimes additional functions.

II.D.2 Structure and characteristics of Sup35p

Full-length Sup35p consists of 685 amino acids and can be divided into three distinct regions (**Figure 13**).
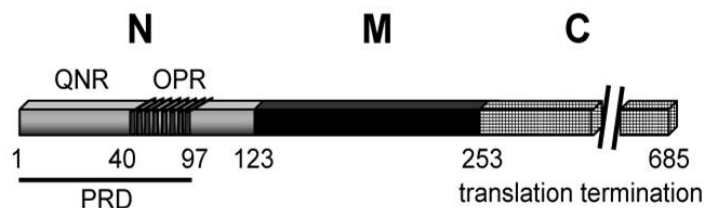
Figure 13. Primary sequence of Sup35p. Sup35p has three regions, the amino-terminal (N), the middle (M) and the carboxyl-terminal (C) region. N consists mainly of the minimal prion forming domain (PRD), that comprises a glutamine- (Q) and asparagine- (N) rich region (QNR) and the oligopeptide repeats (OPR). M is mostly composed of highly charged amino acids and affects the solubility of the protein. The C region is responsible for the translation termination and dispensable for aggregation. Published in (Krammer *et al.* 2008b).

The carboxyl-terminal domain (aa 253-685) has translation termination activity (Chernoff 2004; Ross *et al.* 2005), while the prion status of the protein is governed by the amino-terminal NM region. The N region is indispensable for the conformational alteration and polymerization. It comprises a prion forming domain (PRD, aa 1-97) which is defined to be the minimal region essential for induction and propagation of the prion state (Kushnirov *et al.* 1990; Ter Avanesyan *et al.* 1994; Derkatch *et al.* 1996). The PRD can be further divided into a glutamine (Q)- and asparagines (N)-rich region (QNR, aa 1-40) with a high content of polar and uncharged amino acids (DePace *et al.* 1998) and an oligopeptide repeat region (OPR, aa-41-97). The OPR consists of five imperfect repeats of a glutamine rich sequence bearing a striking resemblance to the octarepeats in mammalian PrP (Wilson & Culbertson 1988; Liu & Lindquist 1999). The QNR region might account for the specificity of intermolecular interactions of Sup35p molecules in the aggregate (Santoso *et al.* 2000; Chien & Weissman 2001) whereas the OPR region is involved in stabilizing aggregates (Parham *et al.* 2001). Interestingly, oligopeptide repeats in Sup35p can significantly modulate conformational conversion and amyloid assembly (Scheibel & Lindquist 2001; Dong *et al.* 2007; Kalastavadi & True 2008).

The [PSI$^+$] determinant spontaneously arises *de novo* in [psi$^-$] cells at a rate of 1:10^6 but its appearance can be increased up to 1:10^1 by over-expression of PRD (Derkatch *et al.* 1996). Furthermore, this region appears to be responsible for formation of nuclei (Krishnan &

Lindquist 2005) and experiments in yeast have demonstrated that the prion domain can confer its aggregation ability to other proteins (Patino *et al.* 1996; Edskes *et al.* 1999; Li & Lindquist 2000). Other than acting as a linker between the N and C region of Sup35p that stabilizes the prion during mitosis and meiosis (Liu *et al.* 2002) and increases the solubility of the protein in the non-prion state (Glover *et al.* 1997), no clear function for the conserved and highly charged M domain has so far been identified (Liebman 2001; Kushnirov & Ter Avanesyan 1998). Solid state nuclear magnetic resonance (NMR) of ^{13}C-1-tyrosine labeled amyloid Sup35p-NM revealed that the distance between two tyrosines averaged 5 Å, indicating a parallel in-register β-sheet structure for Sup35p-NM amyloid (Shewmaker *et al.* 2006) (**Figure 14**). Interestingly, the same structure was also shown for the M domain which is dispensable for [PSI$^+$] propagation (Shewmaker *et al.* 2006).
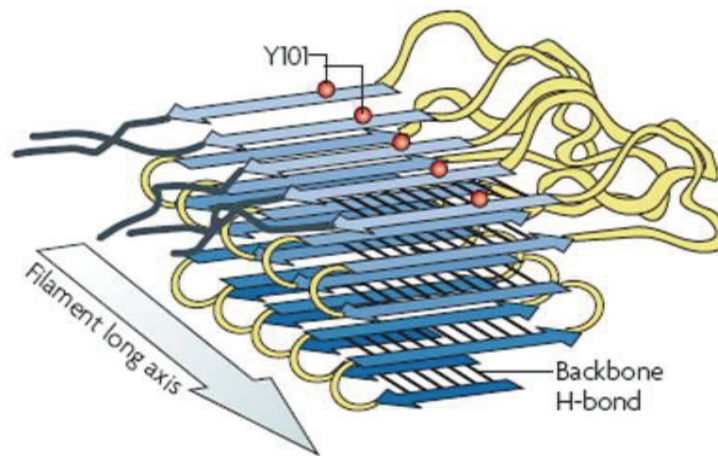
Figure 14. Model of the parallel in-register β-sheet structure of the Sup35p prion domain. β-strands are depicted as blue arrows. They are arranged vertically to the long axis of the filaments. Connecting loops are shown in yellow. The different strands run in parallel leading to an alignment of the same amino acid sequence in the filament as shown for Y101 (red circles). From (Wickner *et al.* 2007).

As known for mammalian PrP, rearrangement to inactive aggregated Sup35p is associated with a change in diverse biochemical properties which can be analyzed by different cell biological, biochemical, and biophysical methods (Patino *et al.* 1996; Paushkin *et al.* 1996) (**Figure 15**).
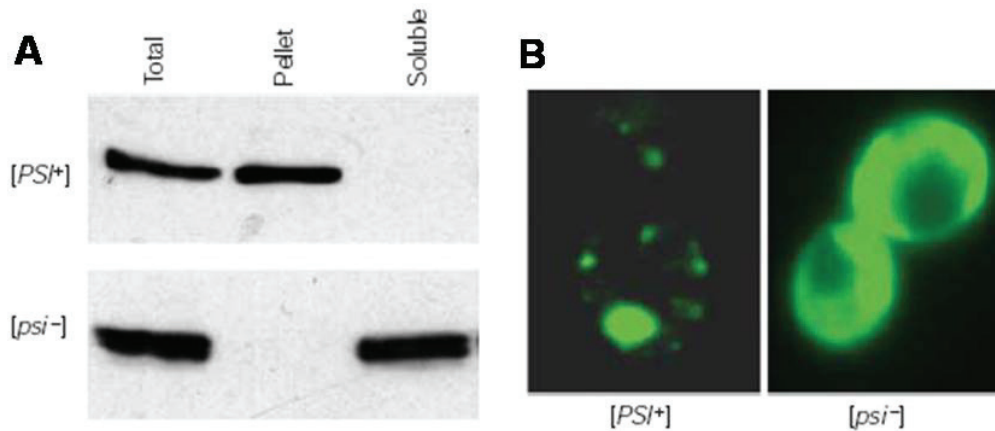
Figure 15. Biochemical differences of Sup35p in [PSI⁺] versus [psi⁻] cells. A: Sup35p in [PSI⁺] cells forms high molecular weight aggregates that can be pelleted by centrifugation while Sup35p remains soluble in [psi⁻] cells. Fractionation of cell lysates via sedimentation assays and subsequent Western blotting can be used to distinguish between these two states. **B**: Fusion of green fluorescence protein (GFP) to the prion forming domain of Sup35p NM visualizes fluorescent aggregates in [PSI⁺] cells in contrast to a diffuse cytosolic staining of NM-GFP in [psi⁻] cells in confocal microscopy images. From (Tuite & Cox 2003).

II.D.3 GENERATION AND PROPAGATION OF THE [PSI⁺] PHENOTYPE

The mechanism of yeast prion formation is thought to proceed according to the nucleated polymerization model proposed for mammalian prions. According to *in vitro* analysis, the amyloid forming process can be divided into two steps, namely nucleation and fibril assembly (Wickner *et al.* 1999; Serio *et al.* 2000). Soluble Sup35p molecules are believed to exist in a steady-state between monomers and oligomers which can spontaneously convert to nuclei by intrinsic conformational rearrangements. Subsequently, they act as seeds for soluble Sup35p and promote its conversion and incorporation into the growing aggregate (Scheibel *et al.* 2004) (**Figure 16**).
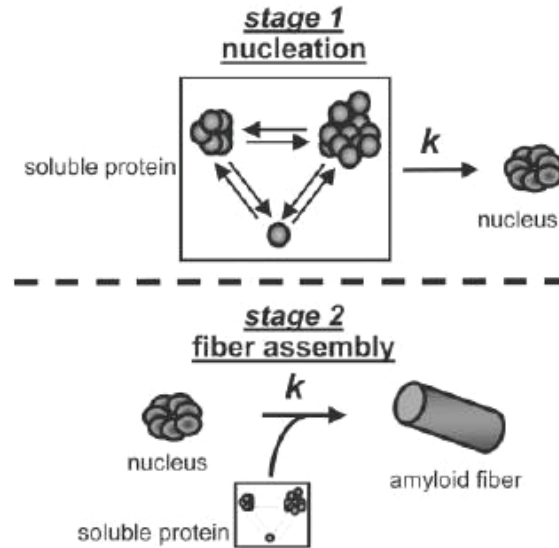
Figure 16. Nucleated conformational conversion (NCC) of Sup35p-NM. In the first stage, soluble NM molecules exist as monomers and different oligomeric forms from which a nucleus can emerge over time. Once established this nucleus is able to seed soluble Sup35p proteins and promote their incorporation into amyloid fibers. From (Scheibel *et al.* 2004).

In contrast to mammalian prions, induction of the prion state as well as the mechanisms of replication are better defined for the yeast [PSI+] determinant. Increased induction of [PSI+] by the over-production of Sup35p or PRD depends on the co-existence of [PIN+] or [URE3], the prion forms of Rnq1p or Ure2p, respectively (Derkatch *et al.* 1997; Bradley *et al.* 2002). Interestingly, they can be substituted by other also non-prion Q/N-rich proteins (Derkatch *et al.* 2001; Osherovich & Weissman 2001) suggesting that heterologous cross-seeding is the underlying mechanism (Vitrenko *et al.* 2007). Reduced amounts of Ssb1 and Ssb2, two ribosome associated Hsp70s, or of Ubc4, an ubiquitin-conjugated enzyme were also shown to cause an enhanced occurrence of the [PSI+] phenotype (Chernoff *et al.* 1999; Allen *et al.* 2007). Thus, a failure of mechanisms ensuring the proper folding of proteins and the degradation of misfolded proteins might promote prion formation. Recent evidence suggests that the cortical actin cytoskeleton might additionally affect [PSI+] induction by providing a scaffold for aggregate assembly (Ganusova *et al.* 2006).

Yeast prion inheritance requires aggregate formation and replication, two events that are strongly dependent on cellular factors. Many chaperones were shown to be important for prion propagation, including Hsp104, Hsp70s, Hsp40s and several co-chaperones (Newnam

et al. 1999; Jung *et al.* 2000; Sondheimer *et al.* 2001; Jones & Masison 2003; Jones *et al.* 2004; Fan *et al.* 2007; Sadlish *et al.* 2008) (**Figure 17**).
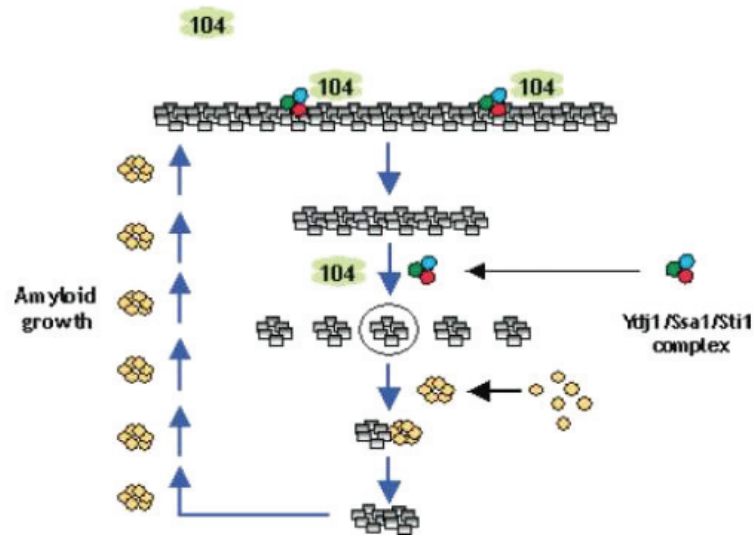
Figure 17. The role of chaperones in yeast prion propagation. Hsp104 (104) activity breaks up pre-existing aggregates to generate small infectious seeds. Hsp70 (e.g., Ssa1) together with Hsp40 (e.g., Ydj1) and various other co-chaperones (e.g., Sti1) are also involved in this process. From (Jones & Tuite 2005).

The disaggregase Hsp104 (Bosl *et al.* 2006) is indispensable for the propagation of all known yeast prions (Chernoff *et al.* 1995; Derkatch *et al.* 1997; Moriyama *et al.* 2000). The fact that Hsp104 activity can be specifically inhibited by millimolar amounts of guanidine hydrochloride (Tuite *et al.* 1981; Ferreira *et al.* 2001; Grimminger *et al.* 2004) makes it easy to study its function in yeast prion propagation. Hsp104 acts in concert with Hsp70s and Hsp40s in disaggregating heat-denatured proteins (Glover & Lindquist 1998) and appears to be crucial for propagon formation for efficient prion transmission to daughter cells by breaking up large amyloid fibrils into smaller seeds (Paushkin *et al.* 1996; Kryndushkin *et al.* 2003; Tuite & Koloteva-Levin 2004; Satpute-Krishnan *et al.* 2007; Byrne *et al.* 2007). Curiously, over-expression of Hsp104 cures [PSI+] but not [URE3] or [PIN+]. However, curing of [PSI+] by Hsp104 over-expression can be inhibited by concomitant over-expression of Ssa1 (Newnam *et al.* 1999) whereas mutants of Ssa1 lose [PSI+] (Jung *et al.* 2000). Detailed analysis revealed that the phosphorylation state of the bound nucleotide determined if Ssa1 had an inhibitory or a supporting effect on [PSI+], demonstrating the important influence of co-chaperones on yeast prion propagation (Jones *et al.* 2004). These data point to

the important intimate interaction of chaperones with each other as well as with their nucleotide exchange factors when interacting with prions.

II.D.4 YEAST PRION VARIANTS AND THE SPECIES BARRIER

A characteristic feature of mammalian prions is the existence of different strains. Yeast prions can also exist as distinct heritable states generally referred to as ´variants` as in yeast the term strain is reserved to distinguish different genetic backgrounds. Fungal prion variants were discovered during experiments on the *de novo* induction of [PSI$^+$] by over-expression of Sup35p (Chernoff *et al.* 1993; Derkatch *et al.* 1996). Yeast prion variants differ in a range of properties like the strength of the associated phenotype (Derkatch *et al.* 1996; Bradley *et al.* 2002), the mitotic stability, and the dependence on molecular chaperones (Kushnirov *et al.* 2000). Yeast prion variants appear to be determined by different amyloid structures of the respective yeast prion proteins. Indeed, it has recently been shown that recombinant NM is able to form multiple distinct fiber types that differ in kinetics (e.g., growth polarity and elongation rate) and seeding specificity (DePace & Weissman 2002). When transformed into yeast, they gave rise to several distinct and heritable traits (DePace & Weissman 2002; Tanaka *et al.* 2004; King & Diaz-Avalos 2004), strongly arguing that conformational variations in the prion protein conformers are the basis for prion strains. A phenomenon similar to the species barrier accounting for the inefficient interspecies transmission of mammalian prions, has been shown for [PSI$^+$] variants of *S. cerevisiae* and *C. albicans* (Chien & Weissman 2001; Chien *et al.* 2003). This elegant work by J. Weissman and co-workers revealed that different conformations of a single polypeptide can determine the specificity of prion propagation and that point mutations are able to create an artificial species barrier by altering the spectrum of possible structures that the respective protein can adopt. Furthermore, they could show that a chimeric protein that harbors sequences of two normally incompatible prion proteins was able to be seeded by the prion forms of both proteins (**Figure 18**), favoring the notion that the species barrier is a variant-specific phenomenon (Collinge & Clarke 2007; Wickner *et al.* 2007).
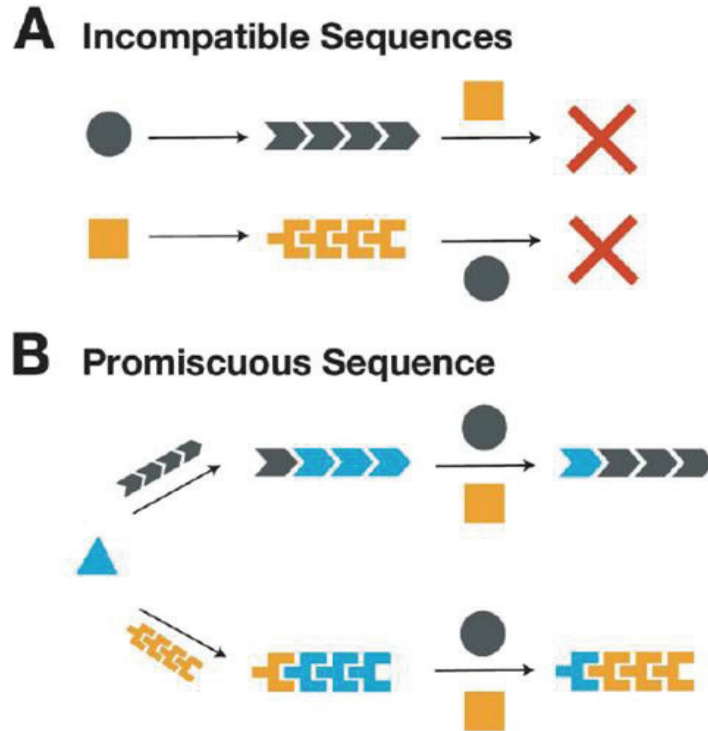
Figure 18. Model to explain the relationship of species barrier and conformation. A: Incompatible conformations of two variants of the prion protein lead to an unbreakable transmission barrier. **B**: If a single amino acid sequence is able to convert into two different structures it can be seeded successfully by two otherwise incompatible prions. From (Chien *et al.* 2004).

II.E SIMILARITIES AND DIFFERENCES BETWEEN MAMMALIAN PRP AND YEAST SUP35P

Sup35p and PrP display no amino acid identity, but the amino-termini of Sup35p and PrP exhibit an unusually high degree of flexibility. Both Sup35p and PrP in their prion states appear to assemble into self-propagating and infectious amyloid fibrils with typical characteristics like PK resistance and detergent insolubility (Patino *et al.* 1996; Paushkin *et al.* 1996; Prusiner 1998a; Wickner *et al.* 2000). Distinct amyloidogenic structures are likely associated with phenotypically distinct prion strains (Chien & Weissman 2001; Clarke *et al.* 2001). Furthermore, structural differences of normal host prion protein and donor prion variant seem to account for a transmission barrier (Collinge & Clarke 2007; Wickner *et al.* 2007). The exact prion-determining elements in PrP remain obscure. In Sup35p, the carboxyl-terminal domain confers the translational termination activity (Chernoff 2004; Ross *et al.* 2005), while the prion status of the protein is governed by the PRD. Thus, the N region

is indispensable for the conformational alteration and polymerization and comprises an oligopeptide repeat region. Oligopeptide repeats are also present in the amino-terminus of PrP. In both cases, oligopeptide repeats can significantly modulate spontaneous prion formation (Prusiner & Scott 1997; Chiesa *et al.* 1998; Liu & Lindquist 1999). Interestingly, recent findings demonstrate that Sup35p oligopeptide repeats can be replaced by PrP repeats, yielding a prion competent molecule (Dong *et al.* 2007). Unlike PrP, Sup35p N additionally contains a Q/N-rich stretch reminiscent of polyQ stretches involved in protein misfolding diseases such as Huntington's disease that critically affect aggregation propensities of Sup35p. Over-expression of N is sufficient to induce the appearance of the [PSI$^+$] phenotype in yeast (Derkatch *et al.* 1996). As aforementioned, the propagation of all known yeast prions depends on the disaggregating activity of Hsp104. Furthermore, several additional chaperones have been identified that modulate yeast prion formation (Jones & Tuite 2005). Unlike in yeast, very little is known about additional co-factors critical for prion induction and propagation in mammals.

An important difference in yeast and mammalian prion biogenesis is the cellular location of prion formation. The Sup35p prion isoform [PSI$^+$] is present in the yeast cytosol. As PrP is attached to the outer leaflet of the membrane via a GPI moiety, conversion to PrP^{Sc} is believed to occur either on the cell surface or along the early endocytic pathway (Caughey & Baron 2006). Elegant experiments have, however, recently demonstrated that GPI anchorage is dispensable for mammalian prion formation (Chesebro *et al.* 2005). Furthermore, aggregated PrP has been shown in the cytosol of mammalian cells (Drisaldi *et al.* 2003; Heller *et al.* 2003; Yedidia *et al.* 2001; Orsi *et al.* 2006). In fact, a prion-like propagation for cytosolic PrP aggregates has been proposed (Ma 2002, Ma and Lindquist, 2002). Thus, while it is unknown if cytosolic PrP assembles into ordered structures with amyloid-like characteristics, these findings clearly demonstrate that the ability of PrP to aggregate is not restricted to the extracellular space or organelle compartments. A summary of similar and different properties of mammalian PrP^{Sc} and yeast Sup35p [PSI$^+$] is given in **Table 4**.

Table 4. Overview of similarities and differences between yeast Sup35p [PSI$^+$] and mammalian PrP^{Sc}.

	PrP^{Sc}	Yeast Sup35p [PSI$^+$]
Function of soluble protein in the non-prion state	Exact function unknown	Translation release factor
Phenotype associated with the prion state of the protein	Pathogenic	Epigenetic factor [PSI$^+$]; suppression of nonsense mutation
Localization	Membrane	Cytoplasm
Co-factor for propagon formation	Unknown	Hsp104
Q/N rich region	No	Yes
Infectivity	Yes	
Species barrier	Yes	
Prion strains	Yes	
Oligopeptide repeat	Yes	
Structure	α-helix → β-sheet	
Partial protease resistance	Yes	
Fiber formation *in vitro*	Yes	
Aggregation *in vivo*	Yes	

II.F YEAST PRIONS AS A MODEL SYSTEM FOR PRION RESEARCH

Several striking similarities between mammalian and yeast prions make the well characterized yeast prion Sup35p an attractive model to elucidate basic mechanisms of prion biogenesis and assembly of aggregation-prone proteins in general (Bousset & Melki 2002; Chernoff 2004; Ross *et al.* 2005; Sigurdson *et al.* 2005). Additionally, yeast prions have proven invaluable in exploring basic mechanisms of prion formation and strain diversity that are also amenable to mammalian prions (Chien & Weissman 2001; Collinge & Clarke 2007; Wickner *et al.* 2007). Sup35p is able to form amyloid fibrils *in vitro* under physiological conditions providing an important tool for studying fundamental aspects of amyloid fibrillization (Scheibel 2004). Undisputable advantages of investigating yeast prions are that they are not pathogenic making *in vivo* studies much easier. Moreover, high-throughput screens for anti-prion compounds are much more tractable and several drugs identified in yeast prion screens were shown to be able to cure mammalian prions, indicating essential common features in mechanisms of yeast and mammalian prion replication (Bach *et al.* 2003; Bach *et al.* 2006; Tribouillard *et al.* 2006).

II.G OBJECTIVE

Striking similarities in the conformational conversion of both proteins make the yeast prion system an interesting model for mammalian prion diseases. The mechanism of mammalian prion replication, the domains in PrP mediating prion assembly and potential co-factors remain elusive. To help unravel several yet unresolved questions in prion disease research comparative analysis of both, yeast Sup35p and mouse prion proteins should be performed. The expression of chimeric proteins of mouse PrP and Sup35p should gain more insights into structural and environmental requirements for protein aggregation. Therefore, it should be investigated if PrP regions that influence mammalian prion formation (such as the PrP aa residues 23-120) can compensate for deletions of the prion domain N in Sup35p. Furthermore, it should be tested if the prion determining regions Sup35p-N and Sup35p-NM are capable of influencing aggregate formation by fusing to the structured domain of mouse PrP (aa 90-230) in order to learn more about the structural driving force for conformational conversion. A well established and in the prion field widely used mouse neuroblastoma cell

line (N2a) model was chosen for the investigations. Diverse other cell lines, like the hippocampal PrP$^{0/0}$ line HpL3-4 and the African green monkey kidney fibroblast-like line COS-7 were used to elucidate cell type specific differences.

Another aim of this study was to investigate the aggregation propensity of ectopically expressed Sup35-NM in N2a cells. First, it should be explored if Sup35p aggregate formation could be induced in mammalian cells by providing appropriate seeds like polyQ protein aggregates or recombinant Sup35p-NM fibrils. Furthermore, potential prion-like properties of NM aggregates should be investigated. Next, we wanted to test if there is a need for additional co-factors for Sup35p-NM aggregate formation and propagation in the mammalian cytosol. Moreover, we aimed to address the question if different Sup35p-NM variants exist in N2a cells. These investigations should shed light on general aspects of prion (variant) formation and propagation and should help to unravel prion propagation mechanisms that are conserved from yeast to mammals.

III. MATERIALS AND METHODS

III.A MATERIALS

III.A.1 CHEMICALS

3-[4,5 dimethylthiazol-2-yl]-2,5-diphenyl tetrazolium bromide (MTT)	Sigma-Aldrich, Steinheim
Agarose	Invitrogen, Karlsruhe
Ammonium peroxodisulfate	Roth, Karlsruhe
Bacillol Plus	Roth, Karlsruhe
Bacto Agar	Becton Dickinson, Heidelberg
Bromphenole blue	Merck, Darmstadt
β-Mercaptoethanol	Sigma-Aldrich, Steinheim
Calcium chloride ($CaCl_2$)	Roth, Karlsruhe
Dimethylsulfoxide	Sigma-Aldrich, Steinheim
Ethanol p. a. 99 %	Roth, Karlsruhe
Ethidium bromide solution (10 mg/ml)	Invitrogen, Karlsruhe
Ethylen diamine tetraacetate, sodium salt (EDTA)	Roth, Karlsruhe
Gelatine 40 % solution	Sigma-Aldrich, Steinheim
Glucose	Sigma-Aldrich, Steinheim
Glycerol	Roth, Karlsruhe
Glycine	Roth, Karlsruhe
Guanidine isothiocyanate (GnSCN)	Roth, Karlsruhe
HCl 37 % (w/w)	Roth, Karlsruhe
Hexadimethrine bromid (Polybrene)	Sigma-Aldrich, Steinheim
Hoechst 33342, trihydrochloride, trihydrate	Sigma-Aldrich, Steinheim
Hybond-P PVDF membrane	GE Healthcare, Freiburg
Isopropanol p. a.	Roth, Karlsruhe
Lactacystin	Calbiochem, San Diego, CA, USA
Lipopolysaccharide	Sigma-Aldrich, Steinheim
Magnesium chloride	Sigma-Aldrich, Steinheim
Magnesium sulfate	Sigma-Aldrich, Steinheim

Methanol p. a.	Roth, Karlsruhe
Natrium chloride	Roth, Karlsruhe
Nocodazole (M1404)	Sigma-Aldrich, Steinheim
N,N,N',N'-Tetramethylenediamine (TEMED)	Sigma-Aldrich, Steinheim
Pefabloc SC	Roche, Mannheim
Permafluor	Beckmann Coulter, Marseille, France
Phosphate buffered saline (PBS)	Invitrogen, Karlsruhe
Potassium chloride (KCl)	Sigma-Aldrich, Karlsruhe
Protogel Ultra Pure 30 %,	
Acrylamide: Bisacrylamide 37,5:1	National Diagnostics; Atlanta, USA
Roti-Histofix	Roth, Karlsruhe
Saponin	Roth, Karlsruhe
Skim milk powder	Merck, Darmstadt
Sodium chloride (NaCl)	Roth, Karlsruhe
Sodium deoxycholate (DOC)	Roth, Karlsruhe
Sodium dodecylsulfate (SDS)	Roth, Karlsruhe
Sodium hydroxide	Roth, Karlsruhe
Tris-hydroxy-methyl-aminomethan (Tris)	Roth, Karlsruhe
Triton X-100	Sigma-Aldrich, Steinheim
Tryptone	Becton Dickinson, Heidelberg
Tween-20	Roth, Karlsruhe
X-ray films Kodak Biomax MS	Sigma-Aldrich, Steinheim
Yeast extract	Becton Dickinson, Heidelberg
7-AminoActinomycin D (7-AAD)	Becton Dickinson, Heidelberg

III.A.2 BUFFERS AND SOLUTIONS

Buffers and solutions are listed in their applied concentration in the context of the described methods.

III.A.3 ANTIBIOTICS

Ampicillin (Amp)   Sigma-Aldrich, Steinheim

Kanamycin (Kan)   Sigma-Aldrich, Steinheim

III.A.4 ENZYMES

Benzonase   Sigma-Aldrich, Steinheim

DNA polymerase Pfu Turbo   Stratagene, Heidelberg

Proteinase K (PK)   Roth, Karlsruhe

T4 DNA ligase (1U/µl)   Invitrogen, Karlsruhe

Trypsin-EDTA   Invitrogen, Karlsruhe

III.A.5 ANTIBODIES

Table 5. Antibodies used in this work (IF: immunofluorescence; WB: Western blot; FACS: fluorescence activated cell sorting; HRP: horseradish peroxidase).

Primary antibody	Source and Reference	Specifity	Application	Dilution
3F4	Mouse monoclonal, provided by Dr. Suzette A. Priola (Rocky Mountain Laboratories, NIH, Hamilton, MT, USA)	Epitope in Syrian hamster and human PrP; aa 109-112 (MKHM)	WB IF FACS	1:5000 1:100 1:100
Anti-hemagglutinin (HA) (F-7)	Mouse monoclonal (Santa Cruz Biotechnology, Santa Cruz, CA, USA)	Epitope of hemagglutinin (YPYDYPDYA)	WB IF FACS	1:1000 1:50 1:50

4H11	Mouse monoclonal (Ertmer *et al.* 2004)	PrP of various species, including mouse and hamster; no linear epitope defined	WB IF FACS	1:1000 1:10 1:10
L42	Mouse monoclonal, provided by Dr. Groschup, INNT, Greifswald (Vorberg *et al.* 1999)	Sheep PrP (aa 145-163)	WB	1:10
A7	Rabbit polyclonal (Gilch *et al.* 2003)	PrP of various species, including mouse and hamster	WB	1:5000
Anti-GFP	Rabbit polyclonal (Santa Cruz Biotechnology, Santa Cruz, CA, USA)	Green fluorescent protein (GFP)	WB	1:5000
Anti-vimetin (H-84)	Rabbit polyclonal (Santa Cruz Biotechnology, Santa Cruz, CA, USA)	Human and mouse vimentin (aa 1-84)	IF	1:100
Anti-γ-tubulin (GTU-88)	Mouse monoclonal (Sigma-Aldrich, Steinheim)	Human and mouse γ-tubulin (aa 38-53)	IF	1:100
Anti-CD107a (LAMP-1)	Rat monoclonal (BD Pharmingen, Heidelberg)	Mouse CD-107a (LAMP-1)	IF	1:100
4A5 (hybridoma supernatant)	Rat monoclonal, provided by Dr. Kremmer, Helmholtz Zentrum, Munich	M domain of Sup35p (aa 229-247)	IF	1:2
7H5 (hybridoma supernatant)	Rat monoclonal, provided by Dr. Kremmer, Helmholtz Zentrum, Munich (Krammer *et al.* 2008b)	N domain of Sup35p (aa 8-27)	WB IF	1:10 1:2

| POM2 | Mouse monoclonal, provided by Prof. Aguzzi, Institute of Neuropathology, University of Zürich (Polymenidou *et al.* 2005) | Octarepeat region of PrP (aa 58–64, 66–72, 74–80, 82–88; QPXXGG/SW) | IF | 1:100 |
| | | | WB | 1:10.000 |

Secondary antibody	Source	Specifity	Application	Dilution
HRP-conj. anti-IgG	Sheep (GE Healthcare, Freiburg)	Mouse IgG	WB	1:7500
HRP-conj. anti-IgG	Donkey (GE Healthcare, Freiburg)	Rabbit IgG	WB	1:7500
HRP-conj. anti-IgG	Goat (GE Healthcare, Freiburg)	Rat IgG	WB	1:5000
Cy2-conj. anti-IgG	Donkey (Dianova, Hamburg)	Mouse IgG	IF	1:100
			FACS	1:100
Cy2-conj. anti-IgG	Donkey (Dianova, Hamburg)	Rabbit IgG	IF	1:100
Cy3-conj. anti-IgG	Donkey (Dianova, Hamburg)	Mouse IgG	IF	1:400
Cy3-conj. anti-IgG	Donkey (Dianova, Hamburg)	Rabbit IgG	IF	1:400
Cy3-conj. anti-IgG	Donkey (Dianova, Hamburg)	Rat IgG	IF	1:400

III.A.6 PLASMID GENERATION

A plasmid coding for a 3F4-tagged mouse PrP (described in (Nunziante *et al.* 2003)) was used as a template for the generation of PrP fragments. Fragments coding for Sup35p domains N, M or NM were amplified using the pJC25-NM expression vector as a template (Scheibel *et al.* 2001). For transient mammalian expression, DNA fragments were cloned into the pcDNA3.1/Zeo expression vector (Invitrogen, Karlsruhe). For stable transduction, NM-HA coding sequences were subcloned into the retroviral vector pSFF (Mann *et al.* 1983;

Miller & Buttimore 1986) as well as into the lentiviral vector LV-PGK-EGFP, containing a phosphoglycerate kinase (PGK) promoter driven EGFP expression cassette (Follenzi *et al.* 2000; Hofmann *et al.* 2003), by replacing the EGFP coding sequence. All constructs were confirmed by DNA sequencing, performed by GATC (Konstanz).

The vector pEGFP-HD72Q (Sittler *et al.* 2001) coding for the huntingtin (htt) exon 1 protein with a polyQ stretch of 72 glutamines was a kind gift of Dr. Erich Wanker (Max Delbrück Center of Molecular Medicine, Berlin). A plasmid coding for Rab4 was kindly provided by M. McCaffrey (University College Cork, Ireland). The ORF of Rab4 was cloned into pcDNA3.1/NT-GFP-TOPO by Gloria Lutzny (Institute of Virology). The vector pEGFP-C1-Rab11 was obtained from D.L. Marks and R.E. Pagano (Mayo Clinic, Rochester, MN, USA). Plasmids were propagated in *E. coli* XL-1 Blue *(sup*E44*, hsd*R17, *end*A1, *rec*A1, *end*A1, *gyr*A46, thi-1, relA1, lac⁻, F`[proABlacl^q, lacZΔM15, Tn 10(ter^R)]) (Stratagene, La Jolla, CA, USA).

III.A.7 OLIGODEOXYNUCLEOTIDES

Primers designed in this work were tested for specificity by BLAST analysis and purchased from Metabion (Martinsried). Oligodeoxynucleotides were synthesized, desalted and purified by HPLC (high performance liquid chromatography). Lyophilized primers were reconstituted in $H_2O_{dest.}$ to a final concentration of 10 µM.

Table 6. Oligodeoxynucleotides used in this work.

Name	Sequence (5' - 3')
PCR primers	
TS 2	ATA TTG AAT TCA ACT TCG TCA TCC ACT TCT TC
TS 3	ATA AAG AAT TCA CCT TGA GAC TGT GGT TG
TS 5	ATA TTG AAT TCA TGT CTT TGA ACG ACT TCC AGG
TS 9	TAA AGG ATC CGT CGC CAC CAT GTC CGA TTC AAA CCA AGG
IV 1	TGG AGA ATT CCA AGG AGG GGG TAC CCA TAA TCA

	GTG G
IV 2	TAA AGC GGC CGC TTA TCA GGA TCT TCT CCC GTC GTA ATA GG
IV 5	TAC CGA ATT CTA CTG CCC CAG CTG CCG CAG CCC CTG C
IV 6	ATC TGG ATC CGT CGC CAC CAT GAA AAA GCG GCC AAA GC
K4-dGFP-rev	GAA TTC TCA AAC TTC GTC ATC CAC
M-PrPfwd	CGC GGA TCC GTC GCC ACC ATG TCT TTG AAC GAC TTT CAA AAG
NM-HA-fw	CGC GGA TCC GTC GCC ACC ATG TCG GAT TCA AAC CAA GGC
NM-HA-rev	GGA ATT CTC AAG CGT AAT CTG GTA CGT CGT ATG GGT AAA CTT CGT CAT CCA
Lenti-HA-rev	ACG TCG ACT CAA GCG TAA TCT GGT ACG TCG TAT GG
Cyto-PrP-re	CCG GAA TTC TCA GGA TCT TCT CCC GTC GTA ATA GGC
PrP90fwd	CGC GGA TCC GTC GCC ACC ATG CAA GGA GGG GGT ACC CAT AAT CAG TGG

Sequencing primers

pSSF-seq	GTA CCT CAC CCT TTC GAG TCG GG
pSSF-seq-rev	CAC AAA GAG TGC AGC AG
pGK-seq-fw	GTG TTC CGC ATT CTG CAA G
pGK-seq-rev	CAA AGG CAT TAA AGC AGC G
pcDNA 3.1+*	CTA TAT AAG CAG AGC TCT C
T7*	TAA TAC GAC TCA CTA TAG GG

* provided by GATC (Konstanz) that performed all sequencing analysis

III.A.8 EUCARYOTIC CELL LINES

Table 7. Eucaryotic cell lines used in this work.

Cell line	Description	Source or reference
N2a	murine neuroblastoma line	ATCC CCL 131 (Butler *et al.* 1988)
HpL3-4	Hippocampal line derived from PrP$^{-/-}$ mice	(Kuwahara *et al.* 1999)
HpLMoPrPL42	HpL3-4 cells ectopically expressing L42 antibody-epitope tagged mouse PrP	Generated by Elke Maas, unpublished
COS-7	African green monkey kidney fibroblast-like cell line	ATCC CRL-1651
PSI2 (Ψ2)	Packaging cell line for retrovirus production; derived from NIH/3T3 TK cells	(Mann *et al.* 1983)
PA317	Packaging cell line for retrovirus production; derived from NIH/3T3 TK cells	ATCC CRL-9078 (Miller & Buttimore 1986)

III.A.9 CELL CULTURE MEDIA AND SUPPLEMENTS

OptiMEM with Glutamax	Invitrogen, Karlsruhe
D-MEM with Glutamax	Invitrogen, Karlsruhe
RPMI 1680	Invitrogen, Karlsruhe
Fetal bovine serum (FCS)	Invitrogen, Karlsruhe
Penicillin/Streptomycin	Invitrogen, Karlsruhe

III.A.10 KITS

Bradford protein assay	Pierce, Bonn, Germany

ECL Plus	GE Healthcare, Freiburg
Fugene 6 Transfection Kit	Roche, Mannheim
GFX PCR DNA and Gel Band Purification Kit	GE Healthcare, Freiburg
GFX Micro Plasmid Prep Kit	GE Healthcare, Freiburg
Lipofectamine 2000	Invitrogen, Karlsruhe
Plasmid Maxi Kit	Qiagen, Hilden
Zero Blunt TOPO PCR Cloning Kit	Invitrogen, Karlsruhe

III.A.11 INSTRUMENTS AND ACCESSORIES

Autoclave V95	Systec, Wettenberg
Fuchs-Rosenthal Hemocytometer	Roth, Karlsruhe
CO_2 Incubator	Heraeus, Hanau
Centrifuges:	
Eppendorf 5417C	Eppendorf-Nethaler-Hinz, Köln
Sigma 4K15	Sigma-Aldrich, Schnelldorf
Beckmann Avanti	Beckmann Coulter, Krefeld
Beckmann TL-100 ultracentrifuge	Beckmann Coulter, Krefeld
Coverslips and slides	Marienfeld, Bad Mergentheim
Cryotubes	Corning Inc., Corning, NY, USA
Electrophoresis Power Supply	Pharmacia Biotech, Sweden
Electrophoresis Power Supply	Consort, Turnhout, Begium
Eppendorf tubes (0.2, 1.5 or 2 ml)	Eppendorf-Nethaler-Hinz, Köln
FACS- polystyrene tubes	Becton Dickinson, Heidelberg
Falcon tubes (15 or 50 ml)	Falcon, Le Pont de Claix, France
Flow cytometer EPICS XL	Beckmann Coulter, Krefeld
Hybond-P PVDF membrane	GE Healthcare, Freiburg
Microscopes:	
Axiovert 40C	Carl Zeiss Jena, Göttingen
Axiovert 200M	Carl Zeiss Jena, Göttingen
LSM510 confocal laser microscope	Carl Zeiss Jena, Göttingen
Midi protein gel chamber	Peqlab Biotechnologie, Erlangen
Optimax X-Ray film processor	PROTEC Medizintechnik, Oberestenfeld

pH-Meter	WTW, Weilheim
Pipets (0.5-10 µl, 10-100 µl, 100-1000 µl)	Eppendorf-Nethaler-Hinz, Köln
Pipet tips	
SafeSeal-Tips (20 µl, 100 µl, 1000 µl)	Biozym, Vienna, Austria
Stripette (5 ml, 10 ml, 25 ml)	Corning, Corning, NY, USA
Pipetus	Hirschmann Laborgeräte, Eberstadt
Power Supply	GE Healthcare, Freiburg
Sonifier	MSE Scientific Instruments, Crawley, Sussex, U.K.
Spectrophotometer	GE Healthcare, Freiburg
Sunrise ELISA Reader	Tecan, Maennedorf, Switzerland
Thermocycler GeneAmp PCR System 9700	Applied Biosystems, Foster City, CA USA
Thermomixer compact	Eppendorf-Nethaler-Hinz, Köln
Tissue culture dishes and plates	Falcon, Le Pont de Claix, France
Trans-Blot SD Semi-dry Transfer Cell	Biorad Laboratories, Munich
ECL Semi-Dry Transfer unit (TE77)	GE Healthcare, Freiburg
Vortex Mixer	NeoLab Migge, Heidelberg
Waterbath	GFL, Burgewede
Whatman paper	Schleicher & Schüll, Dassel

III.B METHODS

III.B.1 BIOLOGICAL SAFETY

Genetical engineering of organisms was accomplished under biosafety level 2 according to the Genoa genetic engineering law of 01.01.2004. Biologically contaminated materials and solutions were collected separately and inactivated according to the lab operating instructions. Inactivation of prions is subject to special regulations. Solutions were incubated with 1 M NaOH for 24 hours. Both liquid and solid prion waste were autoclaved for 60 min at 134° C and 3 bar.

III.B.2 MOLECULAR BIOLOGICAL METHODS

III.B.2.1 Polymerase chain reaction (PCR)

The polymerase chain reaction is an enzymatic procedure for *in vitro* amplification of defined nucleic acid segments through a cyclic repetition of the following steps:

Denaturation: heat denaturation of the template DNA

Annealing: hybridization of oligonucleotides (primers) to a complement target sequence

Elongation: Elongation of primer by a thermo-tolerant polymerase

The annealing temperature is calculated on the basis of the dissociation temperatures of the primers used in the reaction (Suggs *et al.* 1981):

$$T_D\,[°C] = 2 \cdot (A+T) + 4 \cdot (C+G)$$

(A, C, G, T: number of the respective nucleotides)

The elongation time depends on the PCR product length and on the used polymerase (approx. 1 min per 1.5 kb).

Buffers and Solutions:

Oligonucleotides	Metabion, Martinsried
10x PCR reaction buffer	Stratagene, Heidelberg
Desoxinucleotides (dNTPs)	
(1mM each dATP, dTTP, dGTP, dCTP)	GE Healthcare, Freiburg

Reaction mix:

10 %(v/v) (5 µl)	10x PCR reaction buffer
50 µM (2 µl)	dNTP mix
10 µM (2 µl)	of each primer
50-200 ng (1 µl)	template DNA
10 U (1 µl)	Pfu Turbo DNA polymerase
Up to 50 µl	$H_2O_{bidest.}$

Components were added to a 0.2 ml tube and the reaction was carried out in a GeneAmp PCR System 9700 thermo cycler as follows:

Amplification parameters:

Function	temperature	time	
Initial denaturation	95° C	5 min	
Denaturation	95° C	1 min	
Annealing	x° C	45 s	35 Cycles
Elongation	72° C	y s	
Final Elongation	72° C	7 min	

x: calculated annealing temperature for primer pairs (see above)
y: approx. 1 min per 1.5 bp (see above)

PCR products were stored at 4 °C and subsequently separated via agarose gel electrophoresis (*III.B.2.2*) for size determination and purificaton.

III.B.2.2 Agarose gel electrophoresis (AGE)

Buffers and Solutions:

TAE buffer (1x)	40 mM Tris-Acetate
1 mM EDTA; pH 8.0	
DNA loading buffer (5x)	50 % glycerol in TAE-buffer
	0.05 % bromphenol blue
2-log DNA ladder	1.5 µl of 1:1 dilution in 5x DNA loading buffer
	(New England Biolabs, Schwalbach)

For a horizontal 1-2 % agarose gel, 0.5-1 g agarose was boiled in 50 ml TAE. After cooling 1.5 µl ethidium bromide (EtBr) was added and the solution was poured into a gel chamber arranged with a comp. The gel was transferred into an electrophoresis chamber and overlaid with 1x TAE buffer. The PCR products (*III.B.2.1*) were mixed with an adequate volume of the 5 x loading buffer and loaded into the wells. Electrophoretic separation was accomplished at 110 V for 30 min. DNA fragments were visualized under UV-light due to staining with

EtBr which intercalates between the DNA strands. Sizes of PCR products were estimated by comparison with the 2-log DNA ladder as a reference size standard.

III.B.2.3 Elution of DNA fragments from agarose gels

Exact PCR products (*III.B.2.1*) were excised from agarose gels (*III.B.2.2*) and extracted using the GFX PCR DNA and Gel Band Purification Kit according to the manufacturer's protocol. DNA samples were eluted with 30 µl $H_2O_{bidest.}$.

III.B.2.4 TOPO cloning

The Zero Blunt TOPO PCR Cloning Kit was used to insert blunt end PCR products (III.B.2.1) directly into the plasmid vector pCR-BluntII-TOPO. The reaction was carried out according to the manufacturer's instruction (III.A.10).

III.B.2.5 Enzymatic digestion of plasmid DNA

Restriction endonucleases:

Name	cleavage site (5'-3')
BamHI	G↓GATCC
EcoRI	G↓AATTC
NotI	GC↓GGCCGC
SalI	G↓TCGAC

Buffers and Solutions:

10x reaction buffer

100x BSA

All components were obtained from New England Biolabs (Schwalbach) or Roche (Mannheim).

Reaction mix:

5 μg	Plasmid DNA
1x (5 μl)	10x reaction buffer
1x (5 μl)	10x BSA (optional)
10 U (1 μl)	each restriction endonuclease
Up to 50 μl $H_2O_{dest.}$	

Reactions were incubated at least for 2 h at 37 °C. Buffers were chosen as recommended by the manufacturer. This method was used in order to generate DNA fragments from plasmid DNA (*III.A.6*) or PCR products (*III.B.2.1*) with defined 5' and 3' ends according to the applied restriction enzyme for subsequent specific ligation reactions. To verify a correct ligation reaction (*III.B.2.6*) purified plasmid DNA was subjected to an analytic restriction digests. Thereby, only 16 μl of eluted plasmid was used together with the respective smaller amounts of the other components.

III.B.2.6 DNA ligation

Buffers and solutions:

5x T4 ligase buffer	Invitrogen, Karlsruhe
T4 DNA ligase (1U/μl)	Invitrogen, Karlsruhe

Reaction mix:

Approx. 1 μl	vector DNA
Approx. 7 μl	PCR product
1x (3 μl)	5x T4 ligase buffer
1 U (1 μl)	T4 DNA ligase
Up to 15 μl $H_2O_{dest.}$	

A molar ratio of 1:3 to 1:8 of vector (*III.A.6*) and insert DNA (*III.B.2.1*) was mixed with buffer and ligase and incubated over night in a water bath at 14 °C. T4 DNA ligase catalyzes the formation of ATP-dependent phosphodiester bonds between compatible 3'-hydroxyl and 5'-phosphate ends. Therefore, it was used to generate recombinant plasmids of a DNA

fragment and a target vector. The recombinant plasmid was stored at -20°C or subsequently transformed into chemically competent bacteria (*III.B.2.7*).

III.B.2.7 Preparation of chemically competent E. coli

Media and solutions:

Luria-Bertani-(LB) medium	1 % (w/v) (10 g/l)	Bacto Tryptone
	0.5 % (w/v) (5 g/l)	Bacto Yeast extract
	1 % (w/v) (10 g/l)	NaCl
	Up to 1l $H_2O_{dest.}$	

| $MgCl_2$ solution | 100 mM in $H_2O_{dest.}$ |
| $CaCl_2$ solution | 100 mM in $H_2O_{dest.}$ |

A single colony of *E. coli* XL1 Blue (*III.A.6*) was transferred to 5 ml LB medium without antibiotics and incubated over night at 37 °C with constant shaking (180 rpm). The next day, 1 ml of this culture was transferred to 100 ml LB medium and further cultivated at 37 °C with shaking. After the solution had reached an optical density measured at a wavelength (λ) of 600 nm (OD_{600}) of 0.6-0.8, cells were cooled on ice for 10 min prior to sedimentation at 3500 rpm (Sigma 4K15 centrifuge) at 4°C. The pellet was resuspended in 50 ml ice cold sterile $MgCl_2$ solution (100 mM) and incubated for 30 min on ice before the centrifugation step was repeated. The supernatant was discarded and bacteria were resuspended in ice cold sterile $CaCl_2$ solution (100 mM), chilled on ice for 30 min and centrifuged as described above. The cell pellet was resuspended in 2 ml ice cold 100 mM $CaCl_2$ solution and incubated for 24 h on ice. Finally, after addition of 2.5 ml sterile ice cold $CaCl_2$ solution and 0.5 ml glycerol, 100 µl aliquots in 1.5 ml Eppendorf tubes were prepared and immediately frozen at -80 °C.

III.B.2.8 Transformation of E. coli with plasmid DNA

<u>Media:</u>

SOC medium:	2 % (w/v) (20 g/l)	Bacto Tryptone
	0.5 % (w/v) (5 g/l)	Bacto Yeast extract
	10 mM	NaCl
	2.5 mM	KCl
	2 mM	$MgCl_2$
	10 mM	$MgSO_2$
	20 mM	Glucose
		in $H_2O_{dest.}$
LB-agar	1 % (w/v) (10 g/l)	Bacto Tryptone
	0.5 % (w/v) (5 g/l)	Bacto Yeast extract
	1 % (w/v) (10 g/l)	NaCl
	1.5 % (w/v) (15 g/l)	Bacto Agar
	Up to 1l $H_2O_{dest.}$	

One aliquot (50-100 µl) of chemically competent bacteria (*III.B.2.7*) was thawed on ice, and 1 µl of plasmid DNA (*III.A.6*) or 2-6 µl ligation mix (*III.B.2.6*) were added and incubated on ice for 30 min. Immediately after a heat shock of 45 s at 42 °C in a water bath, cells were cooled on ice for 2 min. Addition of 400 µl pre-warmed SOC medium was followed by an incubation step at 37 °C with constant shaking (180 rpm) for 1 h. For selection of transformants adequate volumes (approx. 200-400 µl) of the transformation reaction were plated on LB agar plates containing the appropriate antibiotics (50 µg/ml ampicillin or 50 µg/ml kanamycin) and incubated over night at 37 °C.

III.B.2.9 Isolation of plasmid DNA

III.B.2.9.1 Miniprep
Isolation of plasmid DNA from transformed bacterial cells was achieved using the GFX Micro Plasmid Prep Kit (*III.A.10*) according to the manufacturer's instructions. The purified DNA was eluted in 100 µl autoclaved $H_2O_{dest.}$.

III.B.2.9.2 Maxiprep
To isolate high-copy plasmid DNA in a preparative scale the Qiagen Plasmid Maxi Kit (*III.A.10*) was used according to the manufacturer's instructions. Eluted DNA was precipitated in 0.7 volumes of isopropanol and desalted with 70 % ethanol. Air-dried DNA pellets were redissolved in sterile 200-400 µl $H_2O_{dest.}$.

III.B.2.10 Quantification of nucleic acid

Concentration of DNA was determined by measuring the absorbance at a wave length of 260 nm using a spectrophotometer (GE Healthcare). If diluted in $H_2O_{dest.}$, an absorbance of 1 for a double-stranded (ds) DNA preparation corresponds to 50 µg/ml DNA. The amount of DNA in a sample was calculated according to the Beer-Lambert equation:

$A = \varepsilon \cdot c \cdot l$ A = absorbance (OD unit)

ε = molar extinction coefficient $((\mu g/ml)^{-1} \, cm^{-1})$

$[\varepsilon_{(dsDNA)} = 0.020 \, (\mu g/ml)^{-1} cm^{-1}]$

c = concentration (µg/ml)

l = path length (cm)

As aromatic amino acids, especially tryptophane, have their absorption maximum at OD_{280}, the values at 280 nm were determined to estimate the protein content in the solution. The DNA sample was considered pure if the ratio of OD_{260}/OD_{280} was 1.8 or higher.

III.B.3 PROTEIN BIOCHEMICAL METHODS

III.B.3.1 Preparation of cell lysates from mammalian cells

III.B.3.1.1 Preparation of postnuclear lysates

Buffers and solutions:

Lysis buffer

100 mM NaCl

10 mM Tris-HCl, pH 7.5

10 mM EDTA

0.5 % Triton X-100

0.5 % DOC

In $H_2O_{dest.}$

TNE buffer

50 mM Tris-HCl, pH 7.5

5 mM EDTA

150 mM NaCl

In $H_2O_{dest.}$

Prior to addition of 500 µl lysis buffer (average volume for a 6 cm cell culture dish) cells were rinsed twice with 5 ml PBS. After incubation for 10 min, lysates were supplemented with 0.5 mM Pefabloc protease inhibitor (Roche), transferred to 1.5 ml Eppendorf tubes and cleared of cell membranes and nuclei at 1.000 x g (Eppendorf 5417C) at 4 °C for 1 min. The supernatant was either precipitated to gain total protein or subjected to a sedimentation assay (*III.B.3.4*). For precipitation of proteins, lysates were transferred to 15 ml Falcon tubes and the 2.5 - 5 fold volume of methanol was added before the samples were incubated at -20 °C over night. The next day, precipitated proteins were sedimented by centrifugation for 25 min at 3.500 rpm (Sigma 4K15) at 4 °C. Methanol was discarded, and air-dried protein pellets were resuspended in 50-100 µl TNE buffer. Samples were stored at -20 °C prior to analysis by SDS-PAGE (*III.B.3.6*) and Western blot (*III.B.3.7*).

III.B.3.1.2 Cell lysis for Proteinase K (PK) digestion

<u>Buffers and solutions:</u>

Lysis buffer   0.5 % Triton X-100

                                                   0.5 % DOC

                                                   In PBS

Cells were washed twice with 5 ml ice cold PBS and lysed for 10 min in 200 µl lysis buffer (for a 6 cm cell culture dish) on ice followed by a nucleic acid degradation using 75 U benzonase for 30 min at 4 °C. Lysates were cleared of cell debris by centrifugation at 1.000 x g and 4 °C for 1 min and stored at -20 °C or immediately subjected to a proteinase K (PK) digestion (*III.B.3.3*).

III.B.3.2 Determination of protein concentration by Bradford assay

The Bradford assay (Pierce, Bonn) is a spectroscopic method to measure the concentration of proteins in a solution. It is based on the fact that the dye Coomassie shifts from a red form into Coomassie blue by binding to amino acids. Cell lysates (*III.B.3.1.2*) or proteins dissolved in TNE buffer (*III.B.3.1.1 and III.B.3.4*) were diluted 1:10 in water and 5 µl thereof were transferred in duplicate to a 96-well plate. 5 µl of a protein standard dilution series was pipetted onto the plate and 250 µl Bradford reagent was added. The absorbance was measured at 595 nm and the protein concentrations in the samples were calculated according to the values of the protein standards with defined protein concentrations.

III.B.3.3 Proteinase K (PK) digestion

<u>Buffers and solutions:</u>

6 M   GdnSCN in $H_2O_{dest.}$

Lysate aliquots (*III.B.3.1.2*) with comparable protein contents (*III.B.3.2*) were incubated for 30 min at 37 °C with different amounts (5-50 µg/ml) of proteinase K (PK). Proteolysis was terminated by addition of protease inhibitor Pefabloc (Roche). Samples were incubated with 5 M GdnSCN for 1 h at 37 °C with agitation (180 rpm), precipitated with methanol (*III.B.3.1.1*) and analyzed by SDS-PAGE and Western blot (*III.B.3.6 and III.B.3.7*).

III.B.3.4 Sedimentation assay

Cell lysates devoid of cell debris (*III.B.3.1.1*) were transferred to a 1.5 ml Eppendorf tube and insoluble proteins were sedimented at 20.000 x g and 4 °C for 20 min. Soluble proteins in the supernatant were precipitated with methanol as described (*III.B.3.1.1*). Insoluble fractions (pellet) were resuspended in 50-100 µl TNE buffer and stored at -20 °C until further analysis (*III.B.3.6 and III.B.3.7*).

III.B.3.5 Thermal stability assay

Cell lysates (III.B.3.1.1) were centrifuged at 3800 g for 10 min to discard high-molecular weight NM-HA aggregates. Protein contents in the remaining lysate were quantified (III.B.3.2). Lysates were incubated with 1 % SDS at 25, 37, 50, 60, 70 or 99 °C, respectively, for 15 min. Samples were separated using a one-dimensional SDS gel (12,5 %) (III.B.3.6) followed by electrophoretic transfer to PVDF membrane and Western blot analysis (III.B.3.7). Appropriate volumes were loaded according to the expression levels of NM-HA in individual clones to obtain similar amounts of NM-HA on the gel.

III.B.3.6 Sodium dodecyl sulfate-polyacrylamide gel electrophoresis (SDS-PAGE)

Buffers and solutions:

4 x Lower gel solution	1.5 M	Tris-HCl, pH 8.8
	0.4 % (w/v)	SDS
In $H_2O_{dest.}$		
4 x Upper gel solution	0.5 M	Tris-HCl, pH 6.8
	0.4 % (w/v)	SDS
In $H_2O_{dest.}$		
APS stock solution	10 % (w/v)	APS in $H_2O_{dest.}$

3 x SDS sample buffer	90 mM	Tris-HCl, pH 6.8
	7 % (w/v)	SDS
	30 % (v/v)	Glycerol
	17 % (v/v)	2-mercaptoethanol
	0.01 % (w/v)	Bromphenole blue
	In $H_2O_{dest.}$	

10 x SDS electrophoresis buffer	250 mM	Tris
	2.5 M	Glycine
	1 % (w/v)	SDS
	In $H_2O_{dest.}$	

Resolving gel mixture (for two gels)	20.4 ml	$H_2O_{dest.}$
(12.5 % acrylamide)	15.4 ml	Lower gel solution
	25.9 ml	Protogel acrylamid solution
	192 µl	10 % APS
	90 µl	TEMED

Stacking gel mixture (for two gels)	9.9 ml	$H_2O_{dest.}$
(5 % acrylamide)	4.2 ml	Upper gel solution
	2.8 ml	Protogel acrylamid solution
	168 µl	10 % APS
	30 µl	TEMED

High range protein molecular weight marker	GE Healthcare, Freiburg

The appropriate amount of 3 x SDS sample buffer was added to proteins resuspended in TNE buffer (*III.B.3.1, III.B.3.3 and III.B.3.4*) prior to boiling at 99 °C for 10 min and subsequent SDS-PAGE. Proteins are separated on denaturing SDS gels containing 12.5 % acrylamide according to their molecular mass. Different amounts of samples (5-30 µl), containing equal protein concentrations (*III.B.3.2*) were loaded, together with a molecular weight marker (5

µl). Electrophoresis was accomplished under constant current (30 mA per gel) until the tracking dye reached the bottom of the resolving gel.

III.B.3.7 Western blot (Immunoblot)

Buffers and solutions:

Blotting buffer	20 % (v/v)	Methanol
	3 g	Tris
	14.4 g	Glycine
	Up to 1 l $H_2O_{dest.}$	
10 x TBST	100 mM	Tris-HCl, pH 8.0
	100 mM	NaCl
	0.5 % (v/v)	Tween-20
		In $H_2O_{dest.}$
Blocking buffer	5 %	Skim milk powder in 1 x TBST

The Western blot technique allows the detection of proteins separated by SDS-PAGE (*III.B.3.7*) by specific antibodies (*III.A.5*). Transfer of proteins from the polyacrylamide gel onto a PVDF membrane was accomplished by an electrophoretic, semi-dry method. The membrane was activated by a short incubation in methanol and equilibrated in $H_2O_{dest.}$ before being placed on 3 layers of Whatman paper soaked in blotting buffer. The gel was transferred to on the membrane and covered with 3 additional Whatman papers. A current of approx. 125 mA per gel (calculated as follows: size of the gel in m^2 x 0.8 mA) was applied for a period of 1 hour. Afterwards, the membrane was incubated in blocking buffer at room temperature for 30 min. The primary antibody (*III.A.5*) was diluted in 1x TBST buffer, added to the membrane and incubated on a horizontal shaker at 4 °C over night. After five rinsing steps with 1 x TBST for at least 5 min the secondary antibody (*III.A.5*) in 1 x TBST was added for 60 min at room temperature. After additional 5 washing steps the membrane was rinsed in $H_2O_{dest.}$. For detection of antibody-protein complexes, the membrane was briefly dried between two Whatman papers and covered for 3 min with an appropriate mixture of ECL

solutions, prepared according to the manufacturer's instructions. The membrane was dried quickly between two Whatman papers before exposition to X-ray films for signal detection.

III.B.3.8 Band intensity quantification by ImageQuant TL

Signal intensities were quantified using a ScanJet 4100C scanner (HP) and the Image Quant TL software (GE Healthcare). The Chi-Square (X^2) test or the two-way ANOVA with Bonferroni's multiple comparison test were used for statistical analysis.

III.B.3.9 Fibril assembly

Aliquots containing 10 µM purified, bacterially expressed and soluble recombinant Sup35p-NM protein were kindly provided by Michael Suhre (Spider lab, Prof. Thomas Scheibel, Lehrstuhl für Biomaterialien, Universität Bayreuth). The protein solutions (10 µM in PBS) were aliquoted and rotated (60 rpm) for 24 h at 4 °C or room temperature to generate recombinant NM fibrils.

III.B.3.10 Preparation of AFM samples

Morphology of amyloid fibrils was investigated by contact mode atomic force microscopy (AFM). Samples were placed on freshly cleaved mica attached to 15-mm AFM sample disks (Ted Pella, Redding, CA, U.S.A.). After 3 min of adsorption at room temperature, disks were rinsed several times with Millipore-filtered H_2O. The samples were allowed to air dry. AFM microscopy was carried out by Michael Suhre (Spider lab, Prof. Thomas Scheibel, Lehrstuhl für Biomaterialien, Universität Bayreuth).

III.B.4 CELL BIOLOGICAL METHODS

III.B.4.1 Thawing of mammalian cells

Cells stored in liquid nitrogen were briefly thawed at 37 °C in a water bath. Afterwards, cells were rinsed in 10 ml pre-warmed medium and centrifuged at 1000 rpm (Sigma 4K15 centrifuge), 20 °C, for 10 min to remove DMSO in the cryoconservation medium. The

supernatant was discarded and the cell pellet was gently resuspended in 10 ml fresh culture medium and plated in a 10 cm cell culture dish.

III.B.4.2 Cultivation of cells

The cell line N2a (*III.A.8*) was maintained in Opti-MEM (*III.A.9*), HpL3-4 cells and COS-7 cells (*III.A.8*) were maintained in D-MEM medium (*III.A.9*), and Ψ2 and PA317 cells (*III.A.8*) were maintained in RPMI medium (*III.A.9*) containing 10 % fetal calf serum (FCS) and 1% Pen/Strep (*III.A.9*) in a humidified 5 % CO_2 atmosphere at 37 °C. The medium was changed every 48 h. For further passage, confluent adherent cells were rinsed once with 5 ml PBS and detached from the culture dish using 500 µl Trypsin/EDTA solution. Cells were suspended in 5 ml medium which was subsequently diluted into fresh media to the desired volume and transferred to a new cell culture dish.

III.B.4.3 Cryoconservation of cells

Media:

Cryoconservation medium	90 %	FCS
	10 %	DMSO

At 80 % confluence, cells were detached from the culture dish (*III.B.4.2*), suspended in 7 ml culture medium and centrifuged at 1000 rpm (Sigma 4K15 centrifuge), 4 °C, for 5 min. The cell pellet was resuspended in 3-4 ml cryoconservation medium and 1 ml aliquots in cryovials were immediately placed at -80 °C for at least 24 h before being transferred to liquid nitrogen for long-term storage.

III.B.4.4 Determination of cell numbers

An aliquot of detached and resuspended cells (*III.B.4.2*) was diluted 1:2 in $H_2O_{dest.}$ and 20 µl thereof were transferred to a Fuchs-Rosenthal hemocytometer. The number of cells in 4 diagonally lying squares was counted. One square has an area of 1 mm^2 and a depth of 0.2 mm, thus a volume of 0.2 mm^3. The cell concentration was calculated according to the following formula:

Cell number/ml = counted cells/number of counted squares x dilution factor x 5000

III.B.4.5 Transient transfection of cells

Transient transfections of recombinant plasmids were carried out using the FuGENE transfection Kit (Roche) with N2a and COS-1 cells. For HpL3-4 cells, the Lipofectamine 2000 transfection reagent (Invitrogen) was used. Effectene transfection reagent (Qiagen) was used for Ψ2 and PA317 cells according to the manufacturer's protocols. Briefly, cells were plated on 6 cm dishes and transfected 24 h later. Cells were analyzed 48 h post transfection.

III.B.4.6 Production of retroviral particles

The retroviral expression vector pSFF with the insert of interest was transfected into a mixed culture of Ψ2 and PA317 cells (*III.B.4.5*). These retroviral packaging cells provide genes for gag, pol and env *in trans*, thereby producing replication defective viral particles for subsequent transduction of target cells. As a control, a pSFF plasmid coding for GFP was also transfected. Once the cells were 80-100 % positive for GFP, the supernatant was harvested, cleared of cell debris by centrifugation at 120 x g and 4 °C for 10 min and stored at -80 °C.

III.B.4.7 Transduction of cells

III.B.4.7.1 Transduction of cells with recombinant retrovirus

3×10^5 HpL3-4 cells were plated in 6-well plates. The next day, cells were incubated with 4 g/ml Polybrene (Sigma) for 2h before exposure to 1 ml medium containing retroviral particles over night.

III.B.4.7.2 Transduction of cells with recombinant lentivirus

The day before transduction, 2.5×10^5 N2a cells were plated in 6-well plates. Stable expression of NM-HA was achieved by addition of recombinant lentivirus particles coding for NM-HA (containing 200 ng reverse transcriptase, as measured by ELISA) which were gently provided by Dr. Andreas Hofmann (Laboratory of Prof. Alexander Pfeifer; Institute of Pharmacology and Toxicology, University of Bonn) for 24 h.

III.B.4.8 Aggregate induction assay

N2a cells were plated in 6 cm plates and recombinant NM fibrils were added to the medium at a final concentration of 1 µM for 24 h (if not otherwise stated). Cells were rinsed three times with PBS and subsequently passaged for further analysis.

III.B.4.9 Subcloning of N2a cells by limiting dilution

Detached cells (*III.B.4.2*) were counted (*III.B.4.4*) and diluted several times into medium to a final concentration of 10 cells per ml. 100 µl of this dilution were transferred to a 96-well plate. Wells containing only one cell clone were selected and clones were raised for further analysis.

III.B.4.10 Preparation of cell extracts for infection experiments

Confluent cell monolayers on a 10 cm dish were rinsed with PBS and scraped into 1 ml PBS. After centrifugation (1000 x g, 2-3 min, 4 °C) the supernatant was discarded and the cells were resuspended in 100 µl PBS before being stored at -80 °C for at least 24 h.

III.B.4.11 Infection of cells with cell extracts

On the day of infection cells in PBS (*III.B.4.11*) were thawed and crude cell lysates were generated by a short sonication step (15 - 30 s). Recipient cells plated in 12-well plates were incubated with extracts derived from cells of a whole 10 cm dish. After 24 h cells were rinsed three times with PBS and grown at least one week prior to analysis.

III.B.4.12 Indirect immunofluorescence (IF) analysis

Buffers and solutions:

Quenching solution	50 mM	NH_4Cl
	20 mM	Glycine in PBS
Permeabilization solution	0.1 %	Triton X-100 in PBS

Blocking solution	0.2 %	Gelatine in PBS

Hoechst staining solution	2 µg/ml	Hoechst in PBS

The indirect immunofluorescence technique was used to visualize antigens *in situ* on a single cell level by binding of fluorochrome-labeled secondary antibody to a primary antibody directed against the protein of interest. Cells were plated on 6 cm dishes with glass cover slips. In some experiments, cells were transfected with the respective constructs (*III.B.4.5*). The next day or 48 h post transfection, cover slips were transferred to 12-well culture plates, rinsed 3 x with PBS, and fixed with 500 µl Roti-Histofix for 30 min at room temperature. After removal of the fixation solution cells were quenched with NH_4Cl/glycine solution, permeabilized with 0.1 % Triton X-100 and blocked with blocking solution. Each step was performed for 10 min and terminated by 3 x rinsing steps with PBS. Eventually, the primary antibody (*III.A.5*) diluted in blocking solution was added for 45 min at room temperature in a humid chamber. Samples were rinsed 3 x with PBS prior to addition of the Cy2- or Cy3-conjugated secondary antibody (*III.A.5*) diluted in blocking solution for 30 min at room temperature in the dark. Again, cells were rinsed 3 times and nuclei were stained by incubation with Hoechst DNA staining solution for 10 min at room temperature in the dark. After rinsing cover slips were mounted on microscope slides in anti-fading solution Permafluor and kept dry at -20 °C in the dark. Confocal laser scanning microscopy was carried out using a LSM510 confocal laser microscope (Zeiss).

III.B.4.13 Fluorescence-activated cell sorting (FACS)

Buffers and solutions:

EDTA solution	1mM	EDTA in PBS

FACS buffer	2.5 %	FCS
	0.05 %	NaN_3 in PBS

Saponin buffer	0.1 %	Saponin in FACS buffer

Flow cytometry allows the analysis of single cells in suspension with respect to their size, granularity or fluorescence. Cells were washed twice with PBS and detached from the culture dish using an EDTA solution. Approximately 4×10^5 cells were transferred to FACS tubes and sedimented at 1.200 rpm (Sigma 4K15 centrifuge) at 4 °C for 2 min.

Procedure for cell surface staining:

After resuspension in 500 μl FACS buffer, cells were incubated on ice for 10 min in blocking solution. Again, cells were centrifuged (1.200 rpm, 3 min, 4 °C, Sigma 4K15) before the primary antibody (*III.A.5*) diluted in FACS buffer was added. The samples were vortexed carefully and incubated on ice for 30 min. Three rinsing steps were carried out by repeated sedimentation (1.200 rpm, 3 min, 4 °C, Sigma 4K15) followed by resuspension in 500 μl FACS buffer. The Cy2- or Cy3-conjugated secondary antibody (*III.A.5*) diluted in FACS buffer was added for 30 min on ice in the dark. Rinsing was repeated 3 times in 500 μl FACS buffer and subsequent sedimentation of cells at 1.200 rpm and 4 °C for 3 min. In order to exclude permeabilized or dead cells from analysis, 7-AAD diluted in FACS buffer was added to the samples and incubated for 5 min on ice in the dark immediately prior to the measurement. Cells double stained for secondary antibody and 7-AAD were excluded from the analysis. Permeabilized cells were used as positive controls for 7-AAD staining. Cells lacking 7-AAD staining were used for gating the cell population. Cells not incubated with primary antibody as well as cells not expressing the target protein served as controls. Samples were analyzed in a Coulter EPICS XL apparatus with testing 10.000 cells per experiment.

IV. RESULTS

IV.A CHARACTERIZATION OF SUP35P-NM MOUSE PRP FUSION PROTEINS IN MAMMALIAN CELLS

In contrast to mammalian PrP, the Sup35p domains that are important for prion formation and propagation in yeast are well characterized. To assess structural and environmental requirements for prion protein aggregation in mammalian cells comparative analysis of the aggregation behaviors of Sup35p, PrP and recombinant fusion proteins comprising fragments of both proteins were performed. Important domains known to influence mammalian and yeast prion formation were substituted by the corresponding region of the respective domain of the other prion protein. Sup35p and mouse PrP fusion proteins were transiently expressed in N2a, HpL3-4 and COS cells. Aim of this study was to investigate if a PrP fragment corresponding to aa 23-120 can compensate for the prion forming domain N. Furthermore, it was investigated if fusion of Sup35p domains N, M or NM could modify the aggregation behavior of PrP_{90-230}. Since Sup35p is a cytosolic protein and PrP was shown to be able to form prion-like aggregates when expressed in the cytosol of mammalian cells (Ma & Lindquist 2002), constructs coding for cytosolic proteins were generated.

IV.A.1 CLONING OF VECTORS CODING FOR SUP35P-NM AND MOUSE PRP FUSION PROTEINS

PrP coding sequences were amplified by PCR using a vector coding for 3F4-tagged mouse PrP (described in (Nunziante *et al.* 2003)) as a template. The 3F4 epitope allows recognition of ectopically expressed mouse PrP using the monoclonal antibody (mAb) 3F4 and discrimination from endogenous wild-type mouse PrP. The pJC25-NM expression vector was used as template (Scheibel *et al.* 2001) for amplification of sequences encoding the Sup35p domains N, M and NM. All constructs for transient mammalian expression were cloned into the pcDNA3.1/Zeo expression vector (Invitrogen, Karlsruhe). Insertion of appropriate restriction sites allowed cloning of the respective coding sequences of mouse PrP and Sup35p as fusion proteins. A carboxyl-terminal HA epitope tag for NM expression in mammalian cells was generated using a primer coding for the peptide sequence of hemagglutinin

(YPYDYPDYA) for PCR amplification. Constructs were generated coding for cytosolic PrP (PrP$_{cyto}$, PrP residues 23-230), PrP$_{90-230}$ (PrP comprising residues 90-230), Sup35p-NM (Sup35p residues 1-250) or chimeric proteins thereof. For N-PrP, M-PrP and NM-PrP, residues 1-123, 124-250 or 1-250 of Sup35p were fused to the murine PrP (residues 90-230). In PrP-M, the amino-terminal N region of Sup35p (aa 1-123) was replaced by PrP residues 23-120. If necessary, individual DNA fragments were first cloned into the plasmid vector pCR-BluntII-TOPO prior to introduction into pcDNA3.1/ZEO. A schematic presentation of the cloning strategy showing positions of restriction sites and primers used for each sequence is shown in **Figure 19**. Correct sequences of all constructs were confirmed by DNA sequencing, performed by GATC (Konstanz).
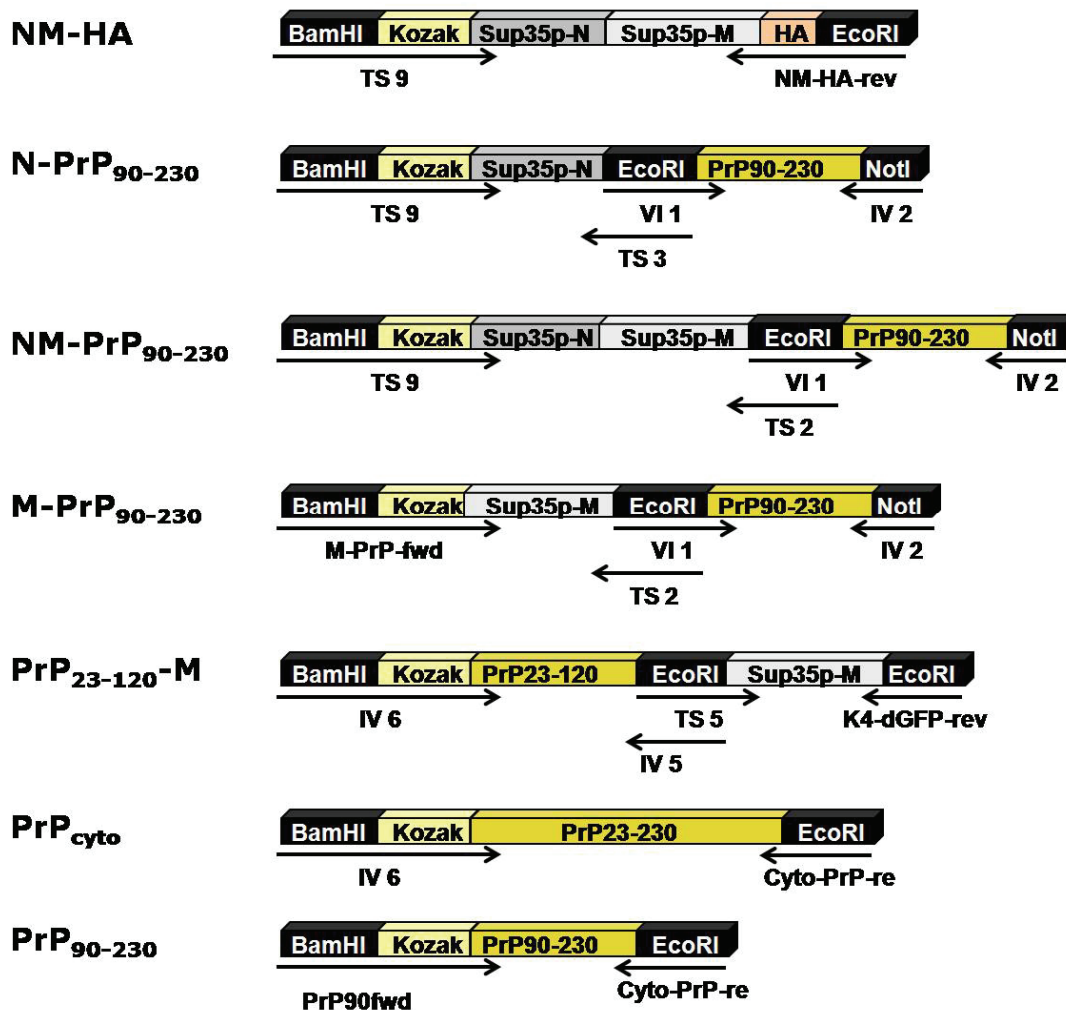
Figure 19. Cloning strategy showing restriction sites and primers used to generate pcDNA3.1/Zeo expression vectors. Detailed primer sequences are listed under III.A.7.

IV.A.2 TRANSIENT EXPRESSION OF PrP$_{90-230}$, PrP$_{CYTO}$, N-PrP, M-PrP AND NM-PrP IN THE MAMMALIAN CYTOSOL LEADS TO AGGREGATE FORMATION

The different constructs listed in **Figure 20** were transfected into N2a cells and 48 h post transfection cells were lysed.
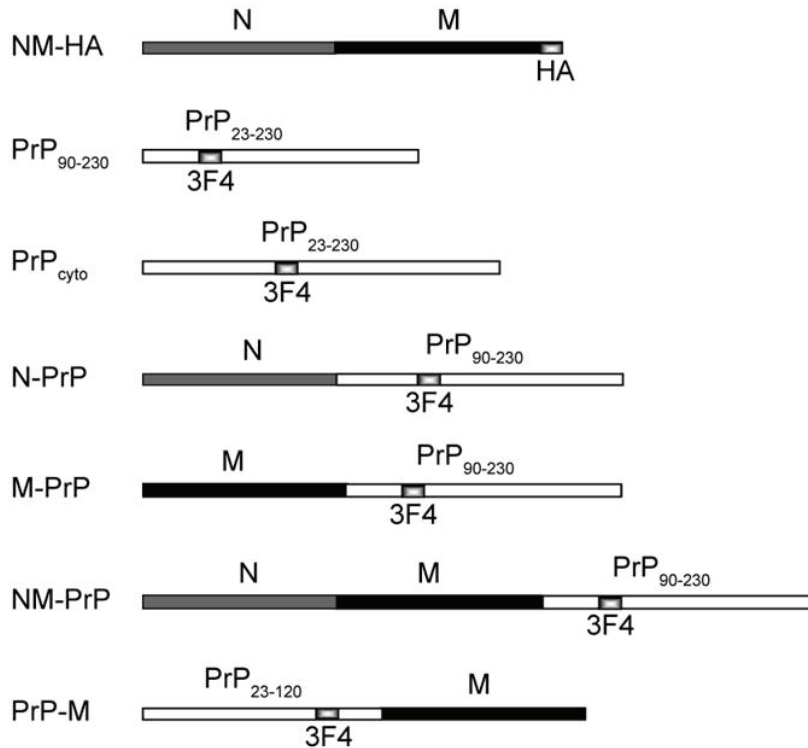

Figure 20. Schematic representation of recombinant proteins. The prion-forming region NM (aa 1-250) of Sup35p contains a C-terminal HA antibody epitope tag for detection purposes in mammalian cells. All proteins harbouring PrP sequences contain a 3F4 antibody epitope that can be detected utilizing the hamster PrP specific antibody 3F4. Modified version published in (Krammer *et al.* 2008b).

Cells expressing fusion proteins showed no overt growth defect for the course of the experiments and no obvious cytotoxic effects, except for cells expressing cytosolic PrP that appeared to be slightly toxic. Western blot analysis revealed that proteins migrated at the expected size of about 17 kDa (PrP$_{90-230}$), 25 kDa (PrP$_{cyto}$), 32 kDa (N-PrP), 45 kDa (M-PrP), 50 kDa (NM-PrP), 35 kDa (PrP-M), and 40 kDa (NM-HA) respectively (**Figure 21**).
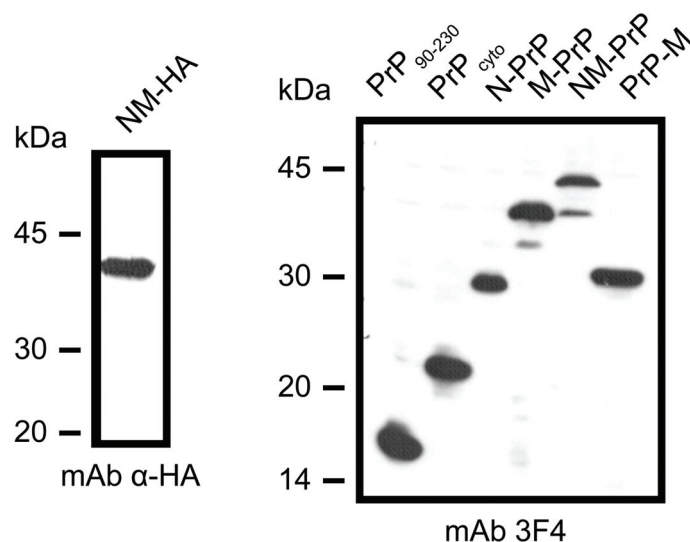
Figure 21. Expression of NM-HA, PrP$_{90-230}$, cytosolic PrP and fusion proteins thereof in the cytosol of N2a cells 48 h post transfection. Cells were lysed and proteins analyzed by SDS gel electrophoresis and Western blot. Proteins were detected using antibodies 3F4 or anti-HA. Modified version published in (Krammer *et al.* 2008b).

Upon over-expression in yeast cells, the prion domain of Sup35p can assemble into aggregates that form visible foci (Zhou *et al.* 2001). Interestingly, 48 h post transfection, NM-HA was almost completely soluble in the cytosol of transfected mammalian cells (**Figure 22**). Similar to NM-HA, expression of PrP-M yielded visible aggregates in only very few cells, while the vast majority of PrP-M was dispersed homogeneously throughout the cytoplasm. By contrast, expression of cytosolic PrP (PrP$_{cyto}$) led to formation of small aggregates (**Figure 22**) (Grenier *et al.* 2006). PrP$_{90-230}$ formed aggregates comparable to PrP$_{cyto}$ in size and localization. Replacement of amino-terminal PrP aa residues 23-89 with Sup35p-N (N-PrP) did not abolish aggregate formation. PrP$_{cyto}$ and PrP$_{90-230}$ formed multiple small aggregates that frequently clustered in one area of the cell. Surprisingly, fusion of M or NM, to the carboxyl-terminal domain of PrP (M- and NM-PrP) led to the spontaneous formation of large, single aggregates (or foci) that strongly differed from the smaller aggregates observed with PrP$_{90-230}$, PrP$_{cyto}$ or N-PrP (**Figure 22**). A significant fraction of cells contained approx. 1-4 dot- and ring-shaped aggregates of M- and NM-PrP reminiscent of Sup35p aggregates associated with the [PSI^{+}] status in yeast (Zhou *et al.* 2001). Multiple ring-shaped aggregates were occasionally present within one cell. Collection of sequential scans along the vertical (z) axis revealed a spherical structure of the giant M- and NM-PrP aggregates. Thus, the ring-like appearance of the aggregates is likely due to the antibody binding only to the surface of the aggregates. The size of single aggregates ranged from small

(PrP$_{90-230}$, PrP$_{cyto}$ and N-PrP, less than 1µm) to big (NM-PrP) with aggregates about 5 µm in diameter. M-PrP foci sometimes even outgrew NM-PrP (up to 10 µm in diameter).
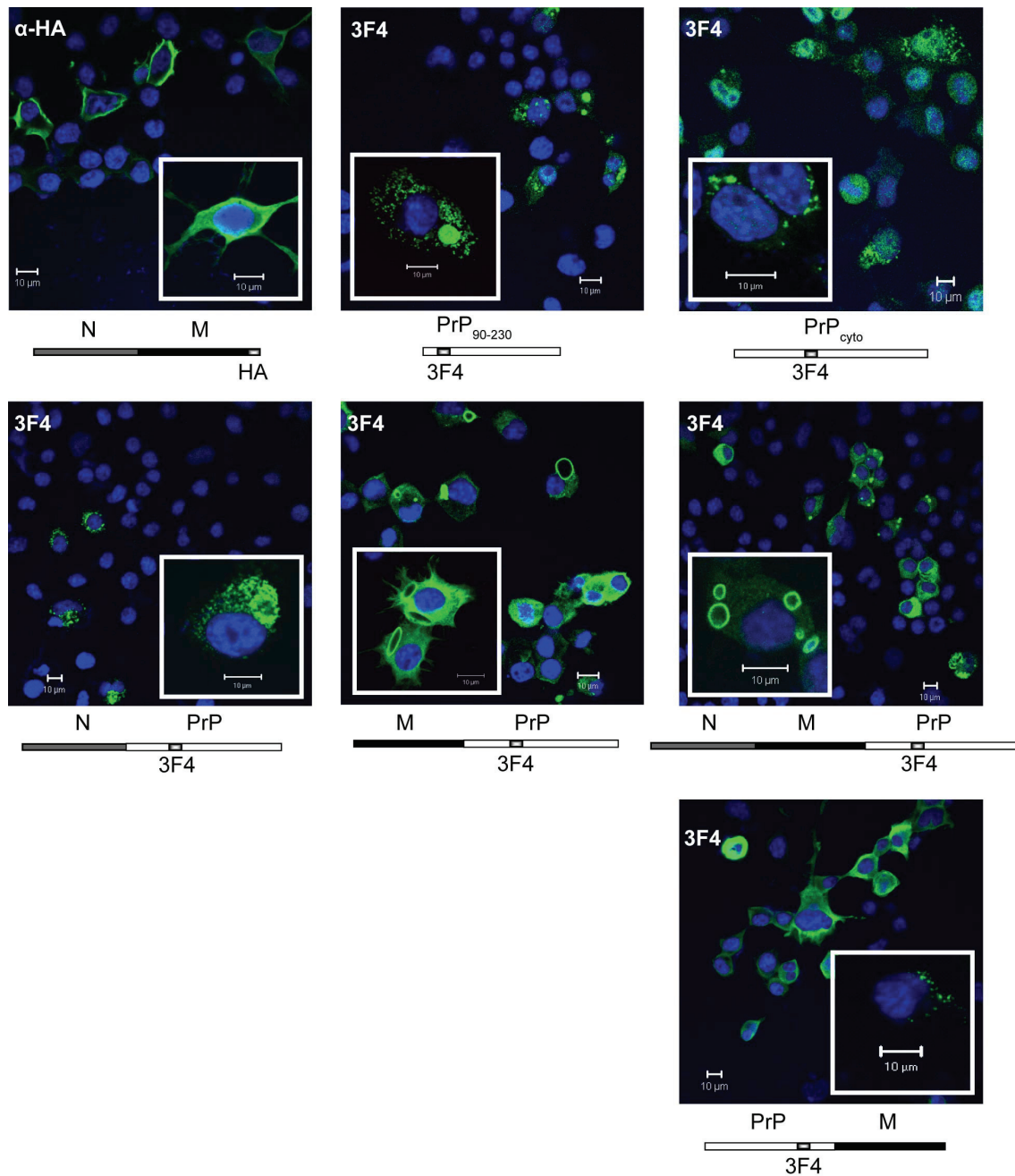

Figure 22. Confocal images of transiently transfected N2a cells subjected to immunofluorescence analysis. Ectopically expressed proteins were stained with 3F4 or anti-HA (green), nuclei were stained with Hoechst (blue). Aggregate formation was observed with PrP$_{90-230}$, PrP$_{cyto}$, N-PrP, M-PrP and NM-PrP, whereas no or very few aggregates were detected in cells expressing NM-HA or PrP-M. Schematic representations of recombinant proteins are depicted below the images. Scale bars: 10 µm. Modified version published in (Krammer *et al.* 2008b).

Confocal microscopy analysis further demonstrated that foci were already present 6 h post transfection, indicating that newly translated proteins were immediately incorporated into the growing aggregates.
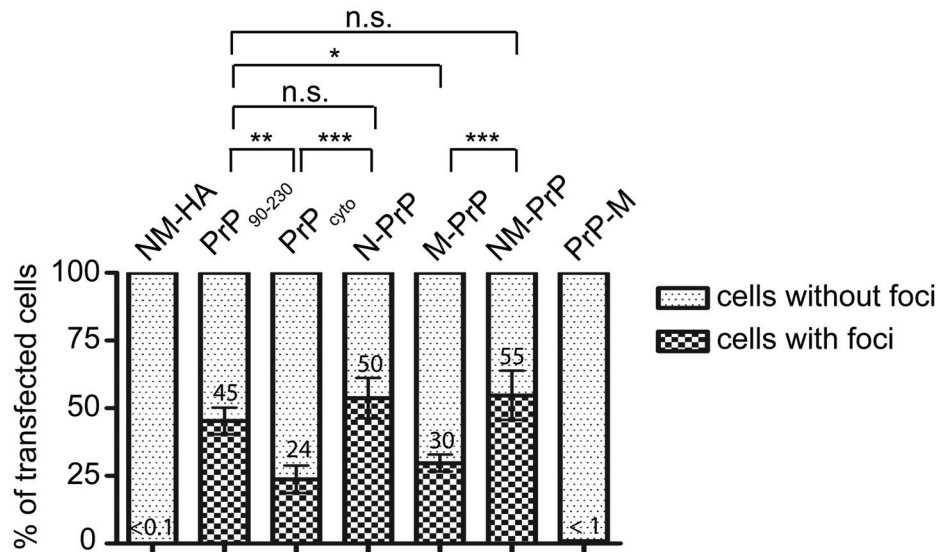

Figure 23. Determination of the ratio of cells that exhibited aggregates to the cells that appeared to express soluble recombinant proteins. For each recombinant protein, protein aggregation was assessed in at least 300 transfected cells in three independent experiments. Aggregate formation was induced at similar levels in cells expressing PrP_{90-230}, N-PrP and NM-PrP. Fewer cells with aggregates were detected when cytosolic PrP or M-PrP was expressed. Marginal aggregate formation was observed in cells expressing PrP-M or NM-HA. The standard deviation of mean is given (S.D.). Statistical analysis were performed using the X^2-test (n.s. = not significant; * = significant with $p<0.05$; ** and *** = highly significant, with $p<0.01$ or $p< 0.001$ respectively). Modified version published in (Krammer *et al.* 2008b).

Comparison of the numbers of cells containing aggregated proteins revealed very few cells containing visible foci of NM-HA or PrP-M (**Figure 23**). By contrast, expression of PrP_{cyto} led to aggregate formation in approximately 24 ± 5 % of transfected cells. Significantly more cells exhibited visible PrP_{90-230} aggregates compared to cells expressing PrP_{cyto} (45 ± 5 % vs. 24 ± 5 %, $p<0.01$), suggesting that the amino-terminal part of PrP had a negative effect on the nucleation rate of PrP_{90-230}. Replacement of the amino-terminal region of PrP with the Sup35p-N or -NM regions significantly increased the number of cells that harboured visible foci to 50 ± 2 % and 55 ± 9 %, respectively, whereas fusion of M to PrP_{90-230} did not. Thus, N had a positive effect on nucleation. Interestingly, the ratio of cells with visible M-PrP aggregates to total M-PrP expressing cells was significantly lower compared to the ratio of cells with visible PrP_{90-230} (30 ± 3 % vs. 45 ± 5 %, $p<0.05$), or NM-PrP foci to

total transfected cells (30 ± 3 % vs. 55 ± 9 %, p<0.001). This suggests that M alone exhibited an inhibitory effect on nucleation similar to the amino-terminal region of PrP, but that this activity could be counter-acted by N.

In conclusion, when transiently expressed in the cytosol of mammalian cells, PrP_{90-230}, PrP_{cyto}, N-PrP, M-PrP and NM-PrP displayed an intrinsic property to aggregate, while NM-HA and PrP-M did not. Interestingly, the frequency of aggregate induction seemed to be influenced by the N and M regions. Furthermore, striking qualitative differences were apparent between PrP_{90-230}, PrP_{cyto} or N-PrP and M- or NM-PrP foci, suggesting that the M region is capable of modulating aggregate size. Thus, the globular domain of PrP promotes aggregate induction whereas N and M domains of Sup35p influence nucleation and seeding.

IV.A.3 CELL TYPE SPECIFIC DIFFERENCES IN NM-PRP AGGREGATE FORMATION

Aggregate formation was also observed in HpL3-4 and COS cells transiently transfected with the respective constructs, except that for NM-PrP some COS cells appeared to harbor more aggregates compared to N2a cells. Confocal microscopy analysis of N2a and COS cells expressing NM-PrP revealed an unexpected high number of aggregates in some COS cells compared to N2a cells. To study if the amount of foci varied dependent on the cell type, 20 cells per N2a and COS cell lines transiently expressing NM-PrP were analyzed for their aggregate contents (**Table 8 and Figure 24**). Due to the small aggregate sizes of N-PrP, PrP_{cyto} and PrP_{90-230} it was not possible to determine if there was a quantitative difference in the number of foci per cell with these chimeric proteins. For N2a and COS cells the amount of NM-PrP aggregates per cell varied greatly. Surprisingly, however, in N2a cells aggregate numbers rarely exceeded 14 aggregates per cells, while in COS cells, 14 and more aggregates (up to 183) where detected in at least half of the studied cells. Notably, the observed differences in aggregate numbers per cell were dependent on N, as M-PrP failed to show a drastic cell type dependent difference in aggregate numbers. These data suggest that N influenced nucleation in a cell-type dependent manner.

Table 8. Number of visible aggregates in COS and N2a transiently expressing M-PrP or NM-PrP. Chimeric proteins were detected by antibodies 3F4 or anti-HA, respectively, and analyzed by confocal microscopy. Visible foci were counted in 20 cells. Mean values of foci per cell are given. Please note that the amount of visible foci can vary greatly between individual cells for NM-PrP but not so much for M-PrP. Published in (Krammer *et al.* 2008b).

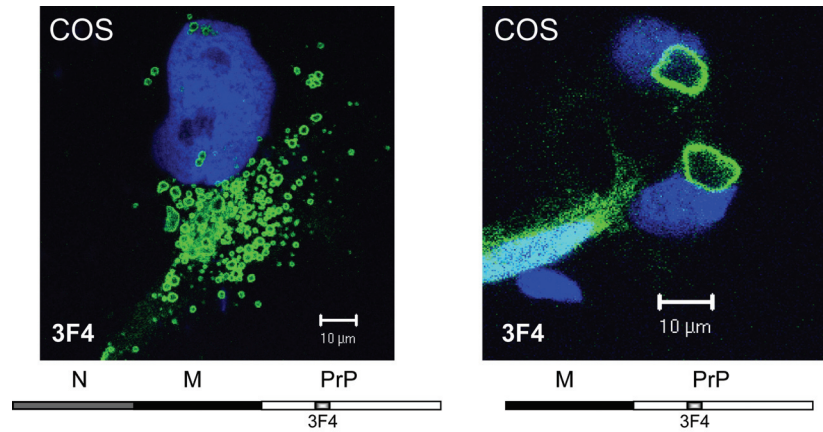|	NM-PrP foci per cell		M-PrP foci per cell	
Cell number	**COS**	**N2a**	**COS**	**N2a**
1	183	9	1	1
2	5	4	1	1
3	20	2	1	1
4	14	2	1	3
5	36	2	2	2
6	11	1	2	1
7	2	1	1	11
8	75	1	1	17
9	54	7	1	16
10	5	2	1	2
11	173	3	2	1
12	1	6	2	2
13	10	1	4	1
14	21	2	3	1
15	29	2	1	4
16	17	4	1	4
17	11	4	2	3
18	4	14	3	2
19	9	7	1	1
20	24	3	4	1
Mean	**35**	**4**	**2**	**4**

Figure 24. Confocal microscopy analysis of COS cells transiently expressing NM-PrP or M-PrP. NM-PrP or M-PrP were detected 48 hours post transfection using mAb 3F4. Representative COS cells harbouring NM-PrP or M-PrP aggregates are shown. NM-PrP or M-PrP were stained with mAb 3F4 (green), nuclei were visualized using Hoechst staining (blue). Scale bars: 10 µm. Published in (Krammer *et al.* 2008b).

IV.A.4 CHIMERIC AGGREGATES LACK CHARACTERISTIC AGGRESOME FEATURES

Misfolded and aggregated proteins that are a potential hazard to the cell can be rapidly eliminated by sequestration into intracellular, perinuclear inclusions, so called aggresomes (Johnston JA *et al.* 1998; Wigley WC *et al.* 1999; Kopito 2000). Aggresome formation is an active cellular process dependent on retrograde protein transport along microtubule tracts leading to protein complex formation around the microtubule organization center. A common feature of aggresomes is therefore the co-localization with centrosome markers (Kopito 2000). Sequestration of misfolded proteins into aggresomes has further been reported to be associated with a collapse of the intermediate filament vimentin forming a cage around the aggresome (Johnston JA *et al.* 1998). However, vimentin was not localized around any of the aggregates formed by PrP_{90-230}, PrP_{cyto}, N-PrP, M-PrP and NM-PrP (**Figure 25**). Unfortunately, the staining of vimentin in N2a cells was relatively diffuse unlike the filamentous (normal) or ring-like (around aggresomes) staining known for COS cells (Garcia-Mata *et al.* 1999) making a definite conclusion impossible. Therefore, co-localization of the proteins with vimentin was also investigated in COS cells (**Figure 26**). However, co-staining did not demonstrate any association of recombinant proteins with vimentin.
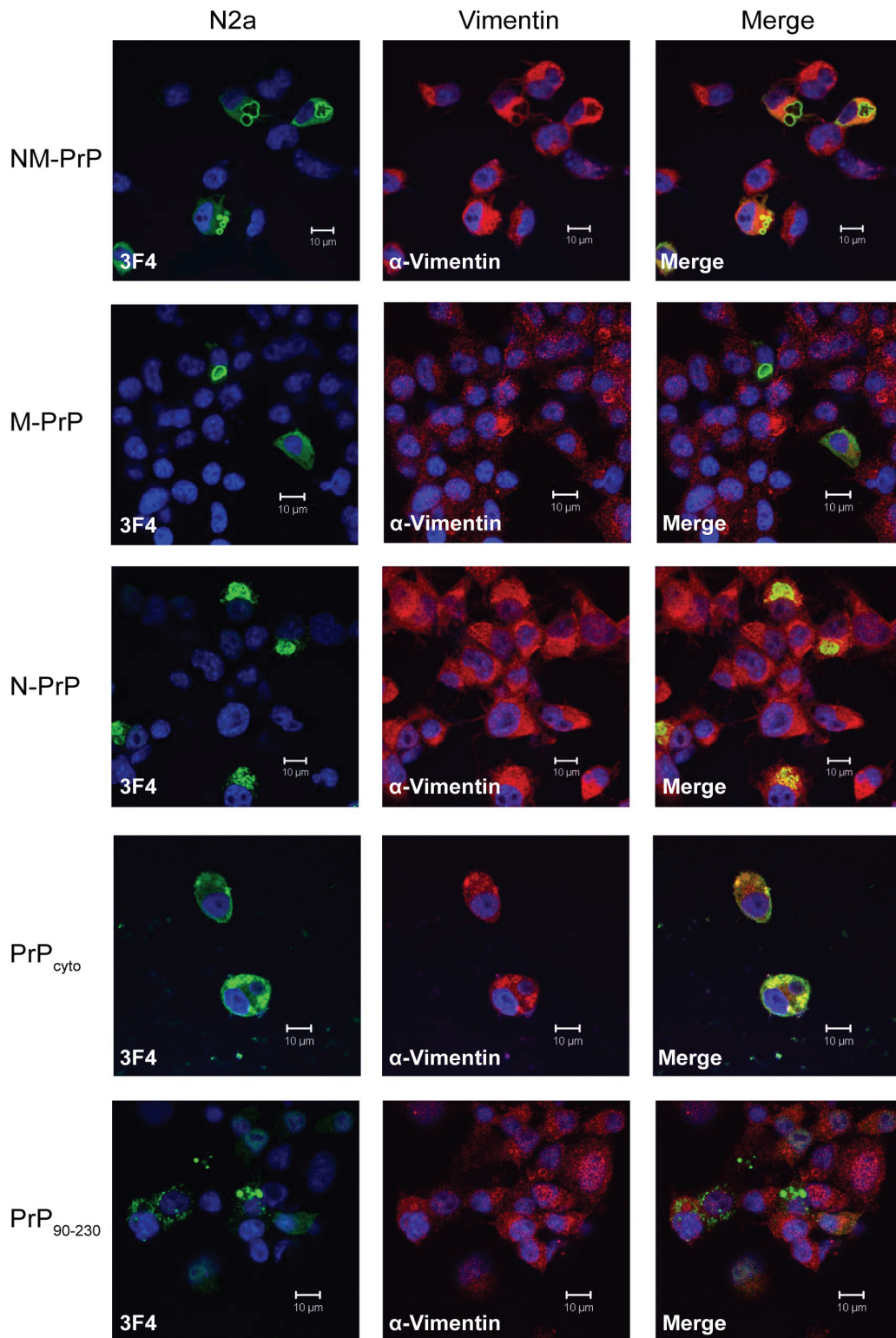
Figure 25. Co-staining of PrP$_{90-230}$, PrP$_{cyto}$, N-PrP, M-PrP and NM-PrP aggregates in N2a cells with the aggresome marker vimentin.
Transfected N2a cells were fixed and co-stained for PrP$_{90-230}$, PrP$_{cyto}$, N-PrP, M-PrP or NM-PrP and vimentin (red). Recombinant proteins were detected using antibody 3F4 (green). Nuclei were stained using Hoechst dye (blue). Only diffuse staining of vimentin was observed. Scale bars: 10 µm. Modified version published in (Krammer *et al.* 2008b).
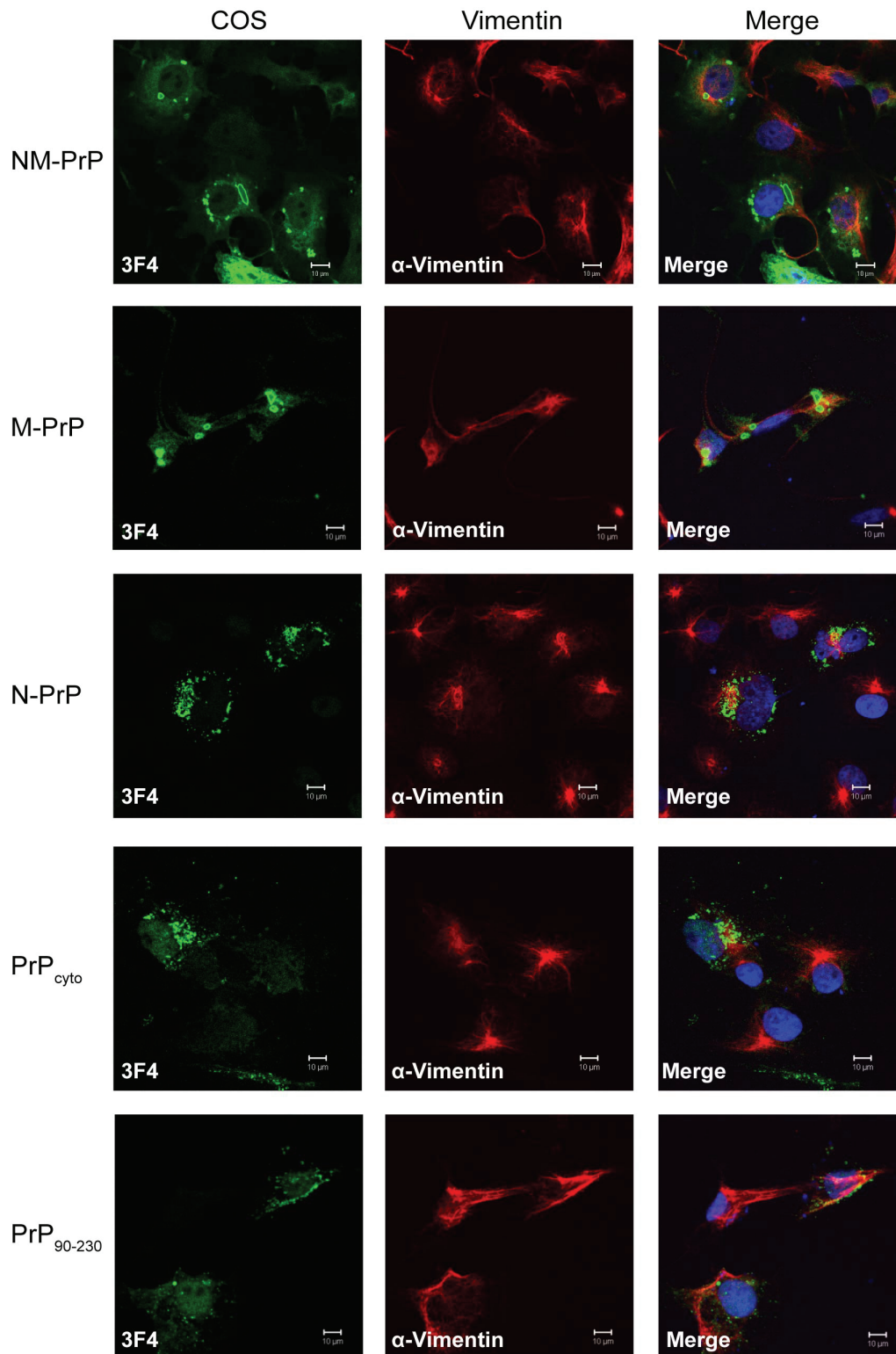
Figure 26. Aggregates in COS cells do not display aggresome characteristics. Transfected COS cells were fixed and co-stained for PrP_{90-230}, PrP_{cyto}, N-PrP, M-PrP or NM-PrP and vimentin (red). Recombinant proteins were detected using antibody 3F4 (green). Nuclei were stained using Hoechst dye (blue) No vimentin cage typical for aggresomes was apparent for any of the aggregates. Scale bars: 10 µm. Modified version published in (Krammer *et al.* 2008b).

As analysis of recombinant proteins gave similar results in the subsequent co-localization studies, only PrP$_{cyto}$, N-PrP, and NM-PrP are shown. Inclusions of recombinant proteins did not appear to be formed in the perinuclear region, suggesting that aggregates differed from conventional aggresomes (**Figure 22**). As expected, staining of N2a cells did not reveal any co-localization of the recombinant proteins with centrosome marker γ-tubulin (**Figure 27**). Additionally, disruption of the microtubule filaments by nocodazole for 24 h beginning at the time of transfection had no influence on aggregate formation, demonstrating that inclusions formed independently of an active transport along microtubule tracts (data not shown). In conclusion, the lack of aggresome markers suggests that PrP$_{cyto}$, N-PrP and NM-PrP aggregates do not evoke an active cellular sequestration into aggresomes.
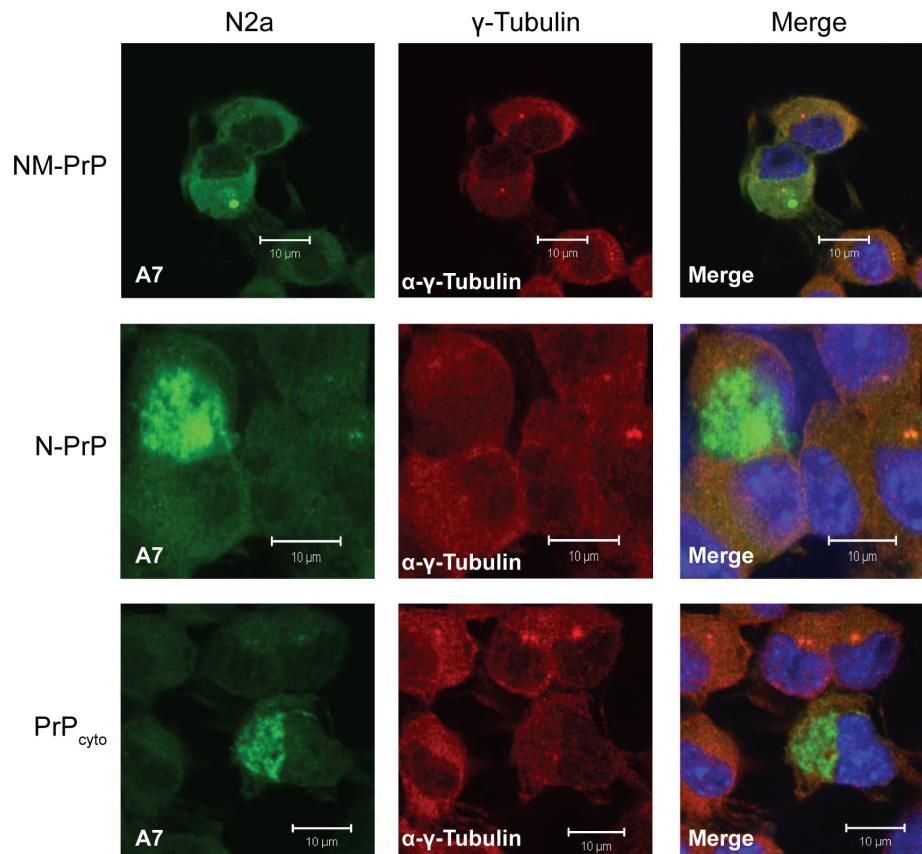

Figure 27. Cytosolic aggregates do not localize at the centrosome. N2a cells expressing chimeric proteins were fixed and stained for, PrP$_{cyto}$, N-PrP, and NM-PrP with polyclonal anti-PrP antibody A7 and aggresome marker γ-tubulin 48 h post transfection. Nuclei were visualized using Hoechst staining. Merged images demonstrate a lack of co-localization of aggregates with the centrosome marker. Scale bars: 10 µm. Modified version published in (Krammer *et al.* 2008b).

IV.A.5 AGGREGATES ARE NOT LOCATED IN CELLULAR COMPARTMENTS

The spheroidal structure of the cytosolic proteins could also result from a potential localization of recombinant proteins in vesicles rather than from intrinsic aggregation. To exclude this possibility, cells expressing recombinant proteins were either co-stained with markers for cellular compartments (**Figure 28**), like Calnexin (marker for ER) and Rab 6 (marker for Golgi), or co-transfected with vectors coding for GFP-tagged Rab 4 and Rab 11 (markers for early and late endosomes, respectively). The use of GFP-tagged marker proteins allows the detection of the respective protein without the need for an additional staining. The confocal microscopy data revealed that there was neither co-localization of PrP_{cyto}, N-PrP, and NM-PrP with markers for the organelles ER and Golgi, nor for early and late endosomes.

Cytosolic protein complexes can also actively be captured into bilammellar autophagosomes (Yorimitsu & Klionsky 2005) that ultimately fuse with lysosomes for acidic hydrolytic degradation (Rubinsztein 2006). To analyze if aggregates formed by PrP_{cyto} and fusion proteins were subjected to lysosomal clearance, cells were co-stained for Lamp-1 that is abundant in lysosomes. None of the aggregated recombinant proteins co-stained with this lysosomal marker (**Figure 29**), demonstrating that protein aggregates were not present in this compartment of the endocytotic pathway.
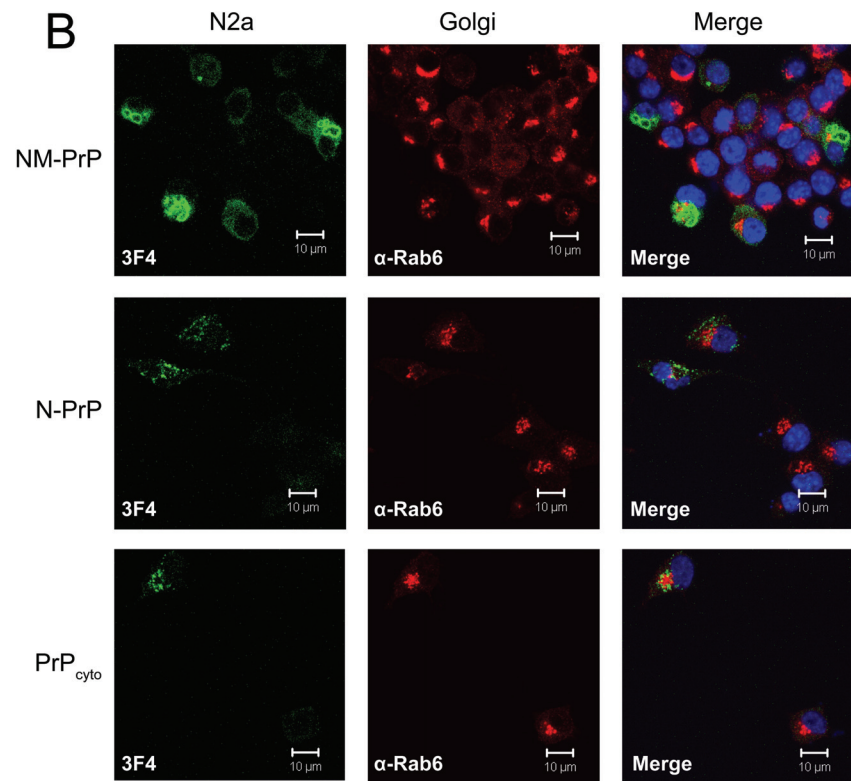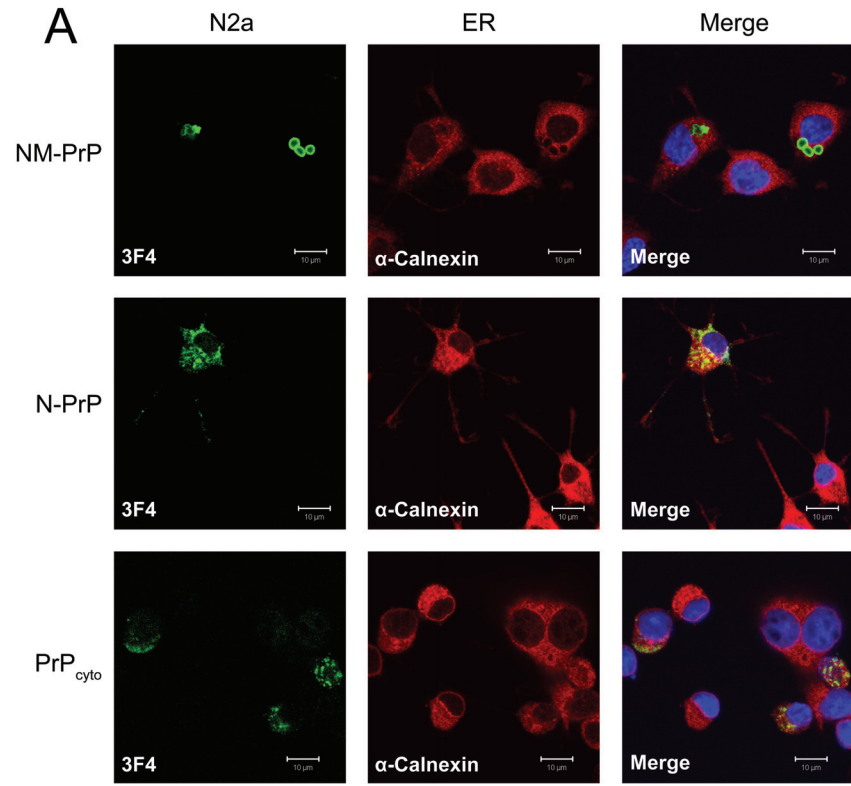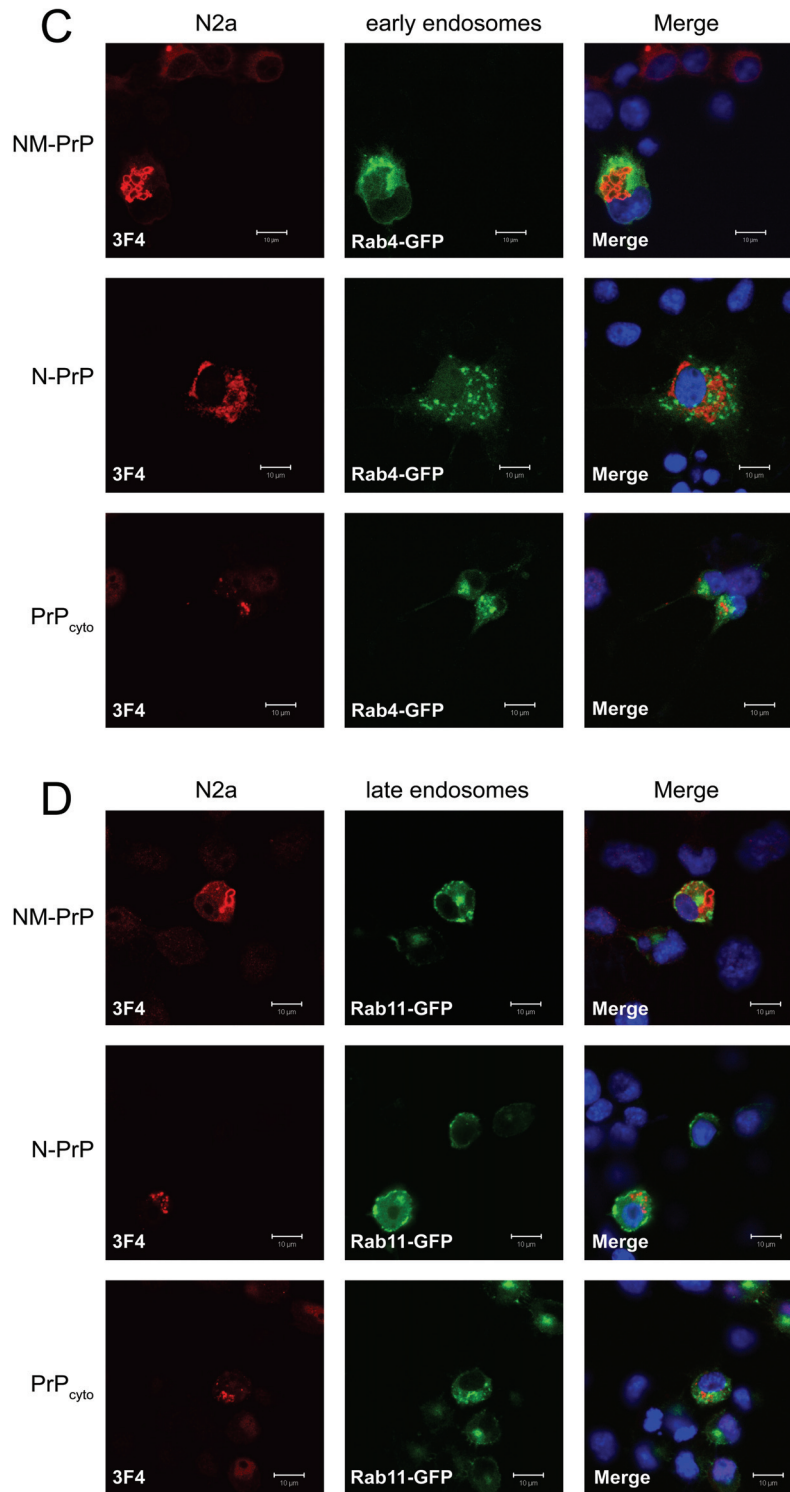
Figure 28. Aggregates are not located in intracellular organelles or vesicles. N2a cells expressing the recombinant proteins were fixed and stained for PrP_{cyto}, N-PrP and NM-PrP. Nuclei were visualized using Hoechst staining. A*:* Co-staining for ER marker Calnexin. B: Transfected N2a cells were co-stained for Rab 6. C: N2a cells were transfected with respective constructs and a construct coding for Rab 4-GFP, a marker for early endosomes. D: N2a cells were co-transfected with the respective constructs and a construct coding for Rab 11-GFP that visualizes late and recycling endosomes. Scale bars: 10 µm. Modified version published in (Krammer *et al.* 2008b).
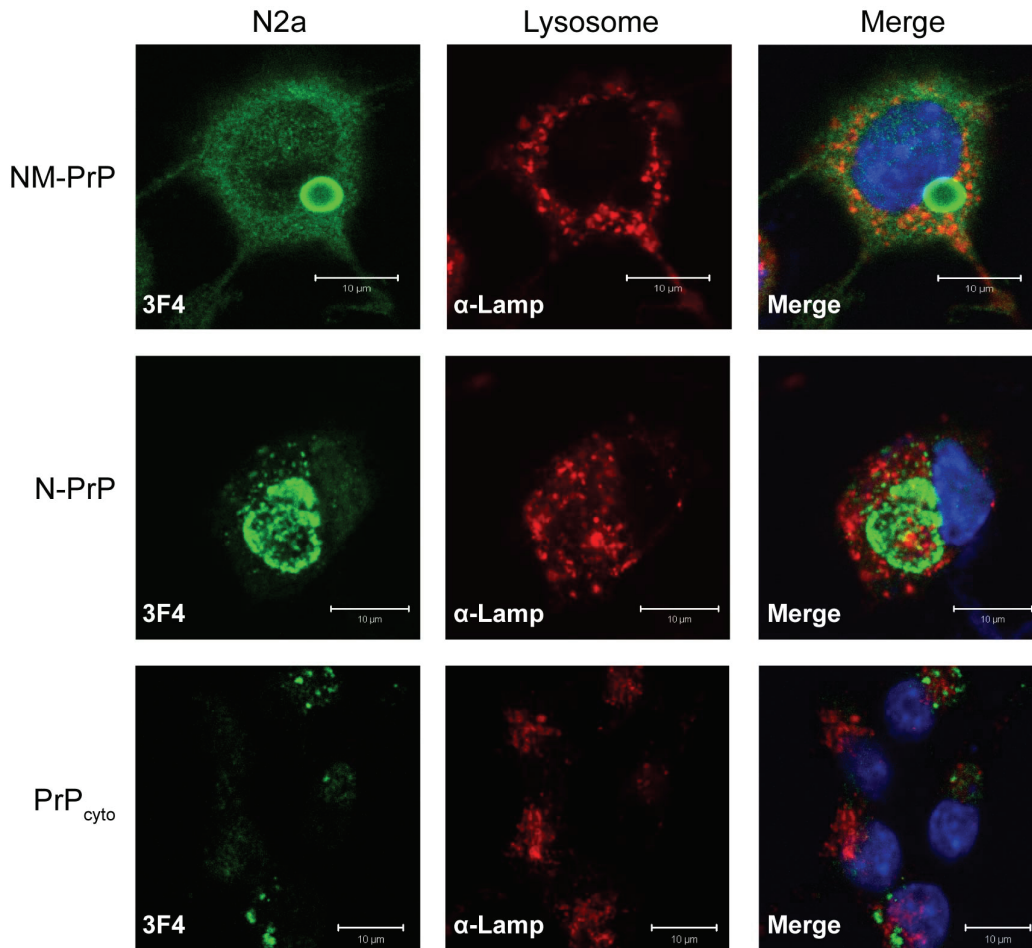
Figure 29. Aggregates were not subjected to lysosomal degradation. Transfected N2a cells were co-stained for the lysosomal marker protein Lamp-1 using the mouse monoclonal anti-CD107a (LAMP-1) antibody and for recombinant proteins using mAb 3F4. The merged image demonstrates a lack of co-localization of aggregates and the lysosomal marker. Scale bars: 10 µm. Published in (Krammer *et al.* 2008b).

These studies revealed that none of the recombinant proteins co-localized with markers for Golgi, ER or early or late endosomes. Furthermore, none of the protein aggregates was targeted to lysosomal degradation. The observed aggregate formation that occurred within 6 h post transfection indicates an intrinsic property of PrP_{90-230}, PrP_{cyto}, N-PrP, M-PrP and NM-PrP to spontaneously aggregate in the cytosol of mammalian cells.

IV.A.6 PrP$_{90\text{-}230}$, PrP$_{\text{CYTO}}$, N-PrP, M-PrP AND NM-PrP FORM INSOLUBLE COMPLEXES IN THE CYTOSOL OF MAMMALIAN CELLS

Fractionation analysis was performed to determine the ratio of insoluble to soluble recombinant proteins in N2a cells transiently transfected with the respective constructs. Whole cell lysates were subjected to centrifugation to separate soluble from insoluble proteins and fractions were analyzed by Western blot. Both NM-HA and PrP-M mainly remained soluble (**Figure 30**). By contrast, PrP$_{90\text{-}230}$, PrP$_{\text{cyto}}$, N-PrP, M-PrP and NM-PrP were detected in the pellet fraction.
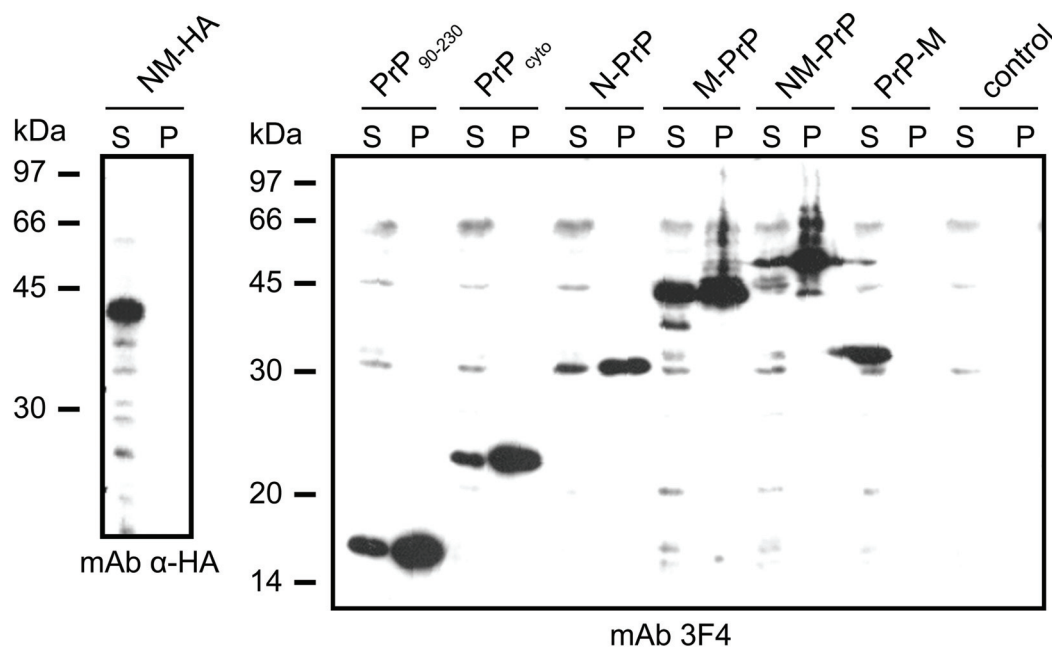
Figure 30. Insoluble protein aggregates in N2a cells expressing PrP$_{90\text{-}230}$, PrP$_{\text{cyto}}$, N-PrP, M-PrP and NM-PrP. N2a cells transiently expressing the respective proteins were lysed and insoluble protein fractions were pelleted by centrifugation. Fractions were subjected to SDS gel electrophoresis and WB analysis. The fractions of insoluble (pellet = P) and soluble recombinant proteins (supernatant = S) are shown. NM-HA was detected using an antibody against the HA tag, all PrP proteins were detected using mAb 3F4. As a control, untransfected cells were lysed and lysates fractioned into soluble and insoluble fractions. Few unspecific bands are apparent in untransfected cells. Modified version published in (Krammer *et al.* 2008b).

Quantification of band intensities revealed that approximately 58 ± 10 % of PrP$_{90\text{-}230}$, 55 ± 13 % of PrP$_{\text{cyto}}$, 68 ± 9 % of N-PrP, 60 ± 2 % of M-PrP and 71 ± 7 % of NM-PrP were sequestered into insoluble complexes that were pelleted by centrifugation (**Figure 31**). Thus, solubility analysis confirmed that PrP$_{90\text{- }230}$, PrP$_{\text{cyto}}$, N-PrP, M-PrP and NM-PrP aggregated into insoluble high molecular mass complexes.
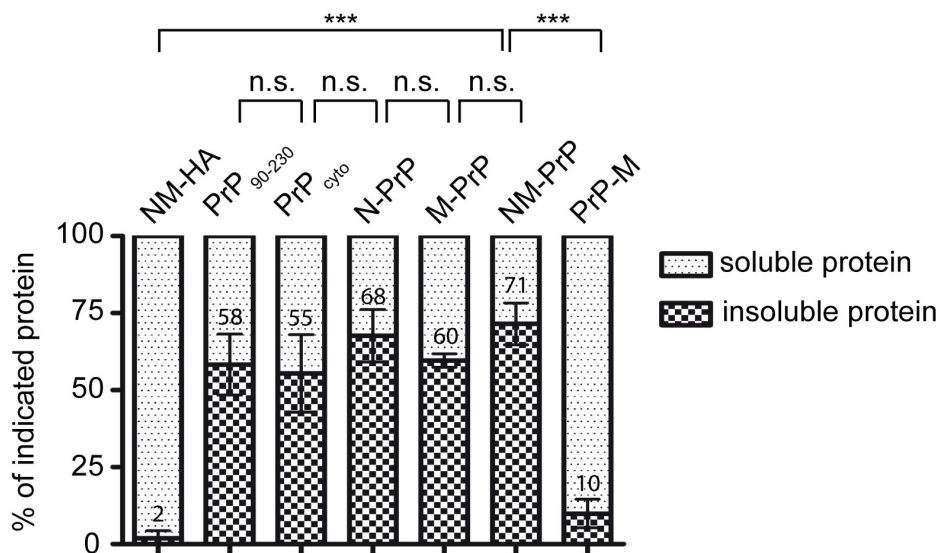
Figure 31. Quantification of recombinant proteins in soluble and insoluble fractions analyzed by SDS-PAGE and WB. Solubility assays were performed three times, and the amounts of pelleted to soluble recombinant proteins were determined. The graph shows the percentage of insoluble to soluble protein for each protein. The standard deviation is given (S.D.). Statistical analysis was performed using the X^2-test (n.s. = not significant; *** = highly significant, p<0.001). Modified version published in (Krammer *et al.* 2008b).

IV.A.7 RECOMBINANT PROTEINS THAT HARBOR THE CARBOXY-TERMINAL PART OF PRP DISPLAY INCREASED RESISTANCE TO PROTEOLYSIS

An increased protease resistance is a characteristic feature of Sup35p in [PSI$^+$] cells and abnormal prion protein (PrP^{Sc}) in mammalian prion diseases. Analysis of PK resistance revealed a complete PK sensitivity of NM-HA (**Figure 32**). PrP$_{90-230}$, PrP$_{cyto}$ and N-PrP displayed increased protease resistance up to 50 µg/ml PK tested (**Figure 32**). Surprisingly, M- and NM-PrP were less PK-resistant, implying that fusion with M altered the aggregate packing, rendering it more amenable to proteolysis. Full length protein was digested upon treatment with 20 µg/ml PK. Thus, resistance to PK appears to be conferred by the globular domain of PrP but can be modulated by the M fragment of Sup35p. Interestingly, PK treatment of PrP$_{90-230}$, PrP$_{cyto}$, N-PrP, M-PrP, NM-PrP, and to a minor extend of PrP-M, produced several low molecular weight fragments which were detected using the 3F4 antibody. Taken together, the globular domain of PrP promotes aggregate induction and is sufficient to confer PK resistance and partial insolubility.
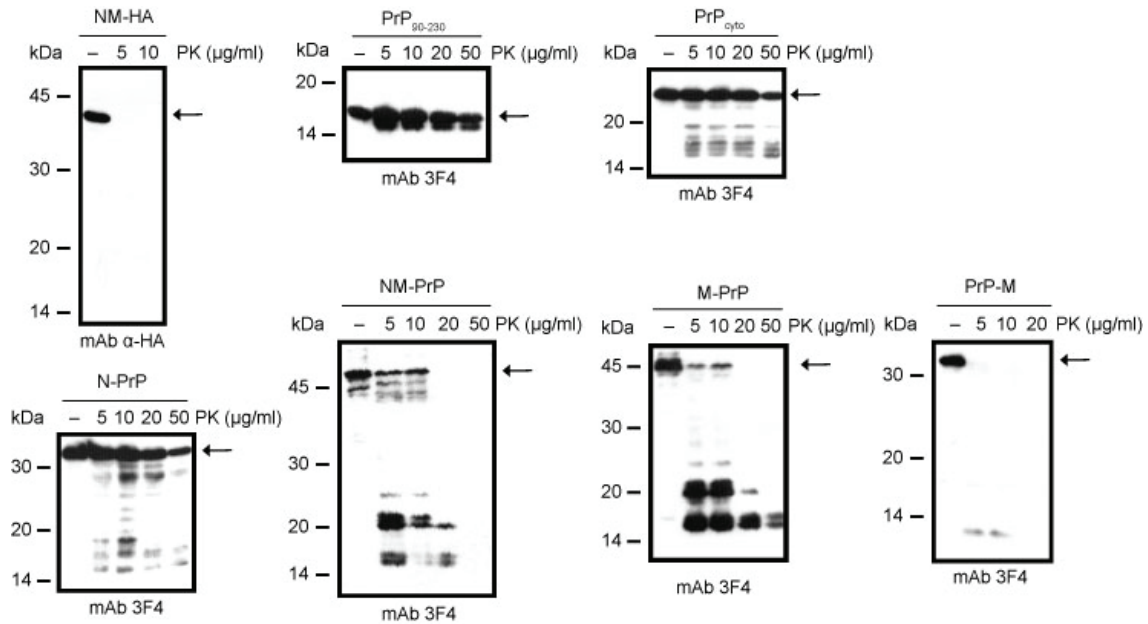
Figure 32 Proteinase K resistance of NM-PrP, M-PrP, N-PrP, PrP$_{cyto}$, and PrP$_{90-230}$. N2a cells were transfected with the respective constructs and harvested 48 h later. Lysates were subjected to PK treatment using the indicated amounts of protease. NM-PrP, M-PrP, N-PrP, PrP$_{cyto}$, PrP$_{90-230}$, and PrP-M were detected using mAb 3F4, while NM-HA was detected using anti-HA. Proteins harboring PrP$_{90-230}$ displayed increased protease resistance compared to NM-HA that was completely digested upon treatment with 5 µg/ml PK for 30 min. Some low molecular weight fragments were observed with PrP-M incubated with PK. Full-length proteins of the expected size are marked with arrows. Modified version published in (Krammer *et al.* 2008b).

IV.A.8 VERIFICATION THAT NM-HA DOES NOT AGGREGATE WHEN EXPRESSED IN N2A CELLS

The HA-tag in NM-HA is located at the very C-terminus of the protein. Therefore, it is possible that it is cleaved off after synthesis or during aggregate formation. In this case potential aggregates would not be detected. To test this possibility, an antibody against the N-terminus of NM (7H5) (generated and kindly provided by Dr. E. Kremmer, Helmholtz Zentrum, München) was used to detect HA-tagged NM in confocal microscopy as well as in WB analysis, respectively (**Figure 33**). A repetition of tests with the use of 7H5 revealed that NM-HA was in its non-aggregated state, soluble and PK sensitive. Hence, these experiments confirmed the results already obtained by using an anti-HA antibody excluding an oversight of NM-HA aggregates due to a possible loss of the HA-tag.
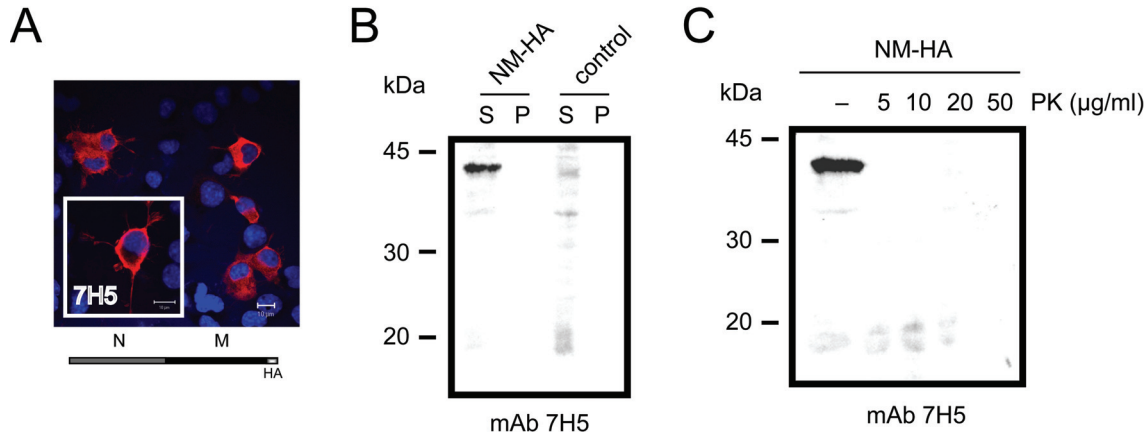
Figure 33. The use of a N-specific antibody confirms that NM-HA does not form detectable aggregates in mammalian cells. N2a cells were transfected with the NM-HA construct and studied 48 h post transfection. NM-HA was detected using rat monoclonal antibody 7H5. **A**: N2a cells expressing NM-HA were fixed and stained for NM-HA (red). Nuclei were visualized using Hoechst staining (blue). No visible foci were observed. Scale bar: 10 µm. **B**: Sedimentation assay of NM-HA. Lysate fractions were subjected to SDS gel electrophoresis. The fractions of insoluble (pellet = P) and soluble recombinant proteins (supernatant = S) are shown. As a control, untransfected cells were used. NM-HA remains exclusively in the supernatant. **C**: Proteinase K digestion of NM-HA. Cell lysates were subjected to PK treatment using the indicated amounts of PK. NM-HA was completely digested upon treatment with 5 µg/ml PK for 30 min. Published in (Krammer *et al.* 2008b).

IV.A.9 CYTOSOLIC PRP AGGREGATES DO NOT SEQUESTER ENDOGENOUS PRP MOLECULES

Aggregated Poly-Q proteins are able to incorporate normal soluble proteins harbouring sequence similarities to the aggregation domain (Haacke *et al.* 2006). PrP^C is located on the cell surface or in endo- and lysosomal vesicles and is therefore unlikely to come into contact with cytosolic aggregates. However, recent studies indicated a possible retrograde transport and cytosolic localization of PrP^C upon stress conditions (Orsi *et al.* 2006). Since the transfection procedure constitutes a stress situation for a cell due to overwhelming protein production it was tested if endogenous PrP is recruited into the cytosolic aggregates. An aliquot of N2a cells transfected with the different constructs was subjected to FACS analysis to detect cell surface PrP (**Figure 34 A**). The remaining cells were lysed and analyzed by Western blot to ensure proper transgenic protein expression (**Figure 34 B**). FACS analysis revealed that surface levels of PrP remained unaltered upon expression of chimeric constructs.
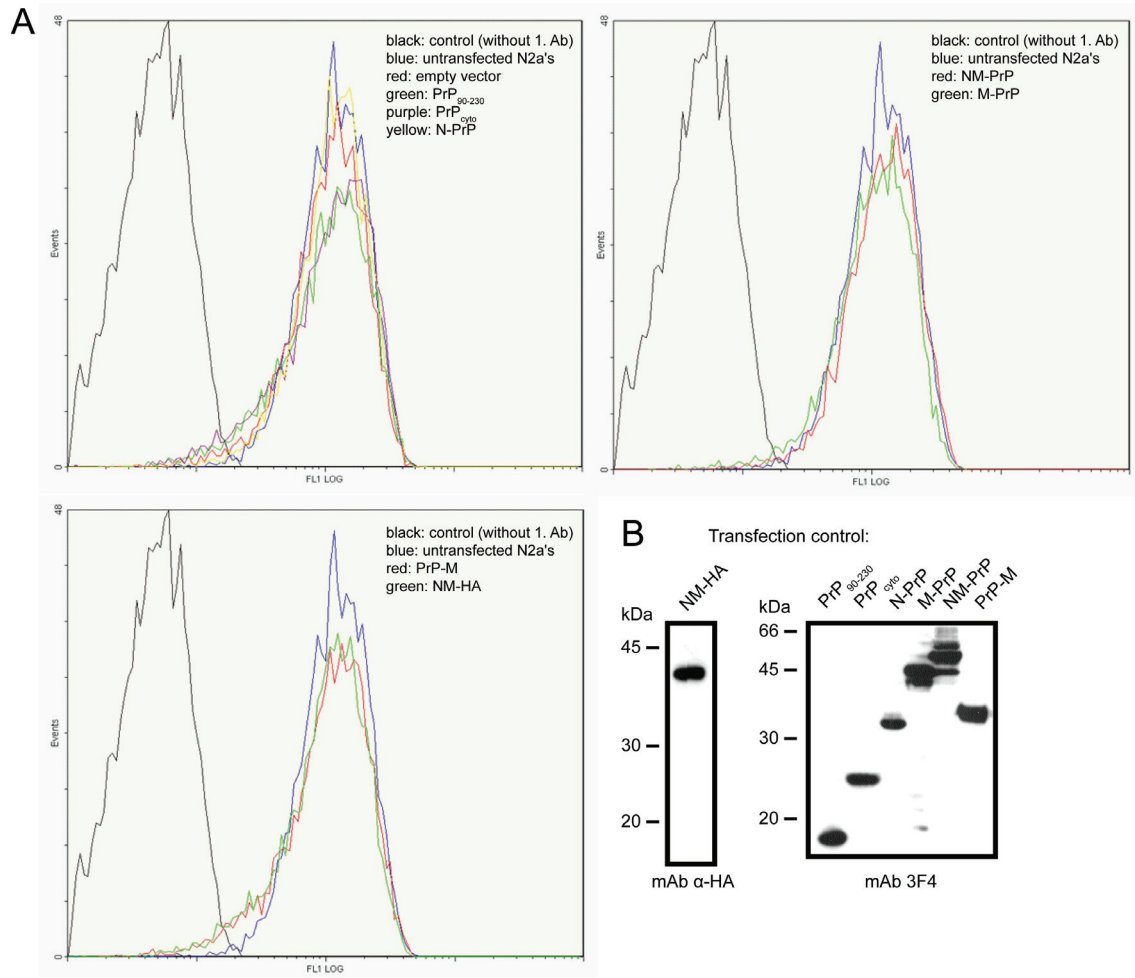
Figure 34. Examination of cell surface PrP expression. A: FACS analysis of cell surface PrP expression. N2a cells transiently transfected with the indicated constructs were harvested 48 h post transfection and surface PrP of unpermeabilized cells was stained with pAb A7 prior to FACS analysis. As controls N2a cells not stained with the primary Ab (black, negative control) and untransfected N2a cells (blue line, positive control) were used. **B**: Verification of cytosolic fusion protein expression. Fractions of transfected cells not used for FACS analysis were lysed and subjected to Western blot for detection of the indicated proteins with mAb 3F4 or anti-HA, respectively.

It could not be entirely ruled out that small amounts of endogenous PrP were incorporated into the aggregates even if the amount of cell surface PrP did not change. To exclude this possibility, a sedimentation assay of cells transfected with the chimeric proteins was performed and a potential shift in the distribution of endogenous PrP from supernatant to the pellet fraction was examined (**Figure 35**). To discriminate between wild-type PrP and the ectopically expressed cytosolic PrP mutants HpLMoPrPL42 cells were used that express only L42-epitope tagged mouse PrP (generated and kindly provided by Elke Maas). This mouse PrP molecule is a GPI-anchored wild-type PrP that harbors the amino acid substitution W144Y (MoPrPL42) (Vorberg *et al.* 1999). By using the antibody L42, only 'endogenous'

L42 epitope tagged PrP can be detected. L42 epitope tagged mouse PrP is expressed properly on the cell surface of HpL3-4 cells (data not shown). This experiment demonstrated that endogenous PrP was not recruited into the cytosolic aggregates.
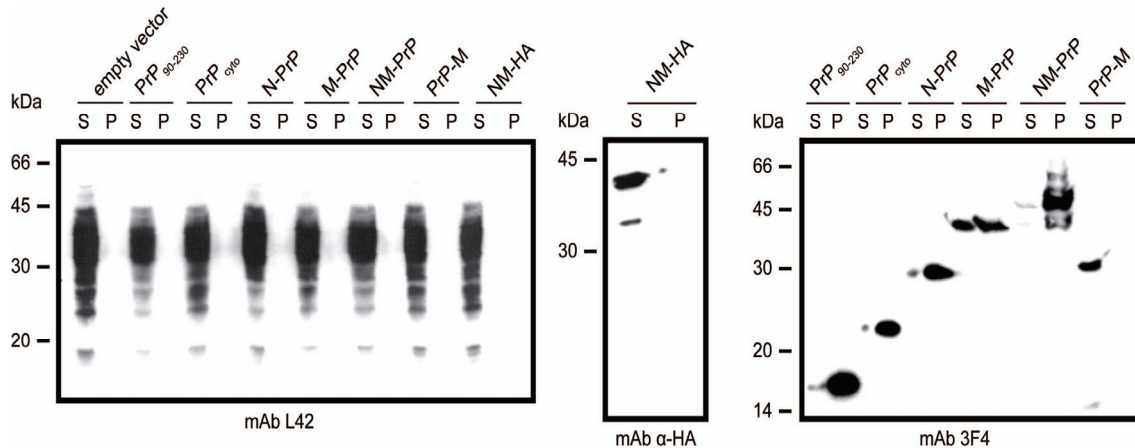

Figure 35. Endogenous L42 epitope tagged mouse PrP in transiently transfected cells is not localized in the pellet fraction. HpLMoPrPL42 cells transfected with the respective constructs were lysed and lysates were subjected to a sedimentation assay. The same supernatant and pellet fractions were loaded on two separate SDS-gels. In the subsequent Western blots, L42-tagged endogenous PrP as well as 3F4- and HA-tagged proteins were detected.

IV.A.10 CO-AGGREGATION OF CO-EXPRESSED CYTOSOLIC RECOMBINANT PROTEINS

Next, it was investigated if the cytosolic recombinant proteins were able to influence the aggregation propensity of another recombinant protein (Krammer *et al.* 2008a). Due to sequence overlap, only some recombinant proteins could be discriminated by the use of different antibodies. Cytosolic PrP was stained with an antibody against the octarepeat region, POM2 (Polymenidou *et al.* 2005), a kind gift of Dr. Polymenidou and Prof. A. Agguzzi (Institute of Neuropathology, University of Zürich). The N and M domains of Sup35p were visualized with the specific antibodies 7H5 or 4A5 (generated in collaboration with Dr. Elisabeth Kremmer; Helmholtz Zentrum München), respectively. First, the construct coding for cytosolic PrP was co-transfected with vectors coding for N-PrP, M-PrP or NM-PrP. Interestingly, PrP$_{cyto}$ and N-PrP localized in the same aggregates (**Figure 36**). Furthermore, M-PrP and NM-PrP also co-aggregated with PrP$_{cyto}$. Surprisingly, only small heterologous aggregates were formed, and the large foci typical for M- and NM-PrP disappeared.
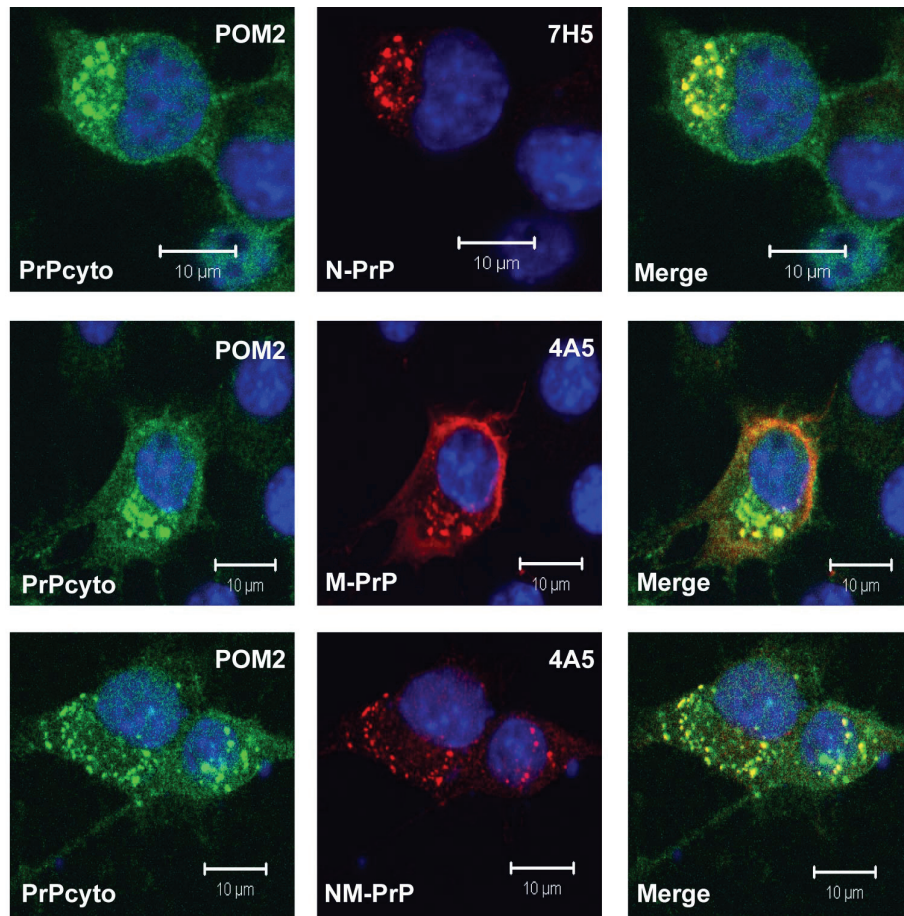
Figure 36. Co-aggregation of cytosolic recombinant proteins. N2a cells were transiently transfected with constructs coding for PrP_{cyto} and N-, M- or NM-PrP. 48 h post transfection cells were stained for PrP_{cyto} (POM2) and N-PrP (7H5), M- or NM-PrP (4A5), respectively, and analyzed by confocal microscopy. Nuclei were visualized using Hoechst staining (blue). Yellow color in the merged pictures indicates co-localization of both recombinant proteins. Scale bars: 10 µm. Published in (Krammer *et al.* 2008a).

Surprisingly, none of the aggregates was able to seed of NM-HA aggregation. Even co-expression of NM-PrP which harbors almost 100 % of the sequence of NM-HA did not lead to NM-HA aggregation (**Figure 37**). Taken together, PrP_{90-230} expression promotes co-seeding of proteins harbouring the PrP globular domain and leads to the appearance of small aggregates. By contrast, proteins that lacked sequence similarity to the globular domain of PrP were not able to co-aggregate. Thus, co-aggregation depends on the globular domain of PrP (Krammer *et al.* 2008a).

Figure 37. Co-expression of NM-HA and NM-PrP. N2a cells were transiently transfected with NM-HA and NM-PrP. 48 h post transfection cells were stained for NM-HA (anti-HA) and NM-PrP (3F4), respectively, for confocal microscopic analy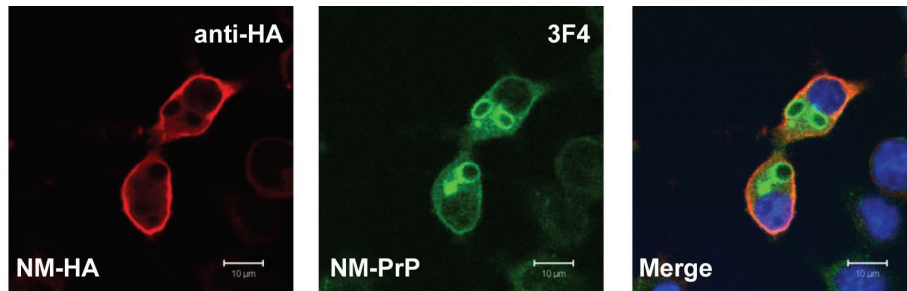sis. Nuclei were visualized using Hoechst staining (blue). No co-aggregation was observed. Scale bars: 10 µm. Published in (Krammer *et al.* 2008a).

IV.B SEEDING OF ECTOPICALLY EXPRESSED SUP35P-NM IN MAMMALIAN CELLS

The examined fusion proteins exhibited several characteristics of prions like an aggregated state, insolubility and partial PK-resistance. However, the induction rate of spontaneous aggregation was much higher (> 30 %) than the normal spontaneous incidence of the prion phenotype (1:10^6 [PSI$^+$] in yeast and sporadic CJD in humans). By contrast, NM-HA seemed to be soluble in the cytosol of mammalian cells even though an aggregation in one per million cells would probably remain undetected. Therefore, we wanted to test if Sup35p-NM aggregation could be seeded in the mammalian cytosol. Furthermore, possible prion-like properties of potential NM-HA aggregates should be investigated.

IV.B.1 SUB-CLONING OF SUP35P-NM-HA INTO RETRO- AND LENTIVIRAL EXPRESSION VECTORS

For the following experiments NM-HA should be stably expressed in N2a cells. In order to achieve this, NM-HA was subcloned from the pcDNA3.1/Zeo plasmid into retro- (pSFF) and lentiviral (LV-PGK) vectors (**Figure 38**). Retroviral particles were generated by transfection of pSFF into a co-culture of Ψ2 and PA317 packaging cells. Recombinant lentivirus was produced by Dr. Alexander Hofmann (laboratory of Prof. Alexander Pfeifer; Institute of Pharmacology and Toxicology, University of Bonn).
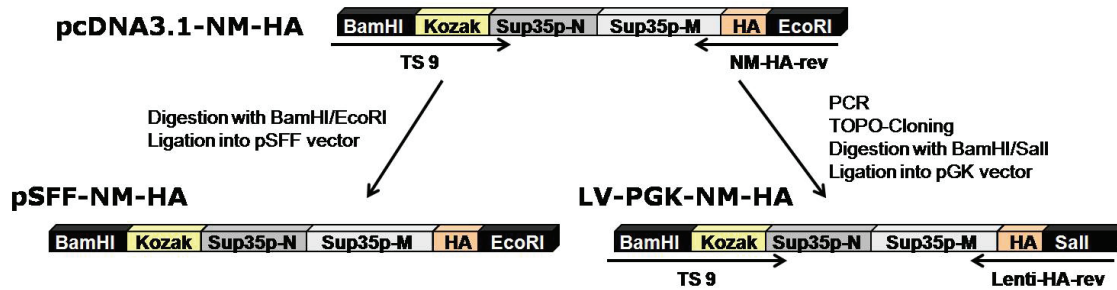
Figure 38. Cloning strategy with indicated restriction sites and/or primers used to generate retro- and lentiviral expression vectors. Detailed primer sequences are listed under III.A.7.

IV.B.2 GENERATION OF HpL3-4 AND N2A CELLS STABLY EXPRESSING NM-HA

HpL3-4 cells are highly susceptible to transduction with a retroviral vector system described previously (Maas *et al.* 2007). Therefore, this system was used to generate HpL3-4 cells stably expressing NM-HA, subsequently referred to as HpL3-4_NM-HA cells. Upon transduction, close to 100 % of the transduced cells expressed NM-HA (**Figure 39**). Unfortunately, this system was not suitable for N2a cells, as only about 40 % of the cells were positive after transduction with the retroviral particles. Therefore, recombinant lentivirus was used for the stable ectopic expression of NM-HA in N2a cells (N2a_NM-HA cells). With this system, almost 100 % of N2a cells were transduced and expressed the transgene (**Figure 39**). Similar to the results obtained with transient expression, NM-HA stayed soluble and was evenly distributed throughout the cytosol.
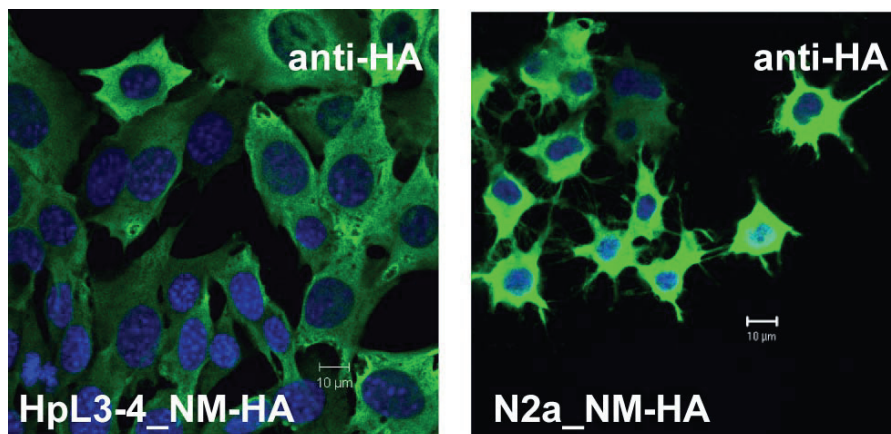

Figure 39. HpL3-4 and N2a cells stably expressing NM-HA. HpL3-4 cells were transduced using retroviral particles, N2a_NM-HA cells were generated using lentiviral particles. Cells were fixed and stained for NM-HA with anti-HA mAb and analized by confocal microscopy. Nuclei were stained with Hoechst dye (blue). No aggregation of NM-HA was observed. Scale bars: 10 μm.

IV.B.3 INDUCTION OF NM-HA AGGREGATION UPON TRANSIENT CO-EXPRESSION WITH POLYQ AGGREGATES

In yeast, *de novo* appearance of [PSI+] and aggregate formation is strongly enhanced in the presence of the host protein Rnq1 in its prion state, [PIN+] (Derkatch *et al.* 1996; Derkatch *et al.* 2000; Sondheimer & Lindquist 2000). Nevertheless, it was shown that other proteins harboring Q/N-rich regions or polyQ moieties can substitute [PIN+], potentially by acting as heterologous seeds (Osherovich & Weissman 2001; Derkatch *et al.* 2004) (**Figure 40 A**). To test if a Q/N-rich protein could also seed NM-HA aggregation in mammalian cells, N2a_NM-HA cells were transiently transfected with pEGFP-HD72Q, a construct encoding the exon 1 of huntingtin protein with a polyQ stretch of 72 glutamines (Sittler *et al.* 2001), kindly provided by Prof. E. Wanker (Max Delbrück Center of Molecular Medicine, Berlin). Indeed, NM-HA co-localized with HD72Q-GFP aggregates 48 h post transfection as assessed by confocal microscopy (**Figure 40 B**). However, NM-HA aggregates disappeared one week post transfection of HD72Q-GFP (**Figure 40 C**). The same results were obtained using HpL3-4_NM-HA cells. Thus, HD72Q-GFP was capable of seeding NM-HA aggregation, but the aggregated state was not maintained (Krammer *et al.* 2008a).
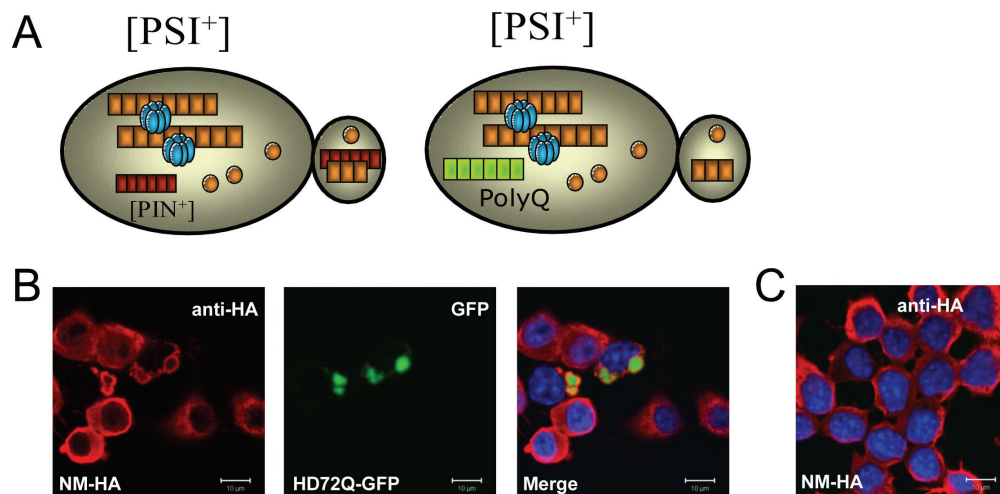
Figure 40. Aggregate induction by Q/N-rich proteins. A: Spontaneous induction of [PSI+] in yeast usually requires the presence of the Q/N-rich protein Rnq1 in its prion state [PIN+], potentially by acting as a heterologous seed for Sup35p aggregation. In [pin-] cells the [PSI+] phenotype can be induced by expression of a polyQ rich protein (Osherovich & Weissman 2001; Derkatch *et al.* 2004). **B**: Induction of NM-HA aggregation in mammalian cells by HD72Q-GFP. N2a cells stably expressing NM-HA (N2a_NM-HA cells) were transiently transfected with a construct coding for HD72Q-GFP. 48 h post transfection cells were stained for NM-HA (anti-HA) for confocal microscopic analysis. NM-HA appeared to aggregate around polyQ aggregates, forming ring-like structures. **C**: NM-HA aggregates did not propagate. One week post transfection cells were stained for NM-HA (anti-HA) and analyzed by confocal microscopy. No aggregates of NM-HA were detected. Nuclei were visualized using Hoechst staining (blue). Scale bars: 10 µm. Modified version published in (Krammer *et al.* 2008a).

IV.B.4 SEEDING OF ECTOPICALLY EXPRESSED NM-HA WITH RECOMBINANT
SUP35P-NM FIBRILS

In vitro formed amyloid fibrils from recombinant fungi prion proteins are infectious in yeast
and fungi providing formal proof of the protein-only hypothesis (Tanaka *et al.* 2004; King &
Diaz-Avalos 2004). According to experiments of the R. Wetzel group cultured cells are able
to take up proteinaceous aggregates from the medium into the cytosol without the necessity
of liposomal packaging (Yang *et al.* 2002). In analogy to these experiments, recombinant
Sup35p NM (kindly provided from Michael Suhre from the laboratory of Prof. Thomas
Scheibel; Lehrstuhl für Biomaterialien, Universität Bayreuth) was fibrillized *in vitro* and
added to N2a_NM-HA cells for 24 h in a final concentration of 1 µM (Krammer *et al.*
2009a). The cartoon (**Figure 41**) outlines the procedure in detail. N2a_NM-HA cells exposed
to NM fibrils were termed N2a_NM-HA+F.
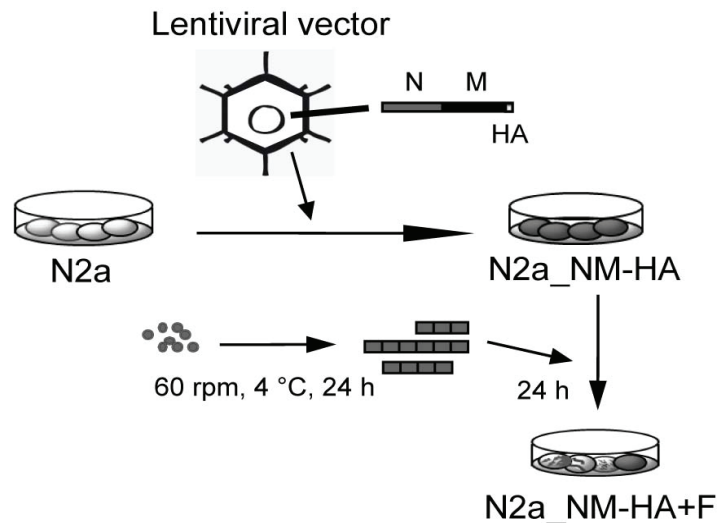
Figure 41. Schematic outline of the generation of N2a_NM-HA cells and the subsequent exposure to NM fibrils. N2a cells were
transduced using lentiviral particles to stably express NM-HA (N2a_NM-HA cells). These cells were treated with recombinant NM fibrils
(made at 4 °C rotating 60 rpm for 24 h) for 24 h, thereafter called N2a_NM-HA+F cells. Modified version published in (Krammer *et al.*
2009a).

The morphology of *in vitro* generated fibrils was investigated by atomic force microscopy
(AFM) with the kind support of Michael Suhre, confirming the formation of recombinant NM
fibrils (**Figure 42**). Additionally, recombinant NM fibrils were stained with our 4A5 mAb
and analyzed by confocal microscopy. Fibrillar structures with comparable sizes to the fibrils
observed by AFM were apparent.
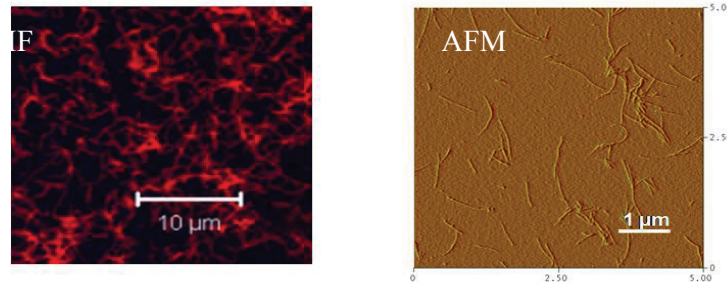
Figure 42. Morphology of NM fibrils. Recombinant NM (10 μM in PBS) was rotated at 60 rpm and 4 °C for 24 h, diluted 1: 10 in $H_2O_{dest.}$ and subsequently subjected to AFM analysis (right panel) or diluted 1:10 into cell culture medium incubated on cover slips, and analyzed by confocal microscopy after staining with 4A5 mAb (left panel). Scale bars: 1 or 10 μm, respectively. Modified version published in (Krammer *et al.* 2009a).

Sedimentation assays 48 h post exposure of cells to recombinant NM fibrils demonstrated insoluble NM-HA in cells exposed to fibrillar NM, while no NM-HA was present in the pellet fraction of untreated N2a_NM-HA cells (**Figure 43 A**). Furthermore, confocal microscopy analysis 48 h post fibril exposure was performed to assess induction of aggregate formation. In line with previous experiments, stably expressed NM-HA remained soluble in N2a_NM-HA cells not exposed to NM fibrils (**Figure 43 B**). By contrast, exposure of N2a_NM-HA cells to recombinant NM fibrils led to aggregation of endogenous NM-HA in about 50-60 % of the cells due to NM fibrils taken up by the cell (**Figure 43 C**), indicating that external addition of NM induced cytosolic co-aggregation with NM-HA.
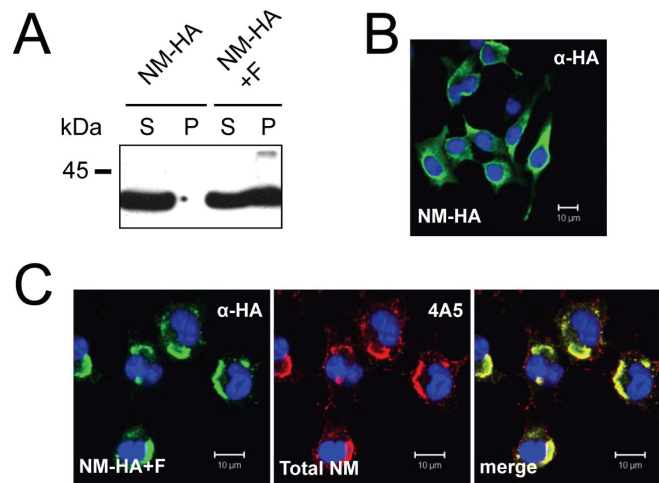
Figure 43. Induction of NM-HA aggregation by exogenous NM fibrils. A: Sedimentation assay of NM-HA in cell lysates upon aggregate induction by exogenous recombinant NM fibrils (NM-HA+F). S: Supernatant; P: Pellet. Antibody: anti-HA (detects only endogenous HA-tagged NM). **B** and **C**: Confocal microscopy analysis of N2a_NM-HA before (B) and after (C) exposure to recombinant NM fibrils. NM-HA was detected using an anti-HA antibody, total NM (endogenous and exogenous) was identified using NM-specific antibody 4A5. Scale bars: 10 μm. Published in (Krammer *et al.* 2009a).

IV.B.5 INDUCTION ACTIVITY CORRELATES WITH THE FIBRILLAR FORM OF RECOMBINANT NM

The recombinant protein solution added to the cells likely contained a mixture of soluble NM and NM fibrils. Therefore, we investigated which conformational state of NM was responsible for aggregation. Vortexing of the fibril suspension previous to dilution into the medium led to increased fibril particles with decreased sizes (**Figure 44 B**). When these fibrils were used for treatment, the induction rate increased to about 70 - 80 %.

The effect of soluble recombinant NM on endogenous NM-HA aggregation could not be assessed under the given experimental conditions, as it readily formed fibrils as soon as 1 h post dilution into cell culture medium (data not shown). Subsequent kinetics of aggregate induction revealed that a 30 min exposure to recombinant NM fibrils was sufficient to induce NM-HA aggregates in N2a_NM-HA cells (**Figure 44 B, C and D**). Under these conditions, the majority of recombinant freshly dissolved NM stayed soluble and failed to induce NM-HA aggregation in N2a_NM-HA cells as determined by confocal microscopy and sedimentation analysis of NM-HA (**Figure 44 B, C and D**), strongly arguing that aggregate inducing activity correlated with the amyloid-like state of recombinant NM. In summary, exogenously added NM-HA fibrils serve as templates for the aggregation of soluble endogenous NM-HA (Krammer *et al.* 2009a).
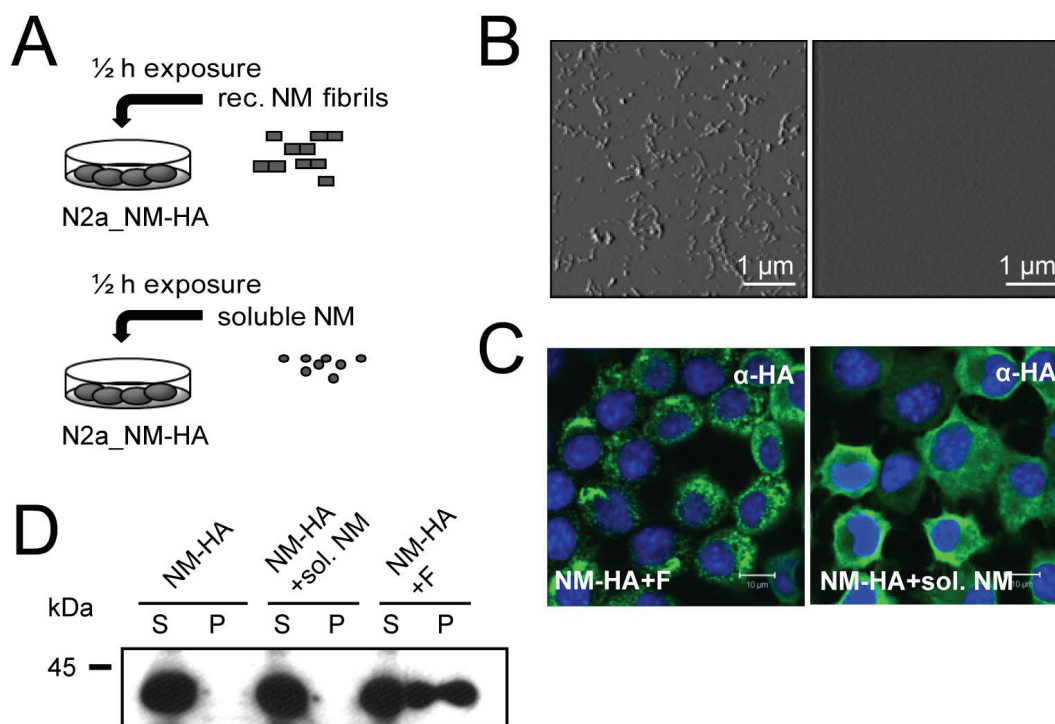
Figure 44. Induction of aggregate formation by recombinant NM is dependent on fibrillar NM. A: The bulk population of N2a_NM-HA cells expressing soluble NM-HA was exposed to recombinant NM fibrils or soluble recombinant NM for 30 min and the aggregation state of endogenous NM-HA was assessed 1 week later. **B**: AFM analysis of recombinant NM used for NM-HA aggregate induction in N2a_NM-HA cells. Left panel: Recombinant NM fibrils (1 µM in cell culture medium) after rotation at 4 °C, 24 h, vortexing and incubation for 30 min at 37 °C (under cell culture conditions). Right panel: recombinant soluble NM (1 µM in cell culture medium) after incubation for 30 min at 37 °C (under cell culture conditions). **C**: Confocal microscopy analysis of N2a_NM-HA cells 1 week post exposure to soluble NM or NM fibrils. Scale bars: 10 µm. **D**: Sedimentation assay of NM-HA expressed by N2a_NM-HA cells 1 week post exposure to soluble NM or NM fibrils. S: Supernatant, P: Pellet. Antibody: anti-HA. Published in (Krammer *et al.* 2009a).

IV.B.6 KINETICS OF ENDOGENOUS AGGREGATE FORMATION

Next, we investigated when endogenous NM-HA begins to aggregate after fibril application. Therefore, N2a_NM-HA cells were treated with 1 µM NM fibrils and cells were fixed for subsequent immunofluorescence analysis at different time points post exposure. Small endogenous NM-HA aggregates were found as soon as 6 h after fibril application (**Figure 45**) while there were no aggregates in control cells incubated with PBS. The shape of the cellular membrane was altered after the addition of fibrils, also in N2a cells not expressing NM-HA (**Figure 45**). These membrane alterations resemble membrane ruffles that are usually associated with uptake of larger particles or bacteria (Steele-Mortimer *et al.* 2000; Chhabra & Higgs 2007).

N2a_NM-HA+PBS
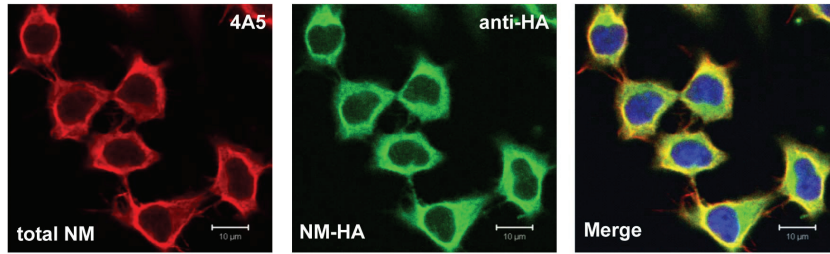
N2a_NM-HA+F 6 h
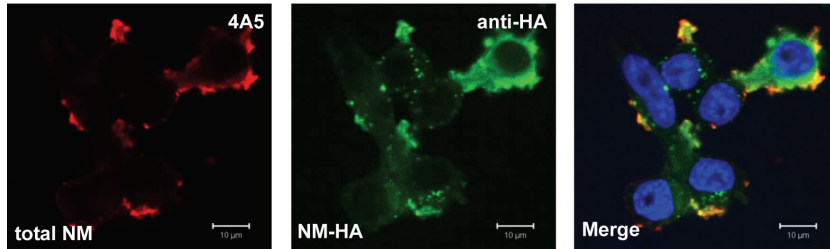
N2a+F 6 h
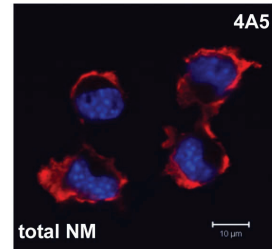
Figure 45. Kinetics of endogenous NM-HA aggregation. N2a_NM-HA cells were treated with PBS (upper panels) or recombinant NM fibrils (lower panels). 6 hours post exposure endogenous NM-HA began to aggregate due to exogenous fibril application while there were no aggregates in N2a_NM-HA cells incubated with PBS. Membrane ruffles were also seen with N2a cells not expressing NM-HA after addition of NM fibrils (right panel). Total amounts of NM were detected with 4A5 mAb, while endogenous NM-HA was visualized using anti-HA antibody. Scale bars: 10 μm.

IV.B.7 NM-HA AGGREGATES ARE HERITABLE IN MAMMALIAN CELLS

Surprisingly, one passage post exposure to recombinant fibrils, approximately 40-60% of cells still contained dot-or spindle-shaped aggregates, while the remainder cells displayed diffuse cytosolic fluorescence. Additionally, a substantial amount of NM-HA was present in the insoluble fraction upon sedimentation, while NM-HA that had not been induced to aggregate remained soluble (**Figure 46 A**). NM-HA aggregation was also evident ten passages post induction, indicating that the aggregated NM-HA state was inherited by daughter cells (**Figure 46 A and B**). Up to now, aggregates were faithfully propagated for more than 30 passages (data not shown). Hence, mammalian cells maintain NM-HA aggregates despite the lack of cytosolic disaggregase Hsp104, an important chaperone for prion propagation in yeast (Chernoff *et al.* 1995), and any known ortholog thereof.
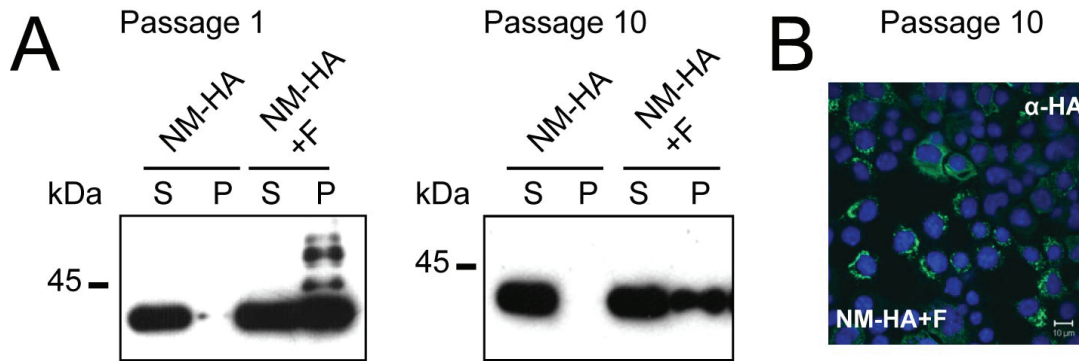
Figure 46. N2a_NM-HA cells were exposed to NM fibril preparations and subsequently passaged one to ten times. A. Sedimentation assay of lysates of cells expressing NM-HA that were not treated with fibrils (N2a_NM-HA) or exposed to fibrils (N2a_NM-HA+F). S: Supernatant; P: Pellet. Anti-HA antibody was used for detection. B. Confocal microscopy analysis of N2a_NM-HA cells ten passages post exposure to fibrils (N2a_NM-HA+F) using HA-specific antibody. Scale bar: 10 μm. Published in (Krammer *et al.* 2009a).

IV.B.8 AGGREGATED NM-HA DISPLAYS SLIGHTLY INCREASED PK RESISTANCE COMPARED TO SOLUBLE NM-HA

Resistance to PK digestion is a characteristic property of PrP^{Sc} and the aggregated form of Sup35p. However, the difference in PK resistance of Sup35p in [psi$^-$] versus [PSI$^+$] cells is not as dramatic as the difference in PK resistance between PrP^C and PrP^{Sc} (Meyer *et al.* 1986; Paushkin *et al.* 1996). Investigations of PK sensitivity of NM-HA in N2a_NM-HA and N2a_NM-HA+F cells revealed a marginally increased PK resistance of NM-HA after aggregate induction with recombinant fibrils (**Figure 47**). Soluble NM-HA originated from uninduced cells was almost fully degraded upon treatment with 1 μg/ml PK. However, uninduced NM-HA exhibited a significant PK-resistance upon digestion with 1 μg/ml PK in N2a cells resulting in a protein band at 30 kDa. Characteristic degradation products were also shown for Sup35p in [psi$^-$] but not in [PSI$^+$] yeast cells (Paushkin *et al.* 1996). Interestingly, a small fraction of NM-HA originated from N2a_NM-HA+F cells was still not degraded by 5 μg/ml PK.
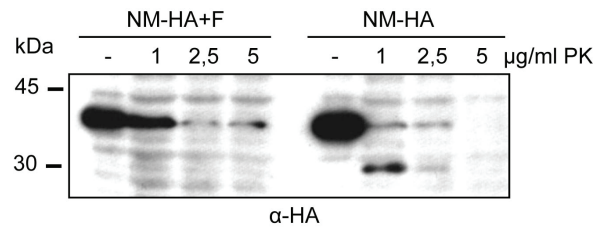
Figure 47. Comparison of PK resistance of induced (NM-HA+F) and not induced HA-tagged Sup35p-NM. N2a cells stably expressing NM-HA before and after induction with recombinant Sup35p-NM fibrils were lysed and lysates treated with the indicated amounts of proteinase K (PK) at 37 °C for 30 min. After SDS-PAGE, the subsequent WB was developed with anti-HA antibodies.

IV.B.9 PHENOTYPICALLY DISTINCT NM-HA AGGREGATES IN PROGENY CELLS

In vitro generated Sup35p-NM molecules are known to form multiple, distinct and faithfully propagated fiber types (DePace & Weissman 2002) and infection of yeast with these different amyloid conformations leads to the emergence of different [PSI+] variants (Tanaka *et al.* 2004). Therefore, we examined if the recombinant Sup35p-NM fibrils we used gave rise to different aggregate types in the induced cells. Indeed, high resolution images of cells exhibiting NM-HA aggregates revealed several phenotypically distinct aggregate types that appeared to be present in different cells (**Figure 48 A**). Some cells contained several larger spindle-shaped NM-HA aggregates, while in others small punctuate NM-HA aggregates occurred at high frequency, and a lot of other intermediate aggregate types were found. Additionally, some cells displaying soluble NM-HA were observed.
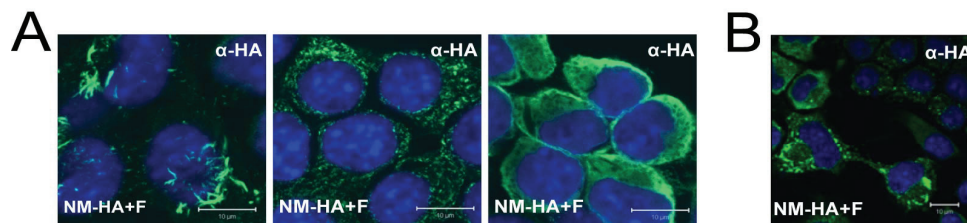
Figure 48. Distinct NM-HA aggregates are heritable. A: Higher resolution images of N2a_NM-HA+F cells reveal distinct aggregate types. **B**: dividing cells indicate hereditary NM-HA aggregates by daughter cells. Antibody: anti-HA. Scale bars: 10 μm. Published in (Krammer *et al.* 2009a).

Cells with similar aggregate types were localized in close proximity and cells undergoing division appeared to transfer only their specific aggregate type to offspring (**Figure 48 B**), indicating that one cell clone might propagate only one aggregate type. To investigate this hypothesis cells were diluted to a single cell level and single clones were raised for analysis (**Figure 49**).
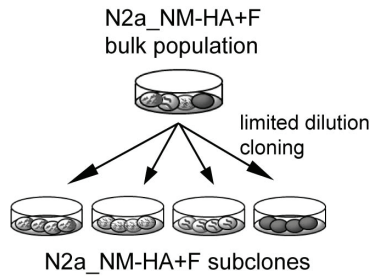
Figure 49. Schematic cartoon of single cell cloning. The N2a_NM-HA bulk population that had been exposed to recombinant NM fibrils was cloned and individual subclones were isolated. Published in (Krammer *et al.* 2009a).

Indeed, distinct NM-HA aggregates in individual clones were stably propagated (**Figure 50 A**).
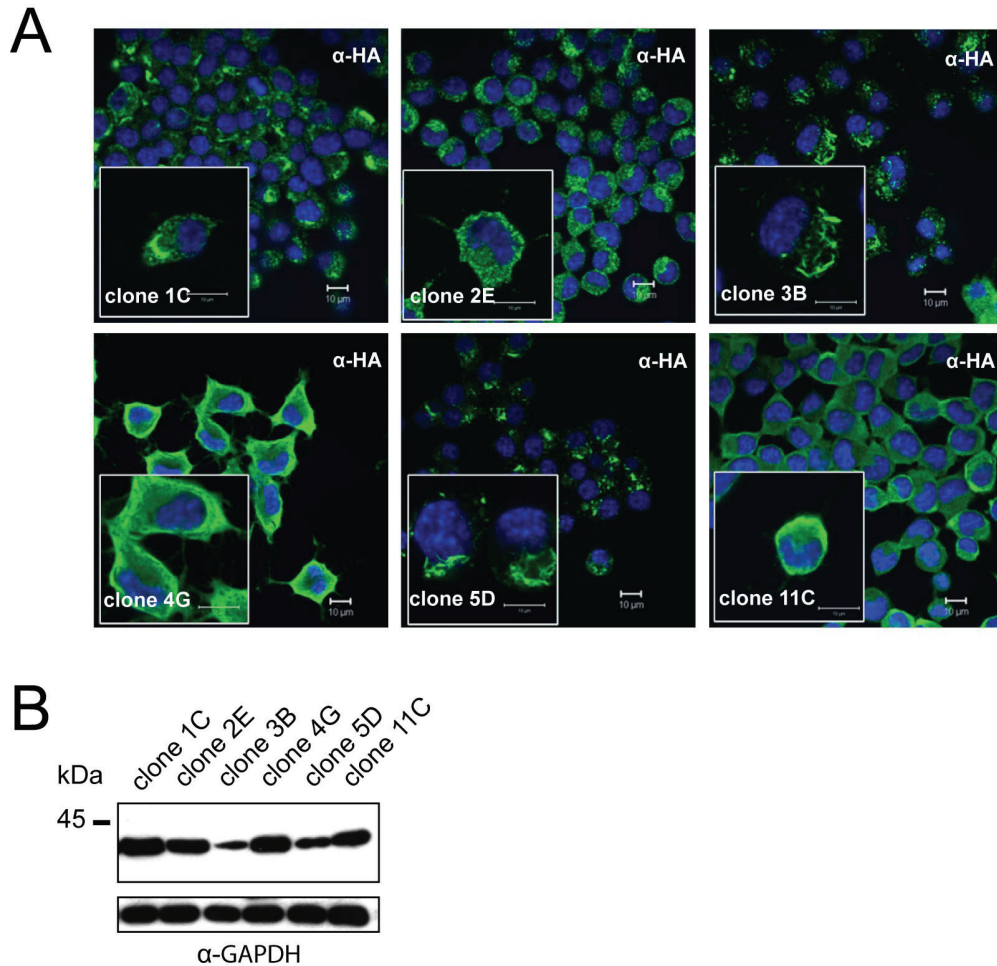
Figure 50. Distinct aggregate phenotypes in progeny cells. A: Confocal microscopy analysis of N2a_NM-HA+F subclones demonstrates inheritance of aggregate phenotypes by progeny cells. Anti-HA antibody. Clones 4G and 11C displayed no visible NM-HA aggregates. Scale bars: 10 µm. **B**: Relative expression levels of NM-HA by individual clones. NM-HA was detected by anti-HA antibody, GAPDH expression demonstrates equal loading of the samples. Published in (Krammer *et al.* 2009a).

The majority of daughter cells displayed similar NM-HA aggregate phenotypes, indicating that only one given variant was faithfully propagated in a certain cell clone once induced (Krammer *et al.* 2009a). Aggregation was observed also in clones with relatively low NM expression levels (compare **Figure 50 A and B**). Thus, aggregate induction did not appear to correlate with increased expression of NM-HA. Clones 3B and 5D that exhibited relatively low expression levels displayed long fibrillar NM-HA aggregates and clone 4G and 11C, which expressed relatively high levels of NM-HA, did not contain visible aggregates. Of note, sedimentation assays confirmed insoluble NM-HA only in clones that displayed NM-HA aggregates by confocal microscopy (**Figure 51**).
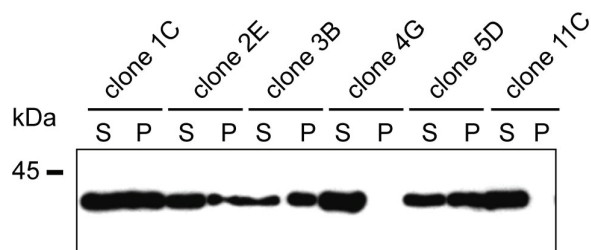
Figure 51. Sedimentation assay of NM-HA in individual cell clones of N2a_NM-HA+F cells. S: Supernatant; P: Pellet. Antibody: anti-HA. Published in (Krammer *et al.* 2009a).

IV.B.10 CELL TYPE DEPENDENT DIFFERENCES IN INDUCED NM-HA PHENOTYPES

Induction of endogenous NM-HA aggregation by addition of recombinant NM fibrils to the medium was also possible in HpL3-4 cells that stably express NM-HA. Similar to aggregates induced in N2a cells, aggregates were heritable and were maintained upon continuous passage. However, HpL3-4_NM-HA+F cells displayed only dot-like aggregates of different sizes; no fibrillar aggregates could be detected (**Figure 52**). Thus, the appearance of phenotypical variants of NM-HA aggregates appears to be cell-type specific.
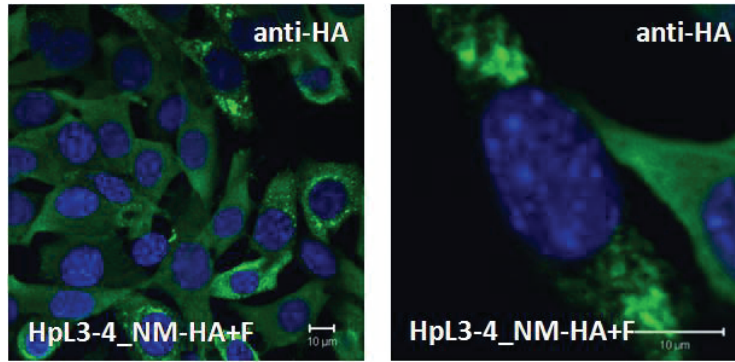
Figure 52. Heritable aggregates in HpL3-4_NM-HA+F cells. HpL3-4 cells stably expressing NM-HA were treated with recombinant NM fibrils and analyzed by confocal microscopy after passage 2. Only dot-like aggregates were found. NM-HA aggregates were stained with anti-HA antibody. Scale bars: 10 μm.

IV.B.11 NM-HA AGGREGATES ARE INFECTIOUS

An extraordinary characteristic that sets prions apart from other misfolded proteins is that they are infectious. To assess if NM-HA aggregates derived from N2a cells were infectious, single cell clones with distinct aggregate phenotypes and bulk N2a_NM-HA expressing soluble NM-HA were sonicated into PBS and cell extracts were incubated with N2a_NM-HA cells for 24 h (**Figure 53**).
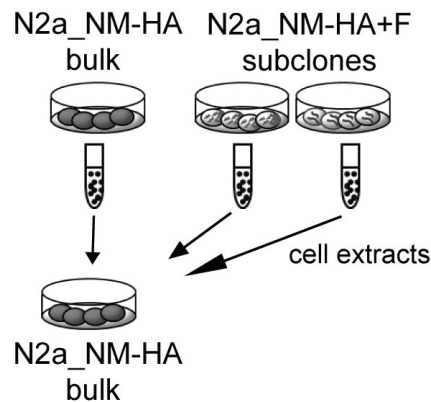
Figure 53. Cartoon of infection assay. The bulk population of N2a_NM-HA cells was exposed to cell extracts of N2a_NM-HA+F subclones 1C and 5D both displaying aggregated NM-HA or to cell lysates of N2a_NM-HA cells expressing soluble NM-HA. Published in (Krammer *et al.* 2009a).

Rinsed cells were passaged one week and studied for endogenous NM-HA aggregation by confocal microscopy. Exposure of wild-type N2a cells to cell extract of clone 5D that displayed visible NM-HA aggregates confirmed that exogenous NM-HA aggregates were no

longer detectable one week post exposure (**Figure 54**, upper panel left). Aggregation was induced only in N2a_NM-HA cells exposed to lysates containing aggregated NM-HA but not in cells incubated with cell lysates containing soluble NM-HA (**Figure 54**). Aggregation of NM-HA was also apparent in subsequent passages of cells exposed to aggregated NM-HA, demonstrating that aggregation was not a transient phenomenon. Interestingly, infection of N2a_NM-HA cells with phenotypically distinct NM-HA aggregates gave rise to NM-HA aggregates of various sizes and shapes similar to N2a_NM-HA cells after induction with recombinant fibrils (**Figure 54**, see two characteristic aggregate types per infection with a lysate of a single cell clone). Thus, NM-HA aggregates are infectious but do not necessarily replicate as the dominant variant of the precursor cell clone (Krammer *et al.* 2009a).
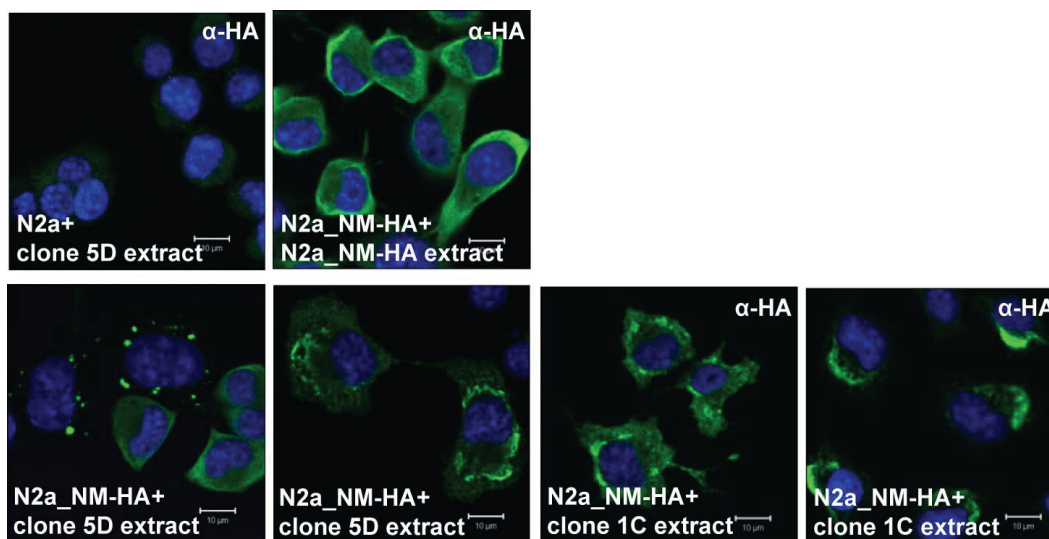
Figure 54. NM-HA aggregates are infectious. Confocal microscopy analysis of cell extract exposed N2a (control) and N2a_NM-HA cells one week post exposure using anti-HA antibody. Note that the aggregate phenotype was not precisely phenocopied upon induction in recipient bulk N2a_NM-HA population. Published in (Krammer *et al.* 2009a).

IV.B.12 CELLULAR FACTORS INFLUENCE AGGREGATE TYPES

Phenotypically distinct aggregate types of donor cells were not faithfully propagated in the infected recipient N2a_NM-HA bulk population, although in this case the infectious agents should consist of only one type of aggregate and not of a mixture as in the case of recombinant NM fibrils used in the first set of experiments. Therefore the cellular influence on aggregate formation was investigated. The bulk population of N2a_NM-HA cells not exposed to recombinant NM fibrils was cloned (**Figure 55**).
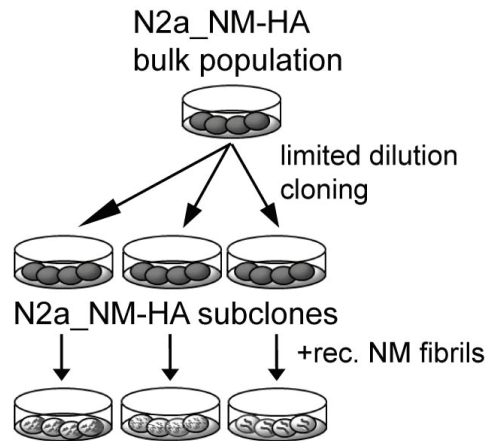
Figure 55. Schematic outline of the experiment. The bulk population of N2a_NM-HA cells was cloned prior to exposure to recombinant NM fibrils. Published in (Krammer *et al.* 2009a).

Ten clones were raised and analyzed. Results of six clones are shown. All studied clones expressed NM-HA as investigated by confocal microscopy (**Figure 56**).
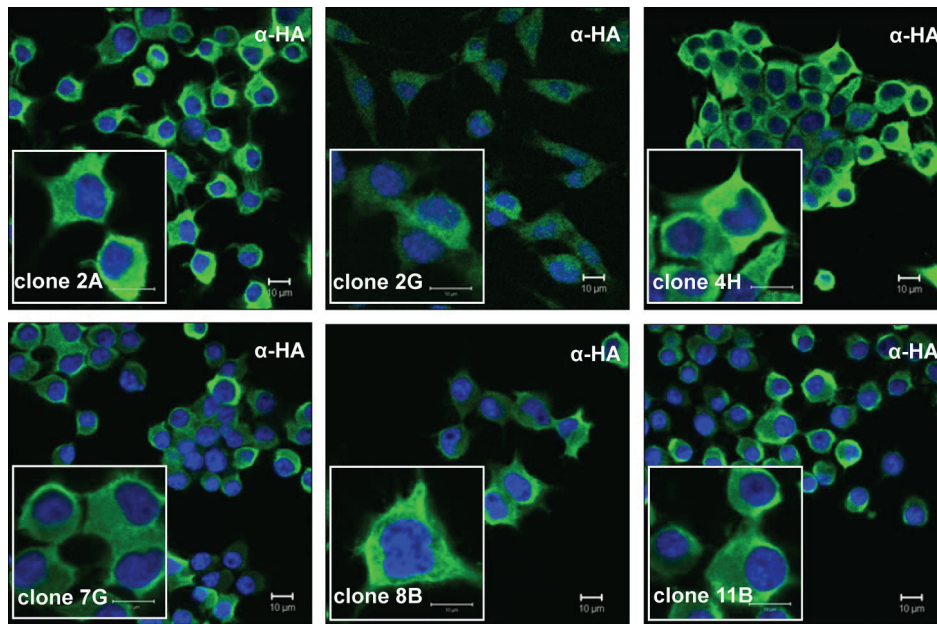
Figure 56. Immunofluorescence analysis of individual N2a_NM-HA subclones. Clones were analyzed for NM-HA solubility by confocal microscopy using anti-HA antibodies. No aggregates were detected. Scale bars: 10 µm. Published in (Krammer *et al.* 2009a).

In a sedimentation assay the NM-HA solubility in the different clones was investigated (**Figure 57**). Of note, for clone 8B a small amount of NM-HA was found in the pellet fraction, indicating NM-HA insolubility before treatment with recombinant NM fibrils, potentially due to high over-expression.
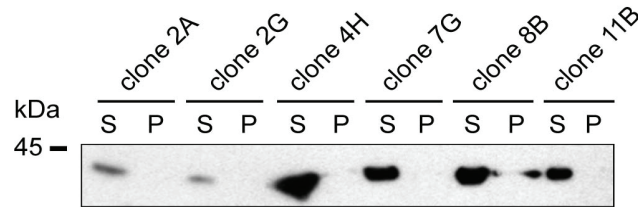
Figure 57. Characterization of NM-HA solubility in individual N2a_NM-HA cell clones. A sedimentation assay was performed to demonstrate solubility of NM-HA before aggregate induction. NM-HA of clone 8B exhibited some insolubility. S: Supernatant, P: Pellet. Antibody: anti-HA. Published in (Krammer *et al.* 2009a).

Single cell clones expressing different amounts of soluble NM-HA (**Figure 58 B**) were subsequently exposed to recombinant NM fibrils. In all ten clones tested (six are shown here), aggregates were induced upon fibril application (**Figure 58 A**).
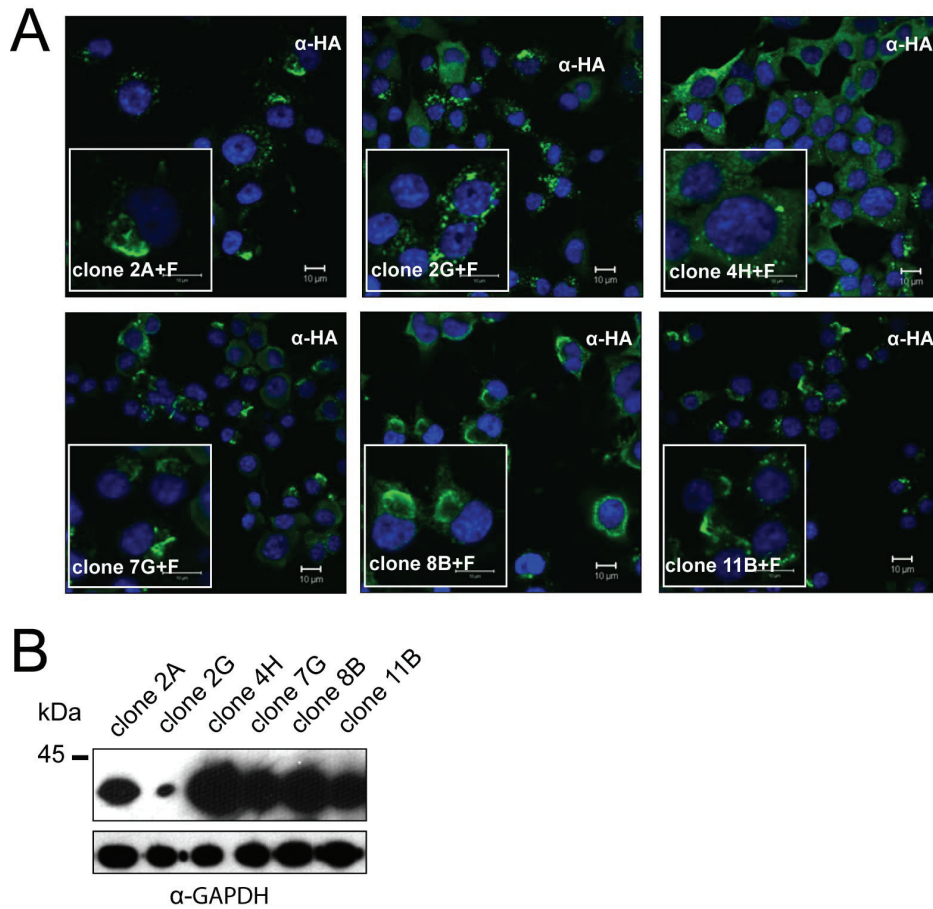
Figure 58. Cellular factors influence the NM-HA aggregate phenotype. A: N2a_NM-HA subclones were exposed to recombinant NM fibrils and analyzed one week later. Individual cells in a given clonal population exhibit similar aggregate phenotypes as assessed by confocal microscopy using anti-HA antibodies. Scale bars: 10 μm. **B**: Relative NM-HA expression levels in N2a_NM-HA cells clones prior to exposure to recombinant NM fibrils. The blot was probed with anti-HA antibodies, GAPDH was detected to demonstrate comparable protein loading. Published in (Krammer *et al.* 2009a).

Interestingly, cell clones preferentially propagated one or sometimes two aggregate types, suggesting a strong clonal effect on variant selection. Fibrillar and dot-like aggregates were comparable to aggregates observed in **Figure 50 A**. Aggregate induction did not appear to correlate with increased expression of NM-HA, as clone 2G exhibited a very low expression level but displayed visible NM-HA aggregates (compare **Figure 58 A** and **B**). A subsequent sedimentation assay confirmed induction of insoluble aggregates upon treatment with recombinant fibrils (**Figure 59**).
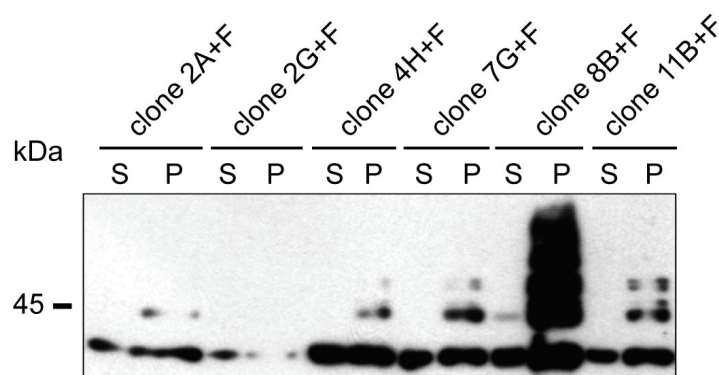
Figure 59. Insolubility of NM-HA in subclones exposed to recombinant NM fibrils. A sedimentation assay was performed to demonstrate insolubility of NM-HA upon aggregate induction. Note the increased amount of insoluble NM-HA in the pellet fraction of clone 8B+F. S: Supernatant, P: Pellet. Antibody: anti-HA. Published in (Krammer *et al.* 2009a).

IV.B.13 VARIATIONS IN TEMPERATURE SENSITIVITY OF PHENOTYPICALLY DISTINCT NM-HA AGGREGATES INDICATES DIFFERENT PROTEIN CONFORMATIONS

The diverse NM-HA aggregate types could result from different amyloid structures of recombinant NM fibrils taken up by single cells. To investigate potential structural variations biochemical characteristics of the different aggregate types were determined. It has previously been shown that fibrils of Sup35p-NM generated *in vitro* at different temperature exhibited differences in resistance to thermal solubilization in the presence of SDS (Tanaka *et al.* 2004). These distinct physical properties indicate different fiber conformations. To detect potential conformational variations, temperature sensitivity of NM-HA in lysates of individual clones was assessed. Cell lysates with equal protein amounts were mixed with 1 % SDS and incubated for 15 min at indicated temperatures (**Figure 60**). Adequate volumes were

loaded on a one-dimensional SDS gel (12,5 %) according to the expression level of NM-HA of individual clones to ensure comparable amounts of NM-HA on the gel.
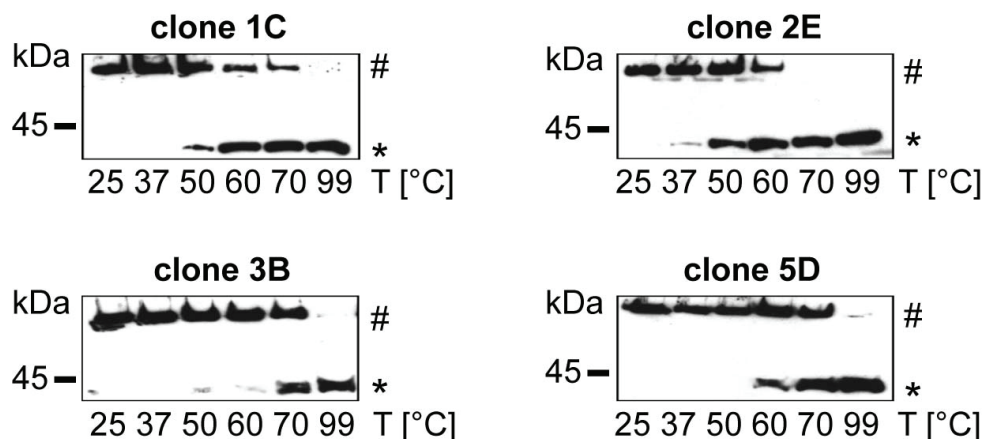
Figure 60. Resistance of NM-HA aggregates from individual N2a_NM-HA+F subclones to thermal denaturation in the presence of SDS. Cell lysates supplemented with 1 % SDS were incubated for 15 min at indicated temperatures. Subsequent SDS-PAGE and Western blot analysis revealed solubilization of NM-HA aggregates in lysates of clones 1C, 2E, 3B, and 5D at different temperatures. The upper bands (marked with #) depict SDS insoluble protein remaining in the pockets of the gel whereas the lower bands represent SDS soluble NM-HA (marked with *). Antibody: anti-HA. Published in (Krammer *et al.* 2009a).

Band intensities were quantified and relative amounts of SDS soluble proteins were plotted against temperature and fitted to a sigmoidal function (Boltzmann equation) (**Figure 61**).

Figure 61. Graphic representation of NM-HA aggregate solubilization. Band intensities of SDS soluble proteins were plotted against temperature and fitted to a sigmoidal function. Statistical analysis was performed using two-way ANOVA with Bonferroni's multiple comparison test and revealed highly significant differences between all curves ($p<0.0001$). Published in (Krammer *et al.* 2009a).

The resulting curves exhibited statistically highly significant differences (two-way ANOVA with Bonferroni's multiple comparison test, $p<0.0001$). NM-HA aggregates from clone 2E displayed the lowest melting temperature (Tm = 45 ± 3 °C), followed by NM-HA aggregates of clone 1C (Tm = 55 ± 3 °C) and clone 5D (Tm = 62 ± 3 °C). NM-HA aggregates of clone 3B were most resistant to thermal denaturation (Tm = 69 ± 3 °C). The melting transition was comparable, only NM-HA aggregates from clone 3B (W = 5 ± 0 °C) differed to some extend from NM-HA aggregates of the other clones 1C (W = 9 ± 6 °C), 2E (W = 15 ± 4 °C) and 5D (W = 11 ± 4 °C). As curves were generated from cells of continuous passages, passage history appeared to have little effect on the relative stabilities of NM-HA aggregates. In summary, NM-HA aggregates from individual clones exhibit different biochemical properties. While the possibility that relative NM-HA expression levels of individual clones may influence the aggregate phenotypes cannot completely be ruled out, it is possible that the distinct NM-HA conformations observed for different cell clones represent diverse NM-HA variants/strains (Krammer *et al.* 2009a).

IV.B.14 OVER-EXPRESSION OF NM-HA AFFECTS THE APPEARANCE OF AGGREGATE TYPES

To investigate the influence of NM-HA expression level on the aggregate phenotype, NM-HA was transiently over-expressed in individual clones exhibiting different phenotypical variants. Clones displaying the highest variation in NM-HA expression levels and aggregate phenotypes were selected and transiently transfected with NM-HA to increase the expression level of NM-HA. (**Figure 62**). The phenotype of the different types of aggregates was altered in individual cells upon transient over-expression of NM-HA, suggesting that the aggregate phenotype is influenced by NM-HA expression levels. The thick and long fibrillar aggregates of clone 3B turned into many smaller and shorter aggregates upon transient over-expression of NM-HA. Interestingly, they clustered in a semi-circular mode and tended to localize along the membrane. A similar phenomenon of aggregate clustering along the membrane has previously been described for yeast over-expressing either NM or wild-type Sup35p (Zhou, 2001). Taken together, the phenotypically distinct appearance of the aggregates appears to be not a direct result of different NM-HA conformations as the aggregate phenotype could be modulated by increasing the amount of NM-HA. Of note, NM-HA over-expression in one clone did not lead to a change into the NM-HA aggregate phenotype of a clone with a higher

NM-HA expression level but rather gave rise to a new phenotypical variant. Thus, aggregate phenotypes of the different clones are changeable but not inter-changeable among each other by elevating levels of NM-HA. It is possible that a higher NM-HA expression level increases the induction rate and thus results in more frequent and smaller aggregates. Of note, the aggregate phenotypes returned to the original phenotypes one week post transfection (data not shown), demonstrating that phenotype changes upon NM-HA over-expression were transient.
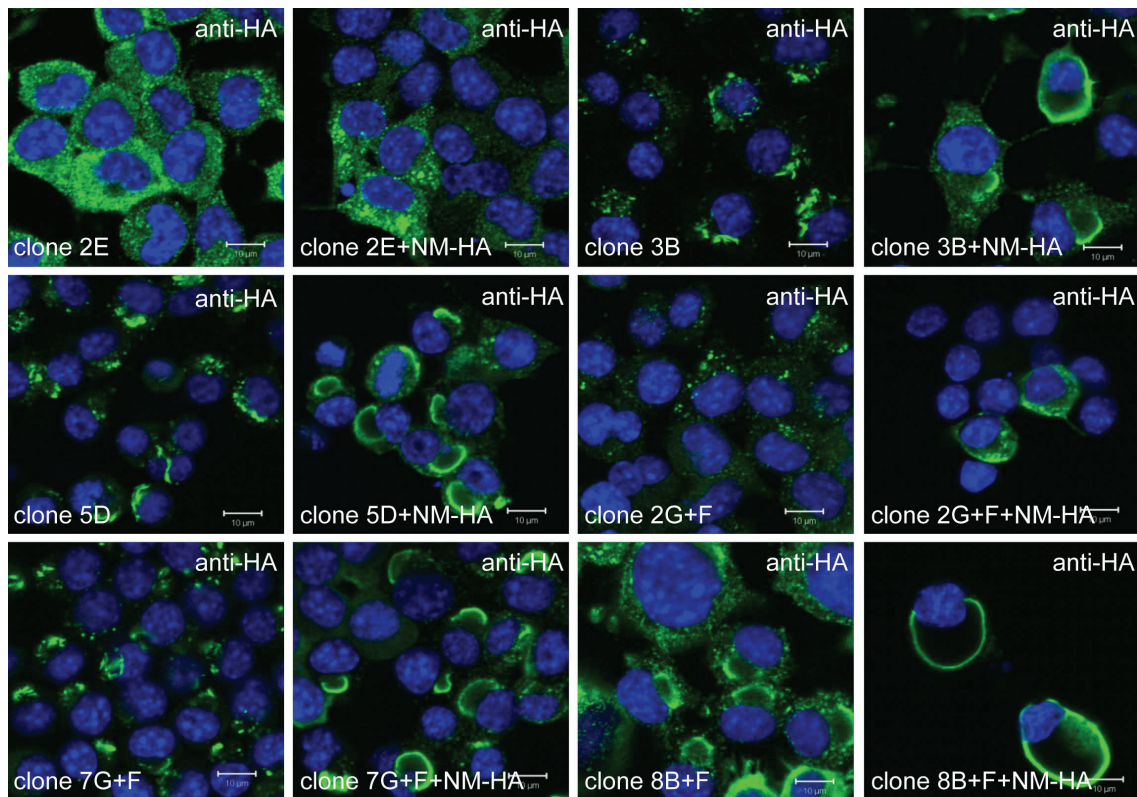
Figure 62. Over-expression of NM-HA changes the phenotype of aggregates propagated in different clones. Three NM-HA+F clones which were cloned after aggregate induction (clone 2E, 3B and 5D) and three NM-HA clones that were first isolated and subsequently exposed to recombinant NM fibrils (clone 2G+F, 7G+F and 8B+F) were chosen for analysis. Cells were transiently transfected with a plasmid coding for NM-HA and analyzed 48 h post transfection by confocal microscopy. Antibody: anti-HA. Scale bars: 10 μm.

IV.B.15 OVER-EXPRESSION OF NM-HA ONLY MARGINALLY INFLUENCES BIOCHEMICAL CHARACTERISTICS OF NM-HA AGGREGATES PROPAGATED BY DIFFERENT CLONES

The results above suggested that phenotypical and possibly also biochemical differences in aggregate types were not indicative of different variants or strains but rather a result of different NM-HA expression levels in individual clones. To test if also biochemical characteristics of aggregates changed, the influence of NM-HA over-expression on the temperature sensitivity of NM-HA aggregates was tested. If the different types of NM-HA aggregates have distinct conformations, then the relative NM-HA expression levels should have no effect on their characteristic melting curve. Clone 3B and 5D were chosen to test this hypothesis. Western blot analysis confirmed that the expression levels of NM-HA in these clones were increased about 2-fold 48h post transfection of pcDNA3.1/Zeo-NM-HA (**Figure 63**).
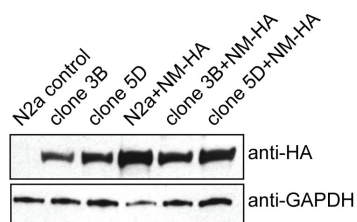
Figure 63. Expression levels of NM-HA after transient over-expression of NM-HA in wild-type N2a and N2a_NM-HA+F subclones 3B and 5D. Cells were transfected with pcDNA3.1/Zeo-NM-HA and lysates were subjected to SDS-PAGE and WB 48 h later. Antibody: anti-HA. Anti-GAPDH was used as a loading control.

The temperature sensitivity of NM-HA aggregates in lysates of clone 3B and 5D after over-expression of NM-HA was assessed as described above (**Figure 64**).
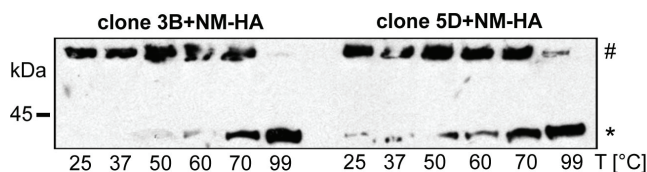
Figure 64. Resistance of NM-HA from clone 3B and 5D to thermal denaturation in the presence of SDS after over-expression of NM-HA. Cell clones were transiently transfected with pcDNA3.1/Zeo-NM-HA and analyzed 48 h later. Lysates supplemented with 1 % SDS were incubated for 15 min at indicated temperatures. Subsequent SDS-PAGE and Western blot analysis revealed solubilization of NM-HA aggregates in lysates of clones 3B+NM, and 5D+NM at different temperatures. The upper bands (marked with #) depict SDS insoluble proteins remaining in the pockets of the gel whereas the lower bands represent SDS soluble NM-HA (marked with *). Antibody: anti-HA.

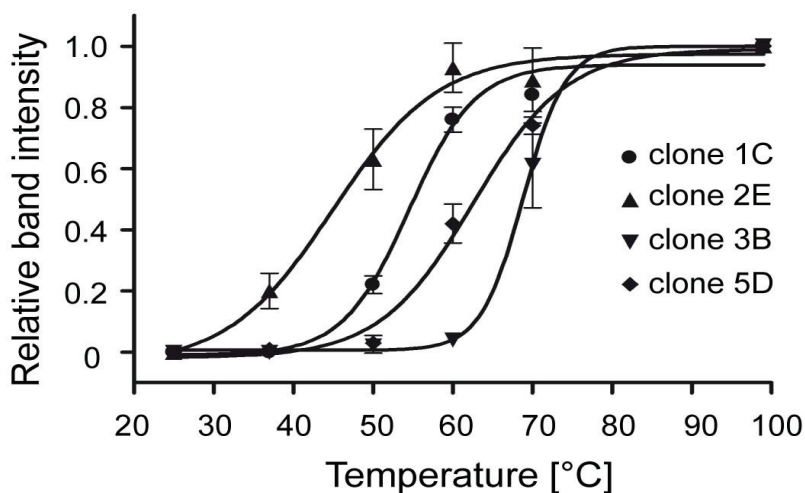As before, band intensities were quantified and relative amounts of SDS soluble proteins were plotted against temperature and fitted to a sigmoidal function (**Figure 65**). Again, the resulting curves highly significantly differed (two-way ANOVA with Bonferroni's multiple comparison test, $p<0.001$). NM-HA aggregates from clone 3B+NM-HA exhibited a melting temperature of Tm = 71 ± 2 °C and a melting transition of W = 7 ± 2 °C, whereas NM-HA aggregates from clone 5D+NM-HA were less resistant to thermal denaturation (Tm = 64 ± 5 °C; W = 11 ± 5 °C). More importantly, the curves of clone 3B+NM-HA and 5D+NM-HA did not significantly differ from the curves of clone 3B and 5D, respectively. Thus, the biochemical properties of the different aggregate types remained stable upon transient over-expression of NM-HA. While the relative NM-HA expression levels of individual clones do influence the aggregate phenotypes, the stable biochemical properties still strongly suggest distinct NM-HA conformations in different cell clones.
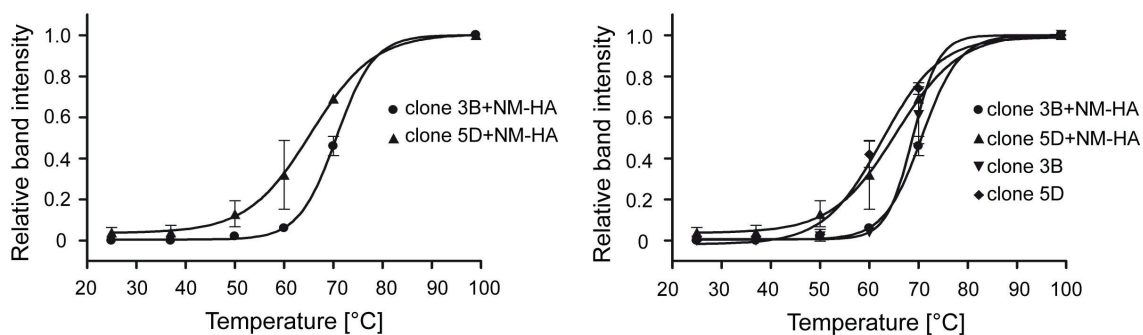
Figure 65. Graphic representation of NM-HA aggregate solubilization. Band intensities of SDS soluble proteins of clone 3B+NM-HA and clone 5D+NM-HA were plotted against temperature and fitted to a sigmoidal function (left panel). The graphs of SDS temperature sensitivity of NM-HA from clone 3B and 5D were added to the graphic for a direct comparison (right panel). Statistical analysis were performed using two-way ANOVA with Bonferroni's multiple comparison test and revealed significant differences between the curves of clone 3B+NM-HA and 5D+NM-HA ($p<0.001$) but no significant differences between the curves of clone 3B and 3B+NM-HA or clone 5D and clone 5D+NM-HA, respectively.

V. DISCUSSION

V.A AGGREGATION PROPENSITIES OF CYTOSOLIC PRP AND PRP/SUP35-NM FUSION PROTEINS

Almost every protein is able to form amyloids *in vitro* (Dobson 2003; Stefani & Dobson 2003). Still, why some proteins also aggregate *in vivo* is poorly understood. Intracellular deposits of misfolded proteins are a feature of many neurodegenerative diseases, but only prions appear to be infectious. Aim of this study was to elucidate general aspects of protein aggregation and the mechanisms of prion formation in mammalian cells. In the first part of this work a model system was established to compare Sup35p and mouse PrP in mammalian cell cultures to elucidate potential *cis* acting elements involved in cytosolic aggregate formation. Here we demonstrate that although both prion proteins were able to form amyloid-like fibrils *in vitro* (Bousset & Melki 2002), they exhibited very different aggregation behaviors when expressed in mammalian cells. While Sup35p-NM remained soluble, all recombinant proteins containing the C-terminal part of PrP (PrP_{90-230}) underwent rapid spontaneous aggregation in N2a cells.

V.A.1 THE NM DOMAIN IS INSUFFICIENT TO PROMOTE AGGREGATION IN MAMMALIAN CELLS

An interesting finding of this work was that the prion forming domain of yeast Sup35p alone was incapable of acquiring an aggregated state when expressed in the cytosol of mammalian cells (**Figures 22, 30, 32, 33 and 39**). The exact mechanism of prion induction in yeast remains enigmatic. *De novo* [PSI+] prion induction in yeast is a rare event (Lund & Cox 1981; Liu & Lindquist 1999) but can be increased up to 1000-fold by over-expression of the Sup35p prion domain (Derkatch *et al.* 1996). However, studies with GFP tagged Sup35p-NM have demonstrated that the *de novo* appearance of [PSI+] upon over-expression of NM-GFP requires the presence of another prion-like element, termed [PIN+] (Derkatch *et al.* 1996; Derkatch *et al.* 1997; Derkatch *et al.* 2000; Osherovich & Weissman 2001; Derkatch *et al.* 2001; Derkatch *et al.* 2004). Alternatively, endogenous Sup35p-NM can be seeded by transformation of *in vitro* converted Sup35p into uninfected yeast cells (Sparrer *et al.* 2000).

These experiments strongly argue that [PIN$^+$] or other aggregation prone Q/N-rich proteins can act *in trans* as a heterologous seeds that support Sup35p aggregate initiation. Proteinaceous deposits that are capable of cross-seeding the aggregation of NM might thus be missing in the cytosol of N2a cells under normal cell culture conditions. This normal solubility of NM is similar to the aggregation behaviour of proteins causing polyQ diseases. The normal cellular proteins are mainly soluble in cell culture, only large extensions of the GAT sequence of the respective genes and/or a proteolytic cleavage results in aggregate formation of the encoded proteins (Taylor *et al.* 2002; Hoffner & Djian 2002; Haacke *et al.* 2006). Therefore, it might be possible, that the Q/N-rich tract in NM is too short to be able to spontaneously aggregate in mammalian cells. However, it is also feasible that aggregated or misfolded NM is recognized by the cell and rapidly destined to cellular degradation. In this case, impairment of protein degradation, for example by inhibition of the proteasome and autophagic system, might facilitate NM aggregate formation, as has been demonstrated for other aggregation-prone proteins, such as membrane-anchored PrP (Mishra *et al.* 2003).

V.A.2 Cytosolic PrP spontaneously forms visible aggregates in N2a cells

Over-expression of PrP$_{cyto}$ in N2a cells led to the formation of visible aggregates in approximately one forth of the transfected cells (**Figure 22**). Cells expressing PrP$_{cyto}$ appeared to grow slower and detached more easily than cells transfected with other constructs or control vector, indicating that PrP$_{cyto}$ exerted at least some toxic effect on cells. Aggregated cytosolic PrP exhibited several biochemical characteristics similar to that of PrP^{Sc}, such as insolubility in non ionic detergents and partial resistance to PK (**Figures 30 and 32**). These findings are in good agreement with previously reported results (Ma & Lindquist 2002; Drisaldi *et al.* 2003; Rambold *et al.* 2006). Several lines of evidence argue that aggregate induction of the fusion proteins was mediated by the globular domain of PrP comprising residues 90-230. First, PrP$_{90-230}$ alone is able to form visible aggregates. Second, fusion of N, M or NM to this PrP region yielded aggregation-prone molecules that readily formed large deposits in mammalian cells, while NM alone appeared to be incapable of forming visible aggregates. Third, replacement of the N domain in Sup35p-NM with the amino-terminal part of PrP (aa 23-120) in PrP-M only led to a very marginal increase in the tendency to spontaneously aggregate. Our data are consistent with recent findings suggesting

that the intracellular aggregation determinant of PrP lies within its globular domain (Grenier *et al.* 2006). Interestingly, the amino-terminal region of PrP (aa 23-89) appeared to negatively influence the nucleation rate of the globular domain of PrP, as deletion of this region (PrP_{90-230}) resulted in a significant increase in the amount of cells with aggregates (**Figure 23**). Thus, fusion of PrP_{23-89} to PrP_{90-230} leads to a lower rate of nucleation. So far no overt cytotoxic effect has been observed for N-PrP, M-PrP and NM-PrP (data not shown). Further studies will be necessary to elucidate if replacement of the amino-terminal part of PrP with Sup35p regions can modulate toxicity of cytosolic PrP.

V.A.3 AGGREGATE FORMATION APPEARS TO BE INDEPENDENT OF AN ACTIVE CELLULAR SEQUESTRATION INTO AGGRESOMES OR LYSOSOMES

Many neurodegenerative diseases and several other systemic diseases are caused by toxic, misfolded proteins that negatively affect cellular function and viability (Scheibel & Buchner 2006). Therefore, cells have evolved several defense mechanisms against potentially dangerous aggregation-prone proteins. The first line of defense constitutes molecular chaperones which are responsible for appropriate folding of nascent proteins. If they fail, proteins that are not properly folded are transported to the ubiquitin-proteasome system for degradation. Large amounts of misfolded proteins would eventually overwhelm these two systems. Thus, misfolded proteins can be sequestered into aggresomes and/or subjected to degradation by autophagy. Recent studies revealed that aggresome formation takes place in several neurodegenerative disorders (Kopito 2000; Taylor *et al.* 2002). However, there are conflicting data about aggresome formation of PrP and its beneficial or disadvantageous effects. Most studies suggested a positive role of aggresome formation rendering aggregation-prone proteins inert and not capable of impairing cellular function (Kopito 2000). By contrast, in permanently scrapie infected cells, PrP^{Sc} was shown to accumulate under mild proteasome impairment. These aggresomes appeared to negatively influence cell viability (Kristiansen *et al.* 2005) while non-disease associated, normal PrP remained soluble, even though it was also localized in the cytosol. Another study reported that transiently over-expressed cytosolic PrP leads to the assembly of aggregated PrP_{cyto} into juxtanuclear aggresome-like structures (Grenier *et al.* 2006). Additionally, mutant GPI-anchored PrP molecules were shown to accumulate in the cytosol in response to proteasome inhibition and were sequestered into aggresomes (Mishra *et al.* 2003). In our hands, transiently expressed

PrP$_{cyto}$ as well as the other fusion proteins readily formed aggregates which were distributed throughout the cytosol. Aggregates neither located in close proximity to the nucleus in the microtubule organization center (MTOC), nor were they encaged by vimentin intermediate filaments. Thus, our results argue that the observed proteinaceous deposits do not constitute classical aggresomes. Moreover, it has been shown that aggresome formation might facilitate the final degradation of aggregation-prone proteins by autophagy (Kopito 2000). Autophagosomes that engulf misfolded proteins subsequently fuse with lysosomes. However, there was no co-staining of any of the visible aggregates with the lysosomal marker Lamp-1, indicating that protein aggregates were not cleared by lysosomes. Furthermore, we have demonstrated that none of the aggregates were enclosed by membranous structures suggesting that aggregation of PrP$_{90-230}$, PrP$_{cyto}$, N-PrP, M-PrP and NM-PrP in the cytosol of mammalian cells is a spontaneous event independent of an active cellular sequestration of misfolded proteins. *In vitro* fibrillization experiments revealed that both NM-HA and NM-PrP are able to form amyloid-like fibrils (Krammer *et al.* 2008b). This fact suggests that conditions in the cellular environment highly influence their ability to aggregate. The following reasons may account for the finding that PrP$_{90-230}$, PrP$_{cyto}$, N-PrP, M-PrP and NM-PrP are capable of accumulating in the cytosol of mammalian cells, while Sup35p NM and PrP-M remain soluble (**Figure 66**).

First, the physiological conditions in the mammalian cytosol per se (e. g., pH) might promote aggregation of the globular domain of PrP, while the same conditions leave soluble NM-HA and PrP-M relatively unaffected. Second, a so far unidentified anti-aggregation molecule (e. g., a chaperone) might bind to NM-HA and PrP-M and thus inhibit aggregation, while this factor is unable to inhibit aggregation of PrP$_{90-230}$, PrP$_{cyto}$, N-PrP, M-PrP and NM-PrP. Third, interaction of an aggregation co-factor with the globular domain of PrP might induce aggregation of PrP$_{90-230}$, PrP$_{cyto}$, N-PrP, M-PrP and NM-PrP. This factor, however, is not able to bind to NM-HA and PrP-M, explaining why these proteins remain soluble. Finally, in mammalian cells a seed composed of aggregated heterologous protein might exist that can specifically cross-seed cytosolic PrP or fusion proteins containing the globular domain of PrP. This seed is incapable of interacting with the NM domain of Sup35p. Further investigations are necessary to confirm this model and to narrow down the important regions in mouse PrP for aggregation as well as to identify potential interaction molecules in the

cytosol. Taken together, cell-specific conditions or factors influence nucleation rate and seeding capacity of N, M and PrP regions.
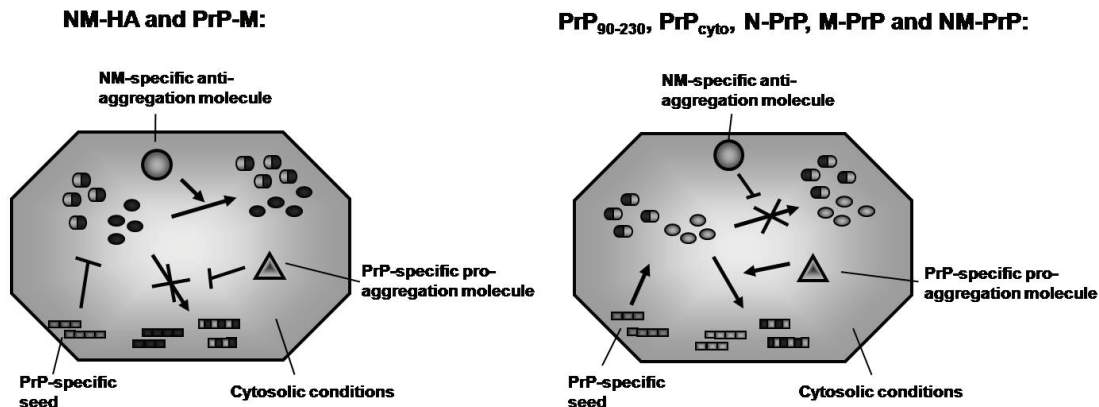
Figure 66. Hypothetical model to explain how aggregation is influenced by the mammalian cell. PrP$_{cyto}$, PrP$_{90-230}$, N-PrP, M-PrP and NM-PrP spontaneously aggregate in the cytosol of mammalian cells, either due to the specific cellular environment, to un-identified pro-aggregation molecules or to cross-seeding by heterologous protein aggregates. Environmental conditions or missing co-factors as well as a NM-specific anti-aggregation molecule might inhibit aggregation of NM-HA. Published in (Krammer *et al.* 2008b).

V.A.4 THE N AND M DOMAINS OF SUP35P MODULATE NUCLEATION AND SIZE OF CYTOSOLIC PRP AGGREGATES

Our data suggest that substitution of the amino-terminus of PrP by N and M confers altered aggregation characteristics to PrP, since fusion of the Sup35p N and M regions to PrP influenced frequency and size of aggregates in the cytosol of mammalian cells. N-PrP mainly formed granular deposits similar to the smaller aggregates observed with PrP$_{cyto}$ (**Figure 22**). By contrast, expression of M- and NM-PrP led to the appearance of large, dot-like or ring-shaped aggregates (**Figure 22**). A similar phenomenon of ring-shaped and dot-like NM aggregates has previously been reported for yeast over-expressing either NM or wild-type Sup35p (Zhou *et al.* 2001). In yeast, worm- or ring-like aggregates appeared frequently during *de novo* prion induction, while they were usually absent when Sup35p was over-expressed in [PSI$^+$] cells. These findings suggest that large aggregates represent intermediates involved in the early stages of [PSI$^+$] formation rather than mature prion aggregates (Zhou *et al.* 2001; Ganusova *et al.* 2006). However, aggregates observed in yeast displayed a true ring structure that could also appear as twisted or branched. Projection of z series demonstrated a spheroidal shape and ball-like structure for M- and NM-PrP aggregates in N2a cells, arguing

that the ring-like appearance observed in our studies was likely due to antibodies solely binding to the outer rim of the dense, large aggregates.

The fact that fusion of Sup35p regions to the globular domain of PrP influenced frequency of aggregate appearance and/or aggregate size indicates that these domains could still exert a modulating activity on PrP aggregation. Here, the nucleation rate was only marginally influenced by the N domain of Sup35p, as fusion of N to PrP$_{90-230}$ did not lead to a higher number of cells displaying visible aggregates (**Figure 23**). The Sup35p-N domain constitutes the prion-forming domain in yeast and comprises oligopeptide repeats as well as a Q/N-rich domain reminiscent to the polyQ stretches in several disease-associated aggregation-prone proteins. Despite the fact that yeast Sup35p and PrP do not share sequence similarities, the amino-termini of both proteins are flexibly unstructured and harbor an oligopeptide repeat region. Expansions of the repeat regions are associated with familial prion diseases in humans and spontaneous induction of the [PSI$^+$] status in yeast (Liu & Lindquist 1999; Scheibel & Lindquist 2001). It was shown recently that in yeast the octarepeat region of human PrP can functionally replace the oligopeptide repeats of Sup35p (Parham *et al.* 2001), giving rise to *de novo* induced [PSI$^+$]. These data argue that both repeat stretches may exert similar functions in aggregation and can be interchangeable. Interestingly, the oligorepeats in Sup35p are longer than that of mouse PrP. This might be the reason why N might positively modulate aggregation when fused to PrP$_{90-230}$ (Liu & Lindquist 1999; Moore *et al.* 2006). Nevertheless, N did not increase nucleation of N-PrP compared to PrP$_{90-230}$ (**Figure 23**). Furthermore, substitution of N with PrP$_{23-120}$ in PrP-M did not change the solubility of the protein, indicating a different role of these domains in mammalian cells compared to yeast cells. However, a precise and concrete evaluation of the influence of N could not be performed, as the very high numbers of aggregates in cells expressing PrP$_{90-230}$ and N-PrP did not allow quantitative analysis.

Fusion of either Sup35p-M or -NM to PrP$_{90-230}$ led to drastic qualitative differences in aggregates suggesting a modulating role of the M domain for aggregate size. Thus, M appears to increase the seeding activity of existing nuclei, potentially by enhancing sequestration of soluble newly formed protein into the growing aggregates. Experiments in yeast demonstrated that deletion of the middle region in Sup35p results in a protein which is mostly insoluble and aggregated and not able to efficiently propagate the [PSI$^+$] status (Liu *et al.* 2002). These and *in vitro* studies clearly demonstrate that the middle region of Sup35p is

important for the solubility of the protein (Liu *et al.* 2002). The decreased resistance of M- and NM-PrP to PK digestion might also be due to the solubilizing effect of Sup35p M domain which could render the protein more sensitive to proteolysis (Liu *et al.* 2002). M additionally decreased the nucleation rate of PrP_{90-230}. The ratio of PrP_{90-230} aggregate containing cells to transfected cells was significantly higher than the ratio of M-PrP foci harboring cells to transfected cells (**Figure 23**). Furthermore, fewer aggregates per single cell were detected for M-PrP compared to PrP_{90-230} (**Figure 22**). Thus, M lowered the nucleation rate like the amino-terminal region of PrP, suggesting that both regions might share at least some function in prion protein aggregate assembly. Interestingly, N counter-acted the solubilizing effect of M when fused to M-PrP. The ratio of cells bearing NM-PrP aggregates to total transfected N2a cells was significantly higher compared to the relative amount of M-PrP foci containing cells (**Figure 23**). Depending on the cell-type, fusion of N to M-PrP increased also the number of aggregates per single cell (**Figure 24**).

Overall, the globular domain of PrP seems to be the driving force for aggregation but both nucleation rate and seeding activity can be modulated by the Sup35p-N and -M regions (**Figure 67**).
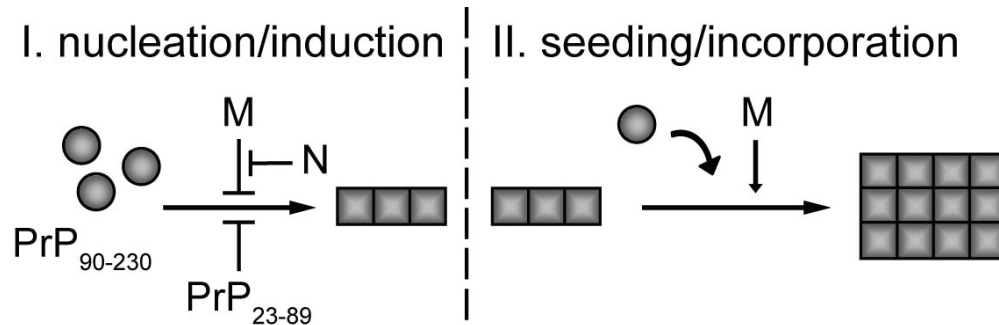
Figure 67. Schematic illustration to explain how N and M modulate PrP_{90-230} aggregation. The globular domain of PrP spontaneously aggregates in the cytosol of mammalian cells. Both PrP_{23-89} and Sup35p-M decrease the nucleation rate when fused to PrP_{90-230}, leading to fewer cells displaying visible aggregates. The influence of M can be counter-acted by N. Fusion of M to PrP_{90-230} increases aggregate size, potentially by an increased seeding capacity. Published in (Krammer *et al.* 2008b).

The here described interplay between N and M domains might also be important for the [PSI$^+$] phenotype in yeast that is known to depend on a crucial equilibration between seed formation and aggregate growth for prion propagation.

V.A.5 CO-AGGREGATION AND SEEDING OF PROTEINS ARE SPECIFIC EVENTS

An accumulation of misfolded proteins is the key event in various proteinopathies. It is commonly anticipated that the toxicity of these proteinaceous deposits is at least partially mediated by sequestering unrelated cellular proteins, thereby disturbing their normal cellular functions (Perutz *et al.* 1994). The different proteins used in this study did not only spontaneously aggregate *per se* but sometimes even co-aggregate with one another. Evidence that aggregation prone proteins can also co-aggregate with heterologous proteins in mammalian cells comes from studies with diverse proteins (Rajan *et al.* 2001). Interestingly, in this study co-aggregation was not driven by a non-specific co-agglomeration of solvent-exposed hydrophobic surfaces. Instead, seeding appeared to occur with extraordinary specificity for example amongst Q/N-rich stretches. Our data are consistent with this study in that PrP_{90-230}-containing proteins were able to co-aggregate. By contrast PrP_{90-230}-containing proteins were not able to interact with NM-HA, while HD72-GFP was (**Figures 36, 37 and 40**). It is likely that co-aggregation of chimeric proteins is due to the aggregated globular domain of PrP that allows correct intermolecular interaction necessary for aggregate formation. Interestingly, PrP_{cyto} can confer its nucleation propensity to other aggregates, enabling them to form more nuclei in concert with PrP_{cyto}. In contrast, seeding of M- and NM-PrP seemed to be less efficient as both chimeric proteins were unable to incorporate PrP_{cyto} into large aggregates (**Figure 36**). However, aggregates containing both proteins, PrP_{cyto} and M-PrP or PrP_{cyto} and NM-PrP, respectively, appeared bigger and less frequent as aggregates of PrP_{cyto} alone, indicating at least a minor influence of M on aggregate size and nucleation frequency. Thus, normally *cis* acting elements can also modulate protein aggregation in *trans*. Unfortunately, quantification was impossible due to the high number of aggregates.

Co-aggregation did not solely depend on a common aggregation-promoting motif. If this was the case, NM-PrP would be able to seed NM-HA as they share almost 100% amino acid sequence in their Q/N-rich region. Our data rather suggest that co-aggregation depends on sequence similarities in the domain that assembles into an ordered aggregate. As the C-terminal domain of PrP is the proposed aggregation domain in all fusion proteins, NM in NM-PrP is likely not in an aggregated state and, therefore, cannot seed NM-HA (**Figure 37**). In contrast, the aggregated domain in HD72-GFP is definitively the polyQ region. In its aggregated state, this polyQ rich region enables NM-HA to sediment around HD72-GFP

aggregates (**Figure 40**). Taken together, this study reveals important details about structural requirements for aggregation and co-aggregation.

V.A.6 DO AGGREGATES DISPLAY PRION-LIKE CHARACTERISTICS?

PrP_{90-230}, cytosolic PrP and chimera of Sup35p N and NM domains and PrP_{90-230} underwent rapid spontaneous aggregation when expressed in the cytosol of mammalian cells. All aggregates observed displayed typical characteristics of both yeast and mammalian prions such as detergent insolubility and at least partial PK resistance. Moreover, *in vitro* studies utilizing purified recombinant NM, PrP-M and NM-PrP confirmed that both NM and NM-PrP were capable of forming amyloid-like fibrils whereas PrP-M was not (Krammer *et al.* 2008b). However, relative PK resistance, insolubility and *in vitro* fibrillization are key characteristics not only of prions but also of amyloid-like proteins in general (Soto *et al.* 2006). Numerous studies reveal striking similarities in assembly pathways of both non-prion amyloidogenic proteins and prions. The extraordinary hallmark that sets prions apart is that they are also infectious. This discrimination between typical amyloid-like proteins and prions has recently been challenged by findings that injection of protein aggregates can at least accelerate aggregation of homologous proteins in some animal models of amyloid diseases (Meyer-Luehmann *et al.* 2006). Elegant experiments that demonstrate that *in vitro* fibrillized NM can increase the rate of prion induction in yeast have been used as evidence that aggregated Sup35p is indeed infectious (King & Diaz-Avalos 2004; Tanaka *et al.* 2004). Interestingly, a self-perpetuating mechanism of aggregate formation for cytosolic PrP has been proposed (Ma & Lindquist 2002). Are the aggregates observed with our recombinant proteins also infectious? Studying if external PrP_{cyto}, N-PrP and NM-PrP aggregates can induce aggregation of their respective soluble counterparts is a difficult task as spontaneous aggregate formation of these proteins already occurs at high frequency in mammalian cells. Experiments are underway to test if PrP_{cyto}, NM-PrP and N-PrP aggregates produced in mammalian cells can seed aggregation of the recombinant soluble proteins *in vitro*. Similar experiments have successfully been performed with yeast derived NM aggregates (Glover *et al.* 1997). Although fibrillization studies already provide evidence that NM and NM-PrP are capable of forming amyloid-like fibrils, aggregates formed by PrP_{90-230}, PrP_{cyto}, N-PrP, M-PrP and NM-PrP in N2a cells may have taken on an alternative fold that might be incapable of promoting assembly of soluble NM or NM-PrP into amyloid-like aggregates *in vitro*.

Indeed, evidence that the same NM can form aggregates that drastically differ in their intermolecular organization also comes from recent *in vitro* studies. Here, NM could form amyloid-like fibrils or alternatively assemble into filaments that appeared to be off-pathway for amyloid formation (Hess *et al.* 2007).

There is increasing evidence that prion propagation in yeast critically depends on Hsp104 that fractionizes growing multimers into seeds that can be transmitted to daughter cells. Thus, it is the disaggregating activity of Hsp104 that actually turns Sup35p aggregates into prions (Chernoff 2004). In mammalian cells, so far no Hsp104 ortholog has been identified in the cytosol that is capable of disaggregating already existing aggregates. In light of this, it will be interesting to study how cellular chaperones or co-expression of Hsp104 in mammalian cells will influence the appearance and/or maintenance of PrP_{90-230}, PrP_{cyto}, N-PrP, M-PrP, and NM-PrP aggregates.

V.B THE YEAST SUP35P NM DOMAIN PROPAGATES AS A PRION IN MAMMALIAN CELLS

Aggregation of Sup35p in yeast leads to modifications in translation termination and the induction of [PSI$^+$] prion phenotype that is associated with changes in growth capabilities on differentiation medium. Spontaneous induction of [PSI$^+$] in yeast is a rare event and occurs at a frequency of $1:10^6$ (Lund & Cox 1981; Liu & Lindquist 1999). Still, the prion phenotype can be induced by over expression of Sup35p or Sup35p-NM in the presence of another prion, termed [PIN$^+$] that appears to cross-seed Sup35p aggregation (Derkatch *et al.* 1996; Derkatch *et al.* 1997; Derkatch *et al.* 2000). In the mammalian cell line N2a, spontaneous NM aggregation was negligible, suggesting that appropriate heterologous seeds were either missing in the cytosol of N2a cells or that the rare event of spontaneous induction was not detected. Aim of the second project was to investigate if addition of recombinant Sup35p-NM fibrils to the medium of mammalian cells ectopically expressing HA-tagged NM could induce endogenous NM aggregation and lead to the propagation of potential NM-HA aggregates as prions.

V.B.1 INDUCTION OF ENDOGENOUS NM-HA AGGREGATION BY ADDITION OF RECOMBINANT SUP35P-NM FIBRILS TO THE CELL CULTURE MEDIUM

Experiments in yeast have demonstrated that *in vitro* fibrillized NM can induce prion formation upon transformation (King & Diaz-Avalos 2004; Tanaka *et al.* 2004). The same results were obtained here with soluble NM in N2a and HpL3-4 cells (Krammer *et al.* 2009a). Here, addition of NM fibrils led to the aggregation of endogenous HA-tagged NM (**Figure 43** and **52**). Surprisingly, active introduction of fibrils into the cytosol by transformation was not necessary. Bacterially expressed, purified NM was efficiently taken up by the cells and eventually even reached the cytosol. These observations were also made by others (Yang *et al.* 2002). It is possible that a net positive charge of proteins might facilitate their transmembrane transport (Yang *et al.* 2002). However, due to protein fibril size, it is very unlikely that they are able to simply penetrate the membrane. Therefore, how fibrils enter the cytosol remains a conundrum. Some viruses enter the cell via endocytosis and eventually escape from endosomal compartments into the cytosol. After clathrin-mediated endocytosis adenovirus escapes from endosomes (Blumenthal *et al.* 1986) by a yet unknown mechanism that probably requires virus induced signaling (Meier & Greber 2003). Interestingly, PrP[Sc] was found in cytosolic aggresomes (Kristiansen *et al.* 2005) implying potential translocation of prion aggregates from endosomal or lysosomal compartments into the cytosol. If this is due to an unspecific leakage in the endocytotic pathway or by a specific mechanism remains enigmatic. Further investigations are necessary to delineate the underlying mechanism.

V.B.2 PROPAGATION OF NM-HA AGGREGATES IN MAMMALIAN CELLS IS INDEPENDENT OF HSP104

Yeast prion inheritance requires aggregate formation and replication, two events that strongly depend on cellular factors. The disaggregase Hsp104 appears to be crucial for both generation and propagation of yeast prions (True 2006). Unlike in yeast, induction of aggregates and their transmission to progeny was independent of Hsp104 expression in N2a cells, as no ortholog of Hsp104 has been discovered in the mammalian cytosol. Our results strongly suggest that other mechanisms promote protein disaggregation in mammals. In this context, another question arises: why were NM aggregates propagated after seeding with recombinant NM fibrils but not upon co-aggregation with HD72-GFP? One reason could be that HD72-

GFP aggregates are slightly toxic (Waelter *et al.* 2001). Thus, cells with HD72-GFP / NM-HA aggregates might die. Indeed, similar to cells expressing PrP_{cyto}, N2a cells with HD72-GFP aggregates grew slower and appeared to be less viable in our hands. However, it is very unlikely that all cells expressing HD72-GFP were killed. It is more likely that cellular factors necessary for prion formation were not able to access NM-HA in HD72-GFP / NM-HA co-aggregates. Which cellular proteins might be involved in the cytosolic propagation of NM-HA as a prion remains to be seen.

One possible candidate factor could be the cortical actin cytoskeleton as it was shown in yeast that deletion of Sla1 which regulates the assembly and disassembly of actin filaments decreased the *de novo* induction of [PSI$^+$] by over-expression of Sup35p (Engqvist-Goldstein & Drubin 2003). Sla1 is involved in the assembly of endocytotic vesicles and excess Sup35p was shown to sediment around these vacuoles (Ganusova *et al.* 2006). Moreover, Sla2, another component of the yeast cytoskeleton machinery and the yeast homolog of mammalian huntingtin-interacting protein Hip1 (Kalchman *et al.* 1997), was found to interact with Sup35p from [psi$^-$] and [PSI$^+$] cells, indicating its possible role in [PSI$^+$] induction (Ganusova *et al.* 2006; Bagriantsev *et al.* 2008). One could imagine that NM fibrils taken up by the cell initially reside within endocytotic vesicles. Cytosolic NM may interact with recombinant NM fibrils near such structures. This interaction could then facilitate not only NM aggregation but also subsequent generation of seeds for transmission to daughter cells (Tuite & Cox 2003). Another reason for the successful propagation of NM-HA aggregates seeded by NM fibrils could be that the preexisting NM fibrils depleted an inhibitor of prion conversion and/or propagation, for example a cytosolic chaperone, whereas HD72-GFP was unable to capture this inhibitor (Derkatch *et al.* 2001).

The fact that anti-prion compounds were found to act on both mammalian and yeast prions indicates that similar targets, thus mechanisms of prion propagation, other than Hsp104, appear to be present in both organisms (Bach *et al.* 2006; Tribouillard *et al.* 2006). The disaggregase Hsp104 is crucially involved in seed formation in yeast for efficient prion transmission to daughter cells (Chernoff *et al.* 1995). As a member of the AAA+ protein superfamiliy, Hsp104 exhibits ATPase activity which mediates ATP-dependend disassembly of protein complexes (Weibezahn *et al.* 2004). Although no known homologs or orthologs of Hsp104 are present in the mammalian cytosol there are other AAA+ proteins which share at least some sequence similarities. One of them is p97/VCP/Cdc48p, a protein involved in the

translocation of misfolded proteins from the ER into the cytosol and their subsequent delivery to the proteasome (Richly *et al.* 2005; Raasi & Wolf 2007). Over-expression of p97/VCP/Cdc48p was shown to suppress the formation of polyQ aggregates (Yamanaka *et al.* 2004), but it failed to promote Sup35p-NM fibril disassembly *in vitro* (Shorter & Lindquist 2004).

With regard to the known complexity of the chaperone-prion interaction in yeast it is very difficult to predict the influence of certain chaperones on NM aggregate propagation in the cytosol of mammalian cells. Despite the dependence on Hsp104, yeast prion dissemination was shown to be influenced by several other chaperones as well as their co-chaperones with homologs in mammals including Hsp70s, Hsp40s, Hsp110s, Fes1 and Sti1 (Tuite & Cox 2003; Jones & Tuite 2005; True 2006; Perrett & Jones 2008). Their impact on prion propagation could be either direct or indirect by interacting with each other, thereby either inhibiting or supporting fibril assembly. Conflicting data exist on the role of these chaperones for prion propagation due to the complexity of interaction and functional redundancy of chaperones. Of note, some Sup35p chimera were able to propagate in the absence of Hsp104 in yeast, thus the existence for Hsp104 is not an absolute requirement (Liu *et al.* 2002; Crist *et al.* 2003; Alexandrov *et al.* 2008). Therefore, it is very likely that other chaperones are able to propagate the prion state of Sup35p-NM also in mammalian cells.

Little information is available on mammalian chaperones involved in prion biogenesis. Several chaperones have been shown to interact with PrP, but if they are required for prion formation remains enigmatic. BiP was shown to bind to native PrP^C and remained associated with a mutant form of PrP for a prolonged period of time (Jin *et al.* 2000). However, BiP resides in the ER. Thus, it is unlikely that BiP plays a role in cytosolic prion formation. The bacterial chaperonin GroEL appears to promote the *in vitro* conversion of PrP^C into a PK-resistant form (DebBurman *et al.* 1997; Stockel & Hartl 2001). Indeed, one mammalian homolog of GroEL, the mitochondrial Hsp60 was identified in a yeast-two-hybrid screen as an interactor of PrP^C (Edenhofer *et al.* 1996). The *in vivo* relevance of these findings remains to be shown. Another chaperone complex, the CCT (cytosolic chaperonin containing T-complex polypeptide-1) or TriC (tailless complex polypeptide-1 [TCP-1] ring complex) belongs to the same class as the bacterial GroEL/ES chaperonin (Spiess *et al.* 2004) and is highly conserved between yeast and humans (Stoldt *et al.* 1996; Spiess *et al.* 2004). This complex was shown to promote the accumulation of polyQ proteins into non-toxic

oligomers in yeast cells (Behrends *et al.* 2006). However, recent data suggest that TriC is not able to influence fibril assembly of the yeast prion protein Ure2 *in vitro* (Savistchenko *et al.* 2008). Inhibition of Hsp90 by geldanamycin leads to a modulation of the structural integrity of PrP[C] (Winklhofer *et al.* 2003; Ochel *et al.* 2003) indicating that Hsp90 might play a role in PrP[C] folding. Unlike the other chaperones Hsp90 seems to have only specific target proteins (Wandinger *et al.* 2008). It remains to be seen if Hsp90 can interact with NM-HA aggregates. The most promising candidates that might effect Sup35p-NM aggregate propagation in the mammalian cytosol are Hsp70s, Hsp40s and other co-chaperones of Hsp70 which were shown to have diverse effects on yeast prions including prion formation, variant determination, propagation and toxicity (Kryndushkin *et al.* 2002; Kryndushkin & Wickner 2007; Lian *et al.* 2007; Fan *et al.* 2007; Sadlish *et al.* 2008; Bagriantsev *et al.* 2008; Douglas *et al.* 2008; Savistchenko *et al.* 2008). Interestingly, scrapie-infected N2a cells (ScN2a) exhibited an impaired stress response compared to uninfected control cells due to an altered regulation of HSF-1 (heat shock factor-1) (Tatzelt *et al.* 1995; Winklhofer *et al.* 2001). Of note, over-expression of heat shock proteins, especially Hsp70 and Hsp40, could counteract the cytotoxic effect of cytosolic PrP (Rambold *et al.* 2006) and inhibited aggregate formation of polyglutamine proteins (Muchowski *et al.* 2000; Sittler *et al.* 2001). An interesting link between yeast prions and mammalian PrP regarding the Hsp90/Hsp70 machinery constitutes the co-chaperone Sti1 which was shown to play a role in [PSI[+]] propagation in yeast (Abbas-Terki *et al.* 2001; Jones *et al.* 2004) and seems to be a ligand for PrP[C] (Zanata *et al.* 2002). It is important to note that the distinct Hsp70 family members are able to work in concert with different co-chaperones and also other chaperones (Kushnirov *et al.* 2000; Jones & Tuite 2005) allowing them to exert different functions. Therefore, it is important to study chaperone networks to provide correct information on chaperone effects on prion formation or propagation. Furthermore, different prion variants have different conformations which might affect the ability of chaperones or chaperone networks to interact with them (Jones & Tuite 2005).

Prion formation and loss was shown to be influenced not only be chaperones but also by ubiquitin system alterations in yeast (Allen *et al.* 2007). Hence, degradation pathways like the proteasome or autophagic activity might be, besides chaperones, reasonable candidates for NM propagon formation in the mammalian cytosol. While the exact factors that allow prion propagation in the mammalian cytosol need to be identified, the artificial prion

transmission across phylogenetic kingdoms by not more than ectopically expressing the responsible gene, suggests that the ability to propagate prions is highly conserved since early life.

V.B.3 ARE THERE CONFORMATIONAL VARIANTS OF NM-HA AGGREGATES IN MAMMALIAN CELLS?

Prions can exist as distinct heritable states defined as prion strains or variants (Derkatch *et al.* 1996) that appear to be based on different conformational states of the prion proteins. It has been postulated that the ability to adopt multiple different aggregation states is an intrinsic propensity of prion proteins and thus independent of cellular factors (DePace & Weissman 2002; Vanik *et al.* 2004; Jones & Tuite 2005; Makarava & Baskakov 2008). Indeed, it has recently been shown that recombinant NM can give rise to several different prion strains when transformed into yeast, suggesting that these phenotypically distinct strains were induced by NM fibrils of different folds (Tanaka *et al.* 2004; King & Diaz-Avalos 2004). It is tempting to speculate that NM-HA aggregates induced by bacterially expressed fibrillized NM in individual cell clones represent prion strains/variants, a hypothesis supported by biochemical analysis of distinct NM-HA aggregate types. While the NM-HA expression levels modulated the phenotypical appearance of specific aggregate types, their biochemical characteristics stayed stable, strongly suggesting distinct NM-HA conformations in individual cell clones. Hence, our results support the hypothesis that prion strains are based on different folds of the same protein as we provided only one exogenous prion protein and obtained a variety of different aggregate phenotypes in cell culture. Furthermore, homogenous aggregate types propagated by individual cell clones strongly argue for a clonal effect on NM aggregation characteristics. Host factors in both yeast and mammals undoubtedly dramatically influence strain propagation efficiencies (Kushnirov *et al.* 2000; Kryndushkin *et al.* 2002; Asante *et al.* 2002; Lloyd *et al.* 2004; Park *et al.* 2006; Kryndushkin & Wickner 2007; Fan *et al.* 2007; Lawson *et al.* 2008). The conformational selection model for prion strain propagation (Collinge 1999) may explain the unexpected finding that infection of N2a_NM-Ha bulk cells with extracts from cell clones propagating one prevalent aggregate type gave rise to a variety of phenotypically distinct aggregate types in recipient cells. According to this model, the primary sequence of prion proteins allows only a certain subset of different folds (**Figure 68**). Prion strains may either exist as ensembles of prion proteins

with different conformations from which the host organism preferentially propagates a prevalent one or a subset of protein conformation variants. Alternatively, they may exist as one clonal protein conformer that might mutate when transferred to another host (Collinge & Clarke 2007).
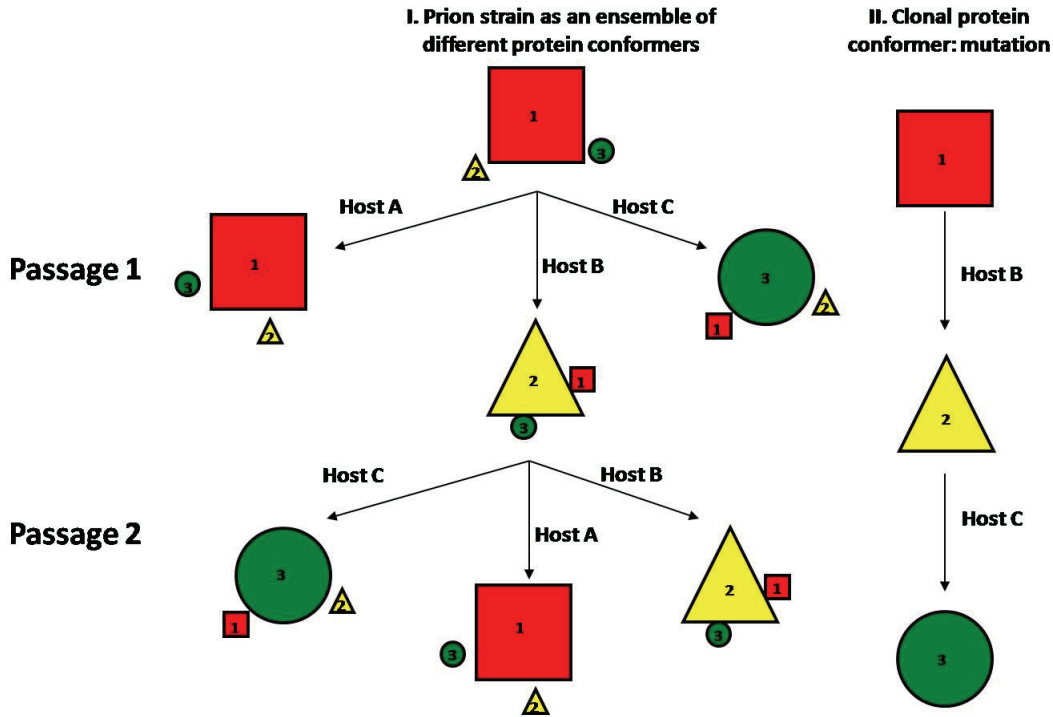
Figure 68. Models to explain prion strain mutations. Prion strains might constitute a mixture of different protein conformers (indicated by different symbols) in a given host with one predominant conformer (indicated by an increased size of the symbol). Upon transmission (passage 1 and 2) to a new host, a non-prevalent conformer is preferentially propagated, associated with a different phenotype. Alternatively, prion strains might constitute a clonal protein conformer that mutates to a new conformer upon transmission to a new host. For details see main text.

The high 'mutation rate' to other variants that was observed when aggregates from one cell clone were used to induce NM-HA aggregates in bulk N2a_NM-HA cells suggests that individual cells of the bulk N2a_NM-HA culture selected out the variant that it could replicate best. If these clones either 'silently' (which means under the detection limit of our conventional methods) propagated also other aggregate types or if the dominant aggregate variant *per se* mutated and refolded due to different host cell factors remains an open question. As prion variants have distinct chaperone requirements for propagation (Kushnirov *et al.* 2000), it is possible that differences in the cellular chaperone environment of individual cells account for the preferential replication of a dominant variant. Recent experiments with

N2a cells and mammalian prions indeed demonstrate that preferential propagation of individual prion strains also occurs in N2a subclones (Mahal *et al.* 2007). In line of this, our work clearly demonstrates the strong influence of the cell's genetic or epigenetic background on conformational selection. Furthermore, HpL_NM-HA cells did not display the same variety of NM aggregate phenotypes indicating a cell-type specific effect. Hence, the great diversity of NM aggregate types is characteristic for N2a cells. If and which host specific factors influence propagation of specific phenotypically and biochemically distinct variants remains to be determined. Due to the fact that recombinant Sup35p NM is known to form diverse types of fibrils (DePace & Weissman 2002) our data prefer a model in which strains exist as a mixture of conformationally different molecules rather than of a molecular clone (Collinge & Clarke 2007). Out of this pool the host cell seems to select one variant which is preferentially propagated and which phenotype becomes subsequently dominant and evident (**Figure 69**).
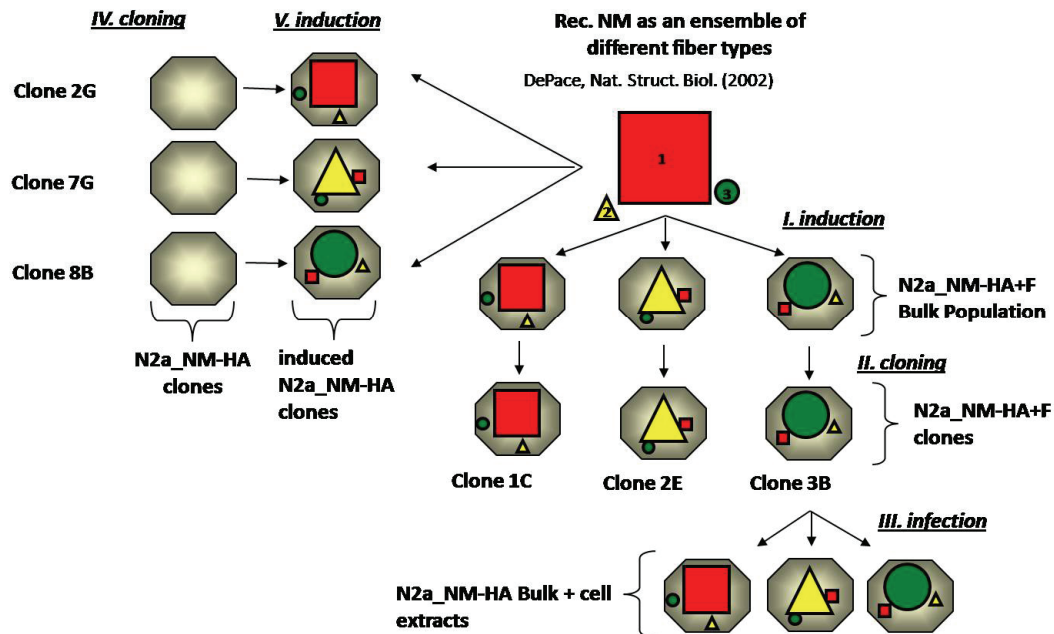
Figure 69. Conformational selection model adapted to NM-HA aggregate propagation. The NM-HA phenotype variation in N2a cells can be explained when we assume that cells propagate an ensemble of aggregate phenotypes with one predominant phenotype (symbolized by squares, circles and triangles). When N2a_NM-HA bulk cells were treated with recombinant Sup35p NM fibrils, the resulting N2a_NM-HA+F cell population exhibited various types of NM-HA aggregates. Single clones of N2a_NM-HA+F cells preferentially propagated one specific phenotypical variant. However, according to this model, also non prevalent variants were concomitantly propagated. Thus, infection of N2a_NM-HA bulk cells with cell extracts of clones showing only one aggregate type gave rise to various different aggregate phenotypes in the recipient cells indicating a strong influence of the host cell on prion variant selection. To confirm this hypothesis, N2a_NM-HA bulk cells were cloned prior to induction with recombinant NM fibrils. Individual N2a_NM-HA clones preferentially propagated one or two distinct aggregate phenotypes.

In collaboration with Dr. Kryndushkin and Prof. R. Wickner (Laboratory of Biochemistry and Genetics, NIH/NIDDK, Bethesda, MD, USA) we showed that mammalian NM prions only inefficiently induced the [PSI$^+$] phenotype in yeast cells (Krammer *et al.* 2009a). A possible explanation could be that NM amyloids have adapted to the cellular environment of mammalian cells and thus lack the chaperone environment necessary for efficient propagation.

V.B.4 EVIDENCE FOR A PRION PROPAGATION MACHINERY IN THE CYTOSOL OF MAMMALIAN CELLS

Amyloids in humans have classically been considered to be detrimental to the host, but increasing evidence accumulates that amyloid formation plays an important role in normal cellular physiology of diverse microorganisms and even mammals. Several physiologically relevant non-prion amyloids have been identified that exert novel biological functions, for example the curli protein of *E. coli* and other bacteria, the hydrophobins of fungi, and human Pmel17 (Fowler *et al.* 2007). Even more intriguingly, elegant studies on the filamentous fungus *Podospora anserina* demonstrate that the prion form of the protein HETs [Het-s] is the biological active form mediating heterokaryon incompatibility (Maddelein *et al.* 2002; Balguerie *et al.* 2003). Thus, it is feasible to assume that prion-based inheritance might also be a natural regulatory process in higher eukaryotes for proteins of diverse function. Still, evidence that prion-like phenomena exist in the mammalian cytosol is missing. Our results show that ectopically expressed Sup35p NM can propagate as a prion in neuroblastoma cells and thus provides proof-of-principle that prion-like inheritance in the mammalian cytosol is possible. Future studies will help to elucidate if mechanisms of prion biogenesis are also of physiological relevance in mammals.

VI. ABBREVIATIONS

A	Adenine, Ampere
Å	Angström
Aa	Amino acid
AAA+	ATPase associated with diverse activities
Ab	Antibody
AFM	Atomic force microscopy
Amp	Ampicillin
APS	Ammoniumpersulfate
Approx.	Approximately
Asn/N	Asparagine
ATCC	American Type Culture Collection
ATP	Adenosintriphosphate
bp	Base pair
BSA	Bovine serum albumin
BSE	Bovine spongiforme enzephalopathy
c	Concentration
C	Cytosine
°C	Degree Celsius
CD	Circular dichroism
CLD	Caveolae-like domains
cm	centimeter
CNS	central nervous system
CWD	Chronic wasting disease
Cys	Cysteine
Da	Dalton
Dest.	Destilled
CJD	Creutzfeldt-Jakob disease
DMEM	Dulbecco's modified Eagle Medium
DMSO	Dimethylsulfoxid
DNA	Deoxyribonucleic acid
DNase	Desoxyribonuclease
dNTP	Desoxyribonucleoside-5'-triphosphate
ddNTP	Didesoxyribonucleoside-5'-triphosphat
d	Day
ds	Double stranded
EDTA	Ethylenediamine-N,N,N´,N´-Tetraacetate
EGFP	Enhanced green fluorescent protein
ER	Endoplasmic reticulum
ERAD	ER associated degradation
Et al.	And others ('et alii')
EtBr	Ethidiumbromide
EtOH	Ethanol
fCJD	familial Creutzfeldt-Jakob disease
FCS	Fetal calf serum

FFI	Fatal familial insomnia
Fig.	Figure
FITC	Fluoresceine isothiocyanate
FSE	Feline spongiforme enzephalopathy
g	Gram; acceleration of gravity
G	Guanine
GFP	Green fluorescent protein
Gln/Q	Glutamine
GPI	Glykosyl-phosphatidyl-inositol
GSS	Gerstmann-Sträußler-Scheinker syndrome
h	Hour
$H_2O_{dest.}$	Destilled water
$H_2O_{bidest.}$	Destilled, deionized water
HA	Hemagglutinin
Hsp	Heat shock protein
IF	Immunofluorescence
Ig	Immune globuline
k	Kilo
kb	Kilo base pairs
kDa	Kilodalton
L	Liter
LB	Luria-Bertani medium
LR	Laminin receptor
LRP	Laminin receptor precursor
LRP1	Lipoprotein receptor- related protein 1
m	Meter, mili
M	Molar
mAb	Monoclonal antibody
mcs	Multiple cloning site
MEM	Minimal essential medium
MetOH	Methanol
min	Minute
mRNA	Messenger RNA
MTOC	Microtubule organization center
n	Nano
NCC	Nucleated conformational conversion
NMR	Nuclear magnetic resonance
OD	Optical density
OPR	Oligopeptide repeats
OR	Octarepeats
ORF	Open reading frame
p	Piko
PA	Polyacrylamide
PAGE	Polyacrylamide gel electrophoresis
pAK	Polyclonal antibody
PBS	Phosphate buffered saline
PCR	Polymerase chain reaction
PFA	Paraformaldehyde

PGK	Phosphoglycerate kinase
PK	Proteinase K
PRD	Prion forming domain
PrP	Prion protein
$PrP^{0/0}$	PrP knock-out
PrP^{C}	Cellular non-pathogenic form of the prion protein
^{Ctm}PrP	Carboxylterminal-trans transmembrane form of PrP
^{Ntm}PrP	Aminoterminal-trans transmembrane form of PrP
PrP^{Sc}	Pathogenic form of the prion protein
PVDF	Polyvinyl difluoride
QNR	Glutamine and asparagine-rich
RNA	Ribonucleic acid
RNase	Ribonuclease
rpm	Rounds per minute
RT	Room temperature
SDS	Sodium dodecyle sulfate
s	Second
S.D.	Standard deviation
ss	Single stranded
t	Time
T	Thymine
Tm	Melting temperature
Tab.	Table
TEMED	N,N,N´,N´-Tetramethylethylendiamin
Tris	Tris-(hydroxymethyl-)aminomethan
tRNA	transfer-RNA
TME	Transmissible mink encephalopathy
TSE	Transmissible spongiform encephalopathy
U	Unit
µ	Micro
UV	ultraviolet
V	Volt
vCJD	variant Creutzfeldt-Jakob disease
Vol.	Volume
Vs.	Versus
W	Watt
WB	Western blot
WT	Wild type
% (v/v)	Volume percentage
% (w/v)	Weight percentage

VII.   REFERENCE LIST

Reference List

Abbas-Terki T, Donze O, Briand PA & Picard D 2001 Hsp104 interacts with Hsp90 cochaperones in respiring yeast. *Mol Cell Biol.* **21** 7569-7575.

Aguzzi A & Haass C 2003 Games played by rogue proteins in prion disorders and Alzheimer's disease. *Science* **302** 814-818.

Aguzzi A & Miele G 2004 Recent advances in prion biology. *Curr.Opin.Neurol.* **17** 337-342.

Aguzzi A & Polymenidou M 2004 Mammalian prion biology: one century of evolving concepts. *Cell* **116** 313-327.

Alexandrov IM, Vishnevskaya AB, Ter Avanesyan MD & Kushnirov VV 2008 Appearance and propagation of polyglutamine-based amyloids in yeast: tyrosine residues enable polymer fragmentation. *J.Biol.Chem.* **283** 15185-15192.

Allen KD, Chernova TA, Tennant EP, Wilkinson KD & Chernoff YO 2007 Effects of ubiquitin system alterations on the formation and loss of a yeast prion. *J Biol.Chem.* **282** 3004-3013.

Alper T, Cramp WA, Haig DA & Clarke MC 1967 Does the agent of scrapie replicate without nucleic acid? *Nature* **214** 764-766.

Alper T, Haig DA & Clarke MC 1966 The exceptionally small size of the scrapie agent. *Biochem Biophys Res Commun.* **22** 278-284.

Anderson RM, Donnelly CA, Ferguson NM, Woolhouse ME, Watt CJ, Udy HJ, Mawhinney S, Dunstan SP, Southwood TR, Wilesmith JW, Ryan JB, Hoinville LJ, Hillerton JE, Austin AR & Wells GA 1996 Transmission dynamics and epidemiology of BSE in British cattle. *Nature* **382** 779-788.

Anfinsen CB 1973 Principles that govern the folding of protein chains. *Science* **181** 223-230.

Arnold JE, Tipler C, Laszlo L, Hope J, Landon M & Mayer RJ 1995 The abnormal isoform of the prion protein accumulates in late-endosome-like organelles in scrapie-infected mouse brain. *J Pathol.* **176** 403-411.

Asante EA, Linehan JM, Desbruslais M, Joiner S, Gowland I, Wood AL, Welch J, Hill AF, Lloyd SE, Wadsworth JD & Collinge J 2002 BSE prions propagate as either variant CJD-like or sporadic CJD-like prion strains in transgenic mice expressing human prion protein. *EMBO J* **21** 6358-6366.

Bach S, Talarek N, Andrieu T, Vierfond JM, Mettey Y, Galons H, Dormont D, Meijer L, Cullin C & Blondel M 2003 Isolation of drugs active against mammalian prions using a yeast-based screening assay. *Nat.Biotechnol.* **21** 1075-1081.

Bach S, Tribouillard D, Talarek N, Desban N, Gug F, Galons H & Blondel M 2006 A yeast-based assay to isolate drugs active against mammalian prions. *Methods* **39** 72-77.

Bagriantsev SN, Gracheva EO, Richmond JE & Liebman SW 2008 Variant-specific [PSI+] Infection Is Transmitted by Sup35 Polymers within [PSI+] Aggregates with Heterogeneous Protein Composition. *Mol.Biol.Cell* **19** 2433-2443.

Balguerie A, Dos RS, Ritter C, Chaignepain S, Coulary-Salin B, Forge V, Bathany K, Lascu I, Schmitter JM, Riek R & Saupe SJ 2003 Domain organization and structure-function relationship of the HET-s prion protein of Podospora anserina. *EMBO J* **22** 2071-2081.

Barron RM, Thomson V, Jamieson E, Melton DW, Ironside J, Will R & Manson JC 2001 Changing a single amino acid in the N-terminus of murine PrP alters TSE incubation time across three species barriers. *EMBO J* **20** 5070-5078.

Basler K, Oesch B, Scott M, Westaway D, Walchli M, Groth DF, McKinley MP, Prusiner SB & Weissmann C 1986 Scrapie and cellular PrP isoforms are encoded by the same chromosomal gene. *Cell* **46** 417-428.

Behrends C, Langer CA, Boteva R, Bottcher UM, Stemp MJ, Schaffar G, Rao BV, Giese A, Kretzschmar H, Siegers K & Hartl FU 2006 Chaperonin TRiC promotes the assembly of polyQ expansion proteins into nontoxic oligomers. *Mol.Cell* **23** 887-897.

Bessen RA & Marsh RF 1992 Identification of two biologically distinct strains of transmissible mink encephalopathy in hamsters. *J Gen Virol.* **73 (Pt 2)** 329-334.

Bessen RA, Raymond GJ & Caughey B 1997 In situ formation of protease-resistant prion protein in transmissible spongiform encephalopathy-infected brain slices. *J Biol.Chem.* **272** 15227-15231.

Blumenthal R, Seth P, Willingham MC & Pastan I 1986 pH-dependent lysis of liposomes by adenovirus. *Biochemistry* **25** 2231-2237.

Borchelt DR, Scott M, Taraboulos A, Stahl N & Prusiner SB 1990 Scrapie and cellular prion proteins differ in their kinetics of synthesis and topology in cultured cells. *J Cell Biol.* **110** 743-752.

Borchelt DR, Taraboulos A & Prusiner SB 1992 Evidence for synthesis of scrapie prion proteins in the endocytic pathway. *J Biol.Chem.* **267** 16188-16199.

Bosl B, Grimminger V & Walter S 2006 The molecular chaperone Hsp104--a molecular machine for protein disaggregation. *J Struct.Biol.* **156** 139-148.

Bousset L & Melki R 2002 Similar and divergent features in mammalian and yeast prions. *Microbes.Infect.* **4** 461-469.

Brachmann A, Baxa U & Wickner RB 2005 Prion generation in vitro: amyloid of Ure2p is infectious. *EMBO J* **24** 3082-3092.

Bradley ME, Edskes HK, Hong JY, Wickner RB & Liebman SW 2002 Interactions among prions and prion "strains" in yeast. *Proc.Natl.Acad.Sci.U.S A* **99 Suppl 4** 16392-16399.

Brandner S, Isenmann S, Raeber A, Fischer M, Sailer A, Kobayashi Y, Marino S, Weissmann C & Aguzzi A 1996 Normal host prion protein necessary for scrapie-induced neurotoxicity. *Nature* **379** 339-343.

Brotherston JG, Renwick CC, Stamp JT, Zlotnik I & Pattison IH 1968 Spread and scrapie by contact to goats and sheep. *J Comp Pathol.* **78** 9-17.

Bruce M, Chree A, McConnell I, Foster J, Pearson G & Fraser H 1994 Transmission of bovine spongiform encephalopathy and scrapie to mice: strain variation and the species barrier. *Philos.Trans.R.Soc.Lond B Biol.Sci.* **343** 405-411.

Bruce ME 2003 TSE strain variation. *Br.Med.Bull.* **66** 99-108.

Bruce ME, Will RG, Ironside JW, McConnell I, Drummond D, Suttie A, McCardle L, Chree A, Hope J, Birkett C, Cousens S, Fraser H & Bostock CJ 1997 Transmissions to mice indicate that 'new variant' CJD is caused by the BSE agent. *Nature* **389** 498-501.

Bueler H, Aguzzi A, Sailer A, Greiner RA, Autenried P, Aguet M & Weissmann C 1993 Mice devoid of PrP are resistant to scrapie. *Cell* **73** 1339-1347.

Bueler H, Fischer M, Lang Y, Bluethmann H, Lipp HP, DeArmond SJ, Prusiner SB, Aguet M & Weissmann C 1992 Normal development and behaviour of mice lacking the neuronal cell-surface PrP protein. *Nature* **356** 577-582.

Butler DA, Scott MR, Bockman JM, Borchelt DR, Taraboulos A, Hsiao KK, Kingsbury DT & Prusiner SB 1988 Scrapie-infected murine neuroblastoma cells produce protease-resistant prion proteins. *J Virol.* **62** 1558-1564.

Byrne LJ, Cox BS, Cole DJ, Ridout MS, Morgan BJ & Tuite MF 2007 Cell division is essential for elimination of the yeast [PSI+] prion by guanidine hydrochloride. *Proc.Natl.Acad.Sci.U.S.A* **104** 11688-11693.

Castilla J, Saa P, Hetz C & Soto C 2005 In vitro generation of infectious scrapie prions. *Cell* **121** 195-206.

Caughey B 2003 Prion protein conversions: insight into mechanisms, TSE transmission barriers and strains. *Br.Med.Bull.* **66** 109-120.

Caughey B & Baron GS 2006 Prions and their partners in crime. *Nature* **443** 803-810.

Caughey B & Raymond GJ 1991 The scrapie-associated form of PrP is made from a cell surface precursor that is both protease- and phospholipase-sensitive. *J Biol.Chem.* **266** 18217-18223.

Caughey B, Raymond GJ, Ernst D & Race RE 1991 N-terminal truncation of the scrapie-associated form of PrP by lysosomal protease(s): implications regarding the site of conversion of PrP to the protease-resistant state. *J Virol.* **65** 6597-6603.

Chernoff YO 2004 Amyloidogenic domains, prions and structural inheritance: rudiments of early life or recent acquisition? *Curr.Opin.Chem.Biol.* **8** 665-671.

Chernoff YO, Derkach IL & Inge-Vechtomov SG 1993 Multicopy SUP35 gene induces de-novo appearance of psi-like factors in the yeast Saccharomyces cerevisiae. *Curr.Genet.* **24** 268-270.

Chernoff YO, Lindquist SL, Ono B, Inge-Vechtomov SG & Liebman SW 1995 Role of the chaperone protein Hsp104 in propagation of the yeast prion-like factor [psi+]. *Science* **268** 880-884.

Chernoff YO, Newnam GP, Kumar J, Allen K & Zink AD 1999 Evidence for a protein mutator in yeast: role of the Hsp70-related chaperone ssb in formation, stability, and toxicity of the [PSI] prion. *Mol Cell Biol.* **19** 8103-8112.

Chesebro B, Trifilo M, Race R, Meade-White K, Teng C, LaCasse R, Raymond L, Favara C, Baron G, Priola S, Caughey B, Masliah E & Oldstone M 2005 Anchorless prion protein results in infectious amyloid disease without clinical scrapie. *Science* **308** 1435-1439.

Chhabra ES & Higgs HN 2007 The many faces of actin: matching assembly factors with cellular structures. *Nat.Cell Biol.* **9** 1110-1121.

Chiarini LB, Freitas AR, Zanata SM, Brentani RR, Martins VR & Linden R 2002 Cellular prion protein transduces neuroprotective signals. *EMBO J* **21** 3317-3326.

Chien P, DePace AH, Collins SR & Weissman JS 2003 Generation of prion transmission barriers by mutational control of amyloid conformations. *Nature* **424** 948-951.

Chien P & Weissman JS 2001 Conformational diversity in a yeast prion dictates its seeding specificity. *Nature* **410** 223-227.

Chien P, Weissman JS & DePace AH 2004 Emerging principles of conformation-based prion inheritance. *Annu.Rev.Biochem* **73** 617-656.

Chiesa R, Piccardo P, Ghetti B & Harris DA 1998 Neurological illness in transgenic mice expressing a prion protein with an insertional mutation. *Neuron* **21** 1339-1351.

Chiti F & Dobson CM 2006 Protein misfolding, functional amyloid, and human disease. *Annu.Rev Biochem* **75** 333-366.

Clarke AR, Jackson GS & Collinge J 2001 The molecular biology of prion propagation. *Philos.Trans.R.Soc.Lond B Biol.Sci.* **356** 185-195.

Clinton J, Royston MC, Gentleman SM & Roberts GW 1992 Amyloid plaque: morphology, evolution, and etiology. *Mod.Pathol.* **5** 439-443.

Cobb NJ, Sonnichsen FD, McHaourab H & Surewicz WK 2007 Molecular architecture of human prion protein amyloid: a parallel, in-register beta-structure. *Proc.Natl.Acad.Sci.U.S.A* **104** 18946-18951.

Cohen FE, Pan KM, Huang Z, Baldwin M, Fletterick RJ & Prusiner SB 1994 Structural clues to prion replication. *Science* **264** 530-531.

Colling SB, Collinge J & Jefferys JG 1996 Hippocampal slices from prion protein null mice: disrupted Ca(2+)-activated K+ currents. *Neurosci.Lett.* **209** 49-52.

Collinge J 1999 Variant Creutzfeldt-Jakob disease. *Lancet* **354** 317-323.

Collinge J 2001 Prion diseases of humans and animals: their causes and molecular basis. *Annu.Rev.Neurosci.* **24** 519-550.

Collinge J 2005 Molecular neurology of prion disease. *J Neurol.Neurosurg.Psychiatry* **76** 906-919.

Collinge J & Clarke AR 2007 A general model of prion strains and their pathogenicity. *Science* **318** 930-936.

Collinge J, Palmer MS, Sidle KC, Gowland I, Medori R, Ironside J & Lantos P 1995 Transmission of fatal familial insomnia to laboratory animals. *Lancet* **346** 569-570.

Collinge J & Rossor M 1996 A new variant of prion disease. *Lancet* **347** 916-917.

Collinge J, Sidle KC, Meads J, Ironside J & Hill AF 1996 Molecular analysis of prion strain variation and the aetiology of 'new variant' CJD. *Nature* **383** 685-690.

Collinge J, Whittington MA, Sidle KC, Smith CJ, Palmer MS, Clarke AR & Jefferys JG 1994 Prion protein is necessary for normal synaptic function. *Nature* **370** 295-297.

Cox BS 1965 [*PSI*], a cytoplasmic suppressor of super-suppressors in yeast. *Heredity* **20** 505-521.

Cox BS 1971 A recessive lethal super-suppressor mutation in yeast and other psi phenomena. *Heredity* **26** 211-232.

Crist CG, Nakayashiki T, Kurahashi H & Nakamura Y 2003 [PHI+], a novel Sup35-prion variant propagated with non-Gln/Asn oligopeptide repeats in the absence of the chaperone protein Hsp104. *Genes Cells* **8** 603-618.

Cuille & Chelle 1939 Experimental transmission of trembling to the goat. *Comptes Rendus des Seances de l'Academie des Sciences* **208** 1058-1160.

DeArmond SJ & Prusiner SB 1995 Etiology and pathogenesis of prion diseases. *Am.J Pathol.* **146** 785-811.

DebBurman SK, Raymond GJ, Caughey B & Lindquist S 1997 Chaperone-supervised conversion of prion protein to its protease-resistant form. *Proc.Natl.Acad.Sci.U.S A* **94** 13938-13943.

DePace AH, Santoso A, Hillner P & Weissman JS 1998 A critical role for amino-terminal glutamine/asparagine repeats in the formation and propagation of a yeast prion. *Cell* **93** 1241-1252.

DePace AH & Weissman JS 2002 Origins and kinetic consequences of diversity in Sup35 yeast prion fibers. *Nat.Struct.Biol.* **9** 389-396.

Derkatch IL, Bradley ME, Hong JY & Liebman SW 2001 Prions affect the appearance of other prions: the story of [PIN(+)]. *Cell* **106** 171-182.

Derkatch IL, Bradley ME, Masse SV, Zadorsky SP, Polozkov GV, Inge-Vechtomov SG & Liebman SW 2000 Dependence and independence of [PSI(+)] and [PIN(+)]: a two-prion system in yeast? *EMBO J* **19** 1942-1952.

Derkatch IL, Bradley ME, Zhou P, Chernoff YO & Liebman SW 1997 Genetic and environmental factors affecting the de novo appearance of the [PSI+] prion in Saccharomyces cerevisiae. *Genetics* **147** 507-519.

Derkatch IL, Chernoff YO, Kushnirov VV, Inge-Vechtomov SG & Liebman SW 1996 Genesis and variability of [PSI] prion factors in Saccharomyces cerevisiae. *Genetics* **144** 1375-1386.

Derkatch IL, Uptain SM, Outeiro TF, Krishnan R, Lindquist SL & Liebman SW 2004 Effects of Q/N-rich, polyQ, and non-polyQ amyloids on the de novo formation of the [PSI+] prion in yeast and aggregation of Sup35 in vitro. *Proc.Natl.Acad.Sci.U.S A* **101** 12934-12939.

Dickinson AG, Stamp JT & Renwick CC 1974 Maternal and lateral transmission of scrapie in sheep. *J Comp Pathol.* **84** 19-25.

Dobson CM 2003 Protein folding and misfolding. *Nature* **426** 884-890.

Doel SM, McCready SJ, Nierras CR & Cox BS 1994 The dominant. *Genetics* **137** 659-670.

Dong J, Bloom JD, Goncharov V, Chattopadhyay M, Millhauser GL, Lynn DG, Scheibel T & Lindquist S 2007 Probing the role of PrP repeats in conformational conversion and amyloid assembly of chimeric yeast prions. *J.Biol.Chem.*

Douglas PM, Treusch S, Ren HY, Halfmann R, Duennwald ML, Lindquist S & Cyr DM 2008 Chaperone-dependent amyloid assembly protects cells from prion toxicity. *Proc.Natl.Acad.Sci.U.S.A* **105** 7206-7211.

Drisaldi B, Stewart RS, Adles C, Stewart LR, Quaglio E, Biasini E, Fioriti L, Chiesa R & Harris DA 2003 Mutant PrP is delayed in its exit from the endoplasmic reticulum, but neither wild-type nor mutant PrP undergoes retrotranslocation prior to proteasomal degradation. *J Biol.Chem.* **278** 21732-21743.

Du Z, Park KW, Yu H, Fan Q & Li L 2008 Newly identified prion linked to the chromatin-remodeling factor Swi1 in Saccharomyces cerevisiae. *Nat.Genet.* **40** 460-465.

Eaglestone SS, Cox BS & Tuite MF 1999 Translation termination efficiency can be regulated in Saccharomyces cerevisiae by environmental stress through a prion-mediated mechanism. *EMBO J* **18** 1974-1981.

Edenhofer F, Rieger R, Famulok M, Wendler W, Weiss S & Winnacker EL 1996 Prion protein PrPc interacts with molecular chaperones of the Hsp60 family. *J Virol.* **70** 4724-4728.

Edskes HK, Gray VT & Wickner RB 1999 The [URE3] prion is an aggregated form of Ure2p that can be cured by overexpression of Ure2p fragments. *Proc.Natl.Acad.Sci.U.S A* **96** 1498-1503.

Engqvist-Goldstein AE & Drubin DG 2003 Actin assembly and endocytosis: from yeast to mammals. *Annu.Rev.Cell Dev.Biol.* **19** 287-332.

Ertmer A, Gilch S, Yun SW, Flechsig E, Klebl B, Stein-Gerlach M, Klein MA & Schatzl HM 2004 The tyrosine kinase inhibitor STI571 induces cellular clearance of PrPSc in prion-infected cells. *J Biol.Chem.* **279** 41918-41927.

Fan Q, Park KW, Du Z, Morano KA & Li L 2007 The role of Sse1 in the de novo formation and variant determination of the [PSI+] prion. *Genetics* **177** 1583-1593.

Ferreira PC, Ness F, Edwards SR, Cox BS & Tuite MF 2001 The elimination of the yeast [PSI+] prion by guanidine hydrochloride is the result of Hsp104 inactivation. *Mol Microbiol* **40** 1357-1369.

Follenzi A, Ailles LE, Bakovic S, Geuna M & Naldini L 2000 Gene transfer by lentiviral vectors is limited by nuclear translocation and rescued by HIV-1 pol sequences. *Nat.Genet.* **25** 217-222.

Fowler DM, Koulov AV, Balch WE & Kelly JW 2007 Functional amyloid--from bacteria to humans. *Trends Biochem.Sci.* **32** 217-224.

Fraser H 2000 Phillips report and the origin of BSE. *Vet.Rec.* **147** 724.

Frolova L, Le G, X, Rasmussen HH, Cheperegin S, Drugeon G, Kress M, Arman I, Haenni AL, Celis JE, Philippe M & . 1994 A highly conserved eukaryotic protein family possessing properties of polypeptide chain release factor. *Nature* **372** 701-703.

Gaedtke L, Lutzny G, Krammer C, Rost R & Vorberg I 2009 The importance of the PrP primary sequence in prion disease transmission. In *Research Signpost* **(in press)**.

Gajdusek DC 1977 Unconventional viruses and the origin and disappearance of kuru. *Science* **197** 943-960.

Ganusova EE, Ozolins LN, Bhagat S, Newnam GP, Wegrzyn RD, Sherman MY & Chernoff YO 2006 Modulation of prion formation, aggregation, and toxicity by the actin cytoskeleton in yeast. *Mol Cell Biol.* **26** 617-629.

Garcia-Mata R, Bebok Z, Sorscher EJ & Sztul ES 1999 Characterization and dynamics of aggresome formation by a cytosolic GFP-chimera. *J.Cell Biol.* **146** 1239-1254.

Gasset M, Baldwin MA, Fletterick RJ & Prusiner SB 1993 Perturbation of the secondary structure of the scrapie prion protein under conditions that alter infectivity. *Proc.Natl.Acad.Sci.U.S A* **90** 1-5.

Ghani AC, Donnelly CA, Ferguson NM & Anderson RM 2002 The transmission dynamics of BSE and vCJD. *C.R.Biol.* **325** 37-47.

Ghani AC, Donnelly CA, Ferguson NM & Anderson RM 2003 Updated projections of future vCJD deaths in the UK. *BMC Infect.Dis.* **3** 4.

Gilch S, Krammer C & Schatzl HM 2008 Targeting prion proteins in neurodegenerative disease. *Expert.Opin.Biol.Ther.* **8** 923-940.

Gilch S, Wopfner F, Renner-Muller I, Kremmer E, Bauer C, Wolf E, Brem G, Groschup MH & Schatzl HM 2003 Polyclonal anti-PrP auto-antibodies induced with dimeric PrP interfere efficiently with PrPSc propagation in prion-infected cells. *J Biol.Chem.* **278** 18524-18531.

Glatzel M & Aguzzi A 2001 The shifting biology of prions. *Brain Res Brain Res Rev.* **36** 241-248.

Glover JR, Kowal AS, Schirmer EC, Patino MM, Liu JJ & Lindquist S 1997 Self-seeded fibers formed by Sup35, the protein determinant of [PSI+], a heritable prion-like factor of S. cerevisiae. *Cell* **89** 811-819.

Glover JR & Lindquist S 1998 Hsp104, Hsp70, and Hsp40: a novel chaperone system that rescues previously aggregated proteins. *Cell* **94** 73-82.

Govaerts C, Wille H, Prusiner SB & Cohen FE 2004 Evidence for assembly of prions with left-handed beta-helices into trimers. *Proc.Natl.Acad.Sci.U.S A* **101** 8342-8347.

Grenier C, Bissonnette C, Volkov L & Roucou X 2006 Molecular morphology and toxicity of cytoplasmic prion protein aggregates in neuronal and non-neuronal cells. *J Neurochem.* **97** 1456-1466.

Griffith JS 1967 Self-replication and scrapie. *Nature* **215** 1043-1044.

Grimminger V, Richter K, Imhof A, Buchner J & Walter S 2004 The prion curing agent guanidinium chloride specifically inhibits ATP hydrolysis by Hsp104. *J Biol.Chem.* **279** 7378-7383.

Haacke A, Broadley SA, Boteva R, Tzvetkov N, Hartl FU & Breuer P 2006 Proteolytic cleavage of polyglutamine-expanded ataxin-3 is critical for aggregation and sequestration of non-expanded ataxin-3. *Hum.Mol.Genet.* **15** 555-568.

Hay B, Barry RA, Lieberburg I, Prusiner SB & Lingappa VR 1987 Biogenesis and transmembrane orientation of the cellular isoform of the scrapie prion protein [published erratum appears in Mol Cell Biol 1987 May;7(5):2035]. *Mol Cell Biol.* **7** 914-920.

Hegde RS, Mastrianni JA, Scott MR, DeFea KA, Tremblay P, Torchia M, DeArmond SJ, Prusiner SB & Lingappa VR 1998 A transmembrane form of the prion protein in neurodegenerative disease. *Science* **279** 827-834.

Heller U, Winklhofer KF, Heske J, Reintjes A & Tatzelt J 2003 Post-translational import of the prion protein into the endoplasmic reticulum interferes with cell viability: a critical role for the putative transmembrane domain. *J Biol.Chem.* **278** 36139-36147.

Heske J, Heller U, Winklhofer KF & Tatzelt J 2004 The C-terminal globular domain of the prion protein is necessary and sufficient for import into the endoplasmic reticulum. *J Biol.Chem.* **279** 5435-5443.

Hess S, Lindquist SL & Scheibel T 2007 Alternative assembly pathways of the amyloidogenic yeast prion determinant Sup35-NM. *EMBO Rep.*

Hewitt PE, Llewelyn CA, Mackenzie J & Will RG 2006 Creutzfeldt-Jakob disease and blood transfusion: results of the UK Transfusion Medicine Epidemiological Review study. *Vox Sang.* **91** 221-230.

Hill AF, Desbruslais M, Joiner S, Sidle KC, Gowland I, Collinge J, Doey LJ & Lantos P 1997 The same prion strain causes vCJD and BSE. *Nature* **389** 448-50, 526.

Hoffner G & Djian P 2002 Protein aggregation in Huntington's disease. *Biochimie* **84** 273-278.

Hofmann A, Kessler B, Ewerling S, Weppert M, Vogg B, Ludwig H, Stojkovic M, Boelhauve M, Brem G, Wolf E & Pfeifer A 2003 Efficient transgenesis in farm animals by lentiviral vectors. *EMBO Rep.* **4** 1054-1060.

Hörnlimann, Riesner & Kretzschmar 2001 Prionen und Prionkrankheiten. *De Gruyter*.

Hundt C, Peyrin JM, Haik S, Gauczynski S, Leucht C, Rieger R, Riley ML, Deslys JP, Dormont D, Lasmezas CI & Weiss S 2001 Identification of interaction domains of the prion protein with its 37-kDa/67-kDa laminin receptor. *EMBO J* **20** 5876-5886.

Jin T, Gu Y, Zanusso G, Sy M, Kumar A, Cohen M, Gambetti P & Singh N 2000 The chaperone protein BiP binds to a mutant prion protein and mediates its degradation by the proteasome. *J Biol.Chem.* **275** 38699-38704.

Johnston JA, Ward CL, and Kopito RR. Aggresomes: a cellular response to misfolded proteins. J Cell Biol. 143[7], 1883-1898. 1998.
Ref Type: Generic

Jones G, Song Y, Chung S & Masison DC 2004 Propagation of Saccharomyces cerevisiae [PSI+] prion is impaired by factors that regulate Hsp70 substrate binding. *Mol Cell Biol.* **24** 3928-3937.

Jones GW & Masison DC 2003 Saccharomyces cerevisiae Hsp70 mutations affect [PSI+] prion propagation and cell growth differently and implicate Hsp40 and tetratricopeptide repeat cochaperones in impairment of [PSI+]. *Genetics* **163** 495-506.

Jones GW & Tuite MF 2005 Chaperoning prions: the cellular machinery for propagating an infectious protein? *Bioessays* **27** 823-832.

Jung G, Jones G, Wegrzyn RD & Masison DC 2000 A role for cytosolic hsp70 in yeast [PSI(+)] prion propagation and [PSI(+)] as a cellular stress. *Genetics* **156** 559-570.

Kalastavadi T & True HL 2008 Prion protein insertional mutations increase aggregation propensity but not fiber stability. *BMC.Biochem.* **9** 7.

Kalchman MA, Koide HB, McCutcheon K, Graham RK, Nichol K, Nishiyama K, Kazemi-Esfarjani P, Lynn FC, Wellington C, Metzler M, Goldberg YP, Kanazawa I, Gietz RD & Hayden MR 1997 HIP1, a human homologue of S. cerevisiae Sla2p, interacts with membrane-associated huntingtin in the brain. *Nat.Genet.* **16** 44-53.

Kanu N, Imokawa Y, Drechsel DN, Williamson RA, Birkett CR, Bostock CJ & Brockes JP 2002 Transfer of scrapie prion infectivity by cell contact in culture. *Curr.Biol.* **12** 523-530.

King CY & Diaz-Avalos R 2004 Protein-only transmission of three yeast prion strains. *Nature* **428** 319-323.

Kopito RR 2000 Aggresomes, inclusion bodies and protein aggregation. *Trends Cell Biol.* **10** 524-530.

Krammer C, Kremmer E, Schatzl HM & Vorberg I 2008a Dynamic interactions of Sup35p and PrP prion protein domains modulate aggregate nucleation and seeding. *PRION* **2** 1-8.

Krammer C, Suhre MH, Kremmer E, Diemer C, Hess S, Schatzl HM, Scheibel T & Vorberg I 2008b Prion protein/protein interactions: fusion with yeast Sup35p-NM modulates cytosolic PrP aggregation in mammalian cells. *FASEB J.* **22** 762-773.

Krammer C, Kryndushkin D, Suhre MH, Kremmer E, Hofmann A, Pfeifer A, Scheibel T, Wickner RB, Schatzl HM & Vorberg I 2009a The yeast Sup35NM domain propagates as a prion in mammalian cells. *Proc.Natl.Acad.Sci.U.S.A* **(in press)**.

Krammer C, Vorberg I, Schatzl HM & Gilch S 2009b Therapy in Prion Diseases: From Molecular and Cellular Biology to Therapeutic Targets. *Infectious Disorders-Drug Targets* **(in press)**.

Krishnan R & Lindquist SL 2005 Structural insights into a yeast prion illuminate nucleation and strain diversity. *Nature* **435** 765-772.

Kristiansen M, Deriziotis P, Dimcheff DE, Jackson GS, Ovaa H, Naumann H, Clarke AR, van Leeuwen FW, Menendez-Benito V, Dantuma NP, Portis JL, Collinge J & Tabrizi SJ 2007 Disease-associated prion protein oligomers inhibit the 26S proteasome. *Mol.Cell* **26** 175-188.

Kristiansen M, Messenger MJ, Klohn PC, Brandner S, Wadsworth JD, Collinge J & Tabrizi SJ 2005 Disease-related prion protein forms aggresomes in neuronal cells leading to caspase activation and apoptosis. *J Biol.Chem.* **280** 38851-38861.

Kryndushkin D & Wickner RB 2007 Nucleotide exchange factors for Hsp70s are required for [URE3] prion propagation in Saccharomyces cerevisiae. *Mol.Biol.Cell* **18** 2149-2154.

Kryndushkin DS, Alexandrov IM, Ter Avanesyan MD & Kushnirov VV 2003 Yeast [PSI+] prion aggregates are formed by small Sup35 polymers fragmented by Hsp104. *J Biol.Chem.* **278** 49636-49643.

Kryndushkin DS, Smirnov VN, Ter Avanesyan MD & Kushnirov VV 2002 Increased expression of Hsp40 chaperones, transcriptional factors, and ribosomal protein Rpp0 can cure yeast prions. *J Biol.Chem.* **277** 23702-23708.

Kushnirov VV, Kryndushkin DS, Boguta M, Smirnov VN & Ter Avanesyan MD 2000 Chaperones that cure yeast artificial [PSI+] and their prion-specific effects. *Curr.Biol.* **10** 1443-1446.

Kushnirov VV & Ter Avanesyan MD 1998 Structure and replication of yeast prions. *Cell* **94** 13-16.

Kushnirov VV, Ter Avanesyan MD, Didichenko SA, Smirnov VN, Chernoff YO, Derkach IL, Novikova ON, Inge-Vechtomov SG, Neistat MA & Tolstorukov II 1990 Divergence and conservation of SUP2 (SUP35) gene of yeast Pichia pinus and Saccharomyces cerevisiae. *Yeast* **6** 461-472.

Kuwahara C, Takeuchi AM, Nishimura T, Haraguchi K, Kubosaki A, Matsumoto Y, Saeki K, Matsumoto Y, Yokoyama T, Itohara S & Onodera T 1999 Prions prevent neuronal cell-line death. *Nature* **400** 225-226.

Lacroute F. Non-Mendelian mutation allowing ureidosuccinic acid uptake in yeast. J Bacteriol. 106[2], 519-522. 1971.
Ref Type: Generic

Lasmezas CI, Deslys JP, Demaimay R, Adjou KT, Lamoury F, Dormont D, Robain O, Ironside J & Hauw JJ 1996 BSE transmission to macaques. *Nature* **381** 743-744.

Lawson VA, Vella L, Stewart JD, Sharples R, Klemm H, Machalek DM, Masters CL, Cappai R, Collins SJ & Hill AF 2008 Mouse-adapted sporadic human Creutzfeldt-Jakob disease prions propagate in cell culture. *Int.J.Biochem.Cell Biol.*

Lee DC, Sakudo A, Kim CK, Nishimura T, Saeki K, Matsumoto Y, Yokoyama T, Chen SG, Itohara S & Onodera T 2006a Fusion of Doppel to octapeptide repeat and N-terminal half of hydrophobic region of prion protein confers resistance to serum deprivation. *Microbiol Immunol.* **50** 203-209.

Lee YJ, Jin JK, Jeong BH, Carp RI & Kim YS 2006b Increased expression of glial cell line-derived neurotrophic factor (GDNF) in the brains of scrapie-infected mice. *Neurosci.Lett.* **410** 178-182.

Legname G, Baskakov IV, Nguyen HO, Riesner D, Cohen FE, DeArmond SJ & Prusiner SB 2004 Synthetic mammalian prions. *Science* **305** 673-676.

Leucht C, Simoneau S, Rey C, Vana K, Rieger R, Lasmezas CI & Weiss S 2003 The 37 kDa/67 kDa laminin receptor is required for PrP(Sc) propagation in scrapie-infected neuronal cells. *EMBO Rep.* **4** 290-295.

Li L & Lindquist S 2000 Creating a protein-based element of inheritance. *Science* **287** 661-664.

Lian HY, Zhang H, Zhang ZR, Loovers HM, Jones GW, Rowling PJ, Itzhaki LS, Zhou JM & Perrett S 2007 Hsp40 interacts directly with the native state of the yeast prion protein Ure2 and inhibits formation of amyloid-like fibrils. *J.Biol.Chem.* **282** 11931-11940.

Liebman SW 2001 Prions. The shape of a species barrier. *Nature* **410** 161-162.

Liu JJ & Lindquist S 1999 Oligopeptide-repeat expansions modulate 'protein-only' inheritance in yeast. *Nature* **400** 573-576.

Liu JJ, Sondheimer N & Lindquist SL 2002 Changes in the middle region of Sup35 profoundly alter the nature of epigenetic inheritance for the yeast prion [PSI+]. *Proc.Natl.Acad.Sci.U.S A* **99 Suppl 4** 16446-16453.

Llewelyn CA, Hewitt PE, Knight RS, Amar K, Cousens S, Mackenzie J & Will RG 2004 Possible transmission of variant Creutzfeldt-Jakob disease by blood transfusion. *Lancet* **363** 417-421.

Lloyd SE, Linehan JM, Desbruslais M, Joiner S, Buckell J, Brandner S, Wadsworth JD & Collinge J 2004 Characterization of two distinct prion strains derived from bovine spongiform encephalopathy transmissions to inbred mice. *J Gen Virol.* **85** 2471-2478.

Lund PM & Cox BS 1981 Reversion analysis of [psi-] mutations in Saccharomyces cerevisiae. *Genet.Res.* **37** 173-182.

Ma J & Lindquist S 2002 Conversion of PrP to a self-perpetuating PrPSc-like conformation in the cytosol. *Science* **298** 1785-1788.

Ma J, Wollmann R & Lindquist S 2002 Neurotoxicity and neurodegeneration when PrP accumulates in the cytosol. *Science* **298** 1781-1785.

Maas E, Geissen M, Groschup MH, Rost R, Onodera T, Schatzl H & Vorberg I 2007 Scrapie infection of PrP deficient cell line upon ectopic expression of mutant prion proteins. *J.Biol.Chem.*

Maddelein ML, Dos RS, Duvezin-Caubet S, Coulary-Salin B & Saupe SJ 2002 Amyloid aggregates of the HET-s prion protein are infectious. *Proc.Natl.Acad.Sci.U.S A* **99** 7402-7407.

Mahal SP, Baker CA, Demczyk CA, Smith EW, Julius C & Weissmann C 2007 Prion strain discrimination in cell culture: the cell panel assay. *Proc.Natl.Acad.Sci.U.S.A* **104** 20908-20913.

Makarava N & Baskakov IV 2008 The same primary structure of the prion protein yields two distinct self-propagating states. *J.Biol.Chem.* **283** 15988-15996.

Mallucci G, Dickinson A, Linehan J, Klohn PC, Brandner S & Collinge J 2003 Depleting neuronal PrP in prion infection prevents disease and reverses spongiosis. *Science* **302** 871-874.

Mallucci GR, Ratte S, Asante EA, Linehan J, Gowland I, Jefferys JG & Collinge J 2002 Post-natal knockout of prion protein alters hippocampal CA1 properties, but does not result in neurodegeneration. *EMBO J* **21** 202-210.

Mallucci GR, White MD, Farmer M, Dickinson A, Khatun H, Powell AD, Brandner S, Jefferys JG & Collinge J 2007 Targeting cellular prion protein reverses early cognitive deficits and neurophysiological dysfunction in prion-infected mice. *Neuron* **53** 325-335.

Mann R, Mulligan RC & Baltimore D 1983 Construction of a retrovirus packaging mutant and its use to produce helper-free defective retrovirus. *Cell* **33** 153-159.

Mc Gowan 1914 Investigation into the disease of sheep called "scrapie" with special reference to its association with sarcospoidiosis. *Rept* **232**.

Mc Gowan 1922 Scrapie in sheep. *Scott.J.Agric.* **5** 365-375.

McKinley MP, Taraboulos A, Kenaga L, Serban D, Stieber A, DeArmond SJ, Prusiner SB & Gonatas N 1991 Ultrastructural localization of scrapie prion proteins in cytoplasmic vesicles of infected cultured cells. *Lab Invest* **65** 622-630.

McLennan NF, Brennan PM, McNeill A, Davies I, Fotheringham A, Rennison KA, Ritchie D, Brannan F, Head MW, Ironside JW, Williams A & Bell JE 2004 Prion protein accumulation and neuroprotection in hypoxic brain damage. *Am.J Pathol.* **165** 227-235.

Meier O & Greber UF 2003 Adenovirus endocytosis. *J.Gene Med.* **5** 451-462.

Meyer RK, McKinley MP, Bowman KA, Braunfeld MB, Barry RA & Prusiner SB 1986 Separation and properties of cellular and scrapie prion proteins. *Proc.Natl.Acad.Sci.U.S A* **83** 2310-2314.

Meyer-Luehmann M, Coomaraswamy J, Bolmont T, Kaeser S, Schaefer C, Kilger E, Neuenschwander A, Abramowski D, Frey P, Jaton AL, Vigouret JM, Paganetti P, Walsh DM, Mathews PM, Ghiso J, Staufenbiel M, Walker LC & Jucker M 2006 Exogenous induction of cerebral beta-amyloidogenesis is governed by agent and host. *Science* **313** 1781-1784.

Miller AD & Buttimore C 1986 Redesign of retrovirus packaging cell lines to avoid recombination leading to helper virus production. *Mol.Cell Biol.* **6** 2895-2902.

Mironov A, Jr., Latawiec D, Wille H, Bouzamondo-Bernstein E, Legname G, Williamson RA, Burton D, DeArmond SJ, Prusiner SB & Peters PJ 2003 Cytosolic prion protein in neurons. *J Neurosci.* **23** 7183-7193.

Mishra RS, Bose S, Gu Y, Li R & Singh N 2003 Aggresome formation by mutant prion proteins: the unfolding role of proteasomes in familial prion disorders. *J Alzheimers.Dis.* **5** 15-23.

Moore RA, Herzog C, Errett J, Kocisko DA, Arnold KM, Hayes SF & Priola SA 2006 Octapeptide repeat insertions increase the rate of protease-resistant prion protein formation. *Protein Sci.* **15** 609-619.

Moriyama H, Edskes HK & Wickner RB 2000 [URE3] prion propagation in Saccharomyces cerevisiae: requirement for chaperone Hsp104 and curing by overexpressed chaperone Ydj1p. *Mol Cell Biol.* **20** 8916-8922.

Muchowski PJ, Schaffar G, Sittler A, Wanker EE, Hayer-Hartl MK & Hartl FU 2000 Hsp70 and hsp40 chaperones can inhibit self-assembly of polyglutamine proteins into amyloid-like fibrils. *Proc.Natl.Acad.Sci.U.S.A* **97** 7841-7846.

Newnam GP, Wegrzyn RD, Lindquist SL & Chernoff YO 1999 Antagonistic interactions between yeast chaperones Hsp104 and Hsp70 in prion curing. *Mol Cell Biol.* **19** 1325-1333.

Nonno R, Di Bari MA, Cardone F, Vaccari G, Fazzi P, Dell'Omo G, Cartoni C, Ingrosso L, Boyle A, Galeno R, Sbriccoli M, Lipp HP, Bruce M, Pocchiari M & Agrimi U 2006 Efficient transmission and characterization of Creutzfeldt-Jakob disease strains in bank voles. *PLoS Pathog.* **2** e12.

Novitskaya V, Bocharova OV, Bronstein I & Baskakov IV 2006 Amyloid fibrils of mammalian prion protein are highly toxic to cultured cells and primary neurons. *J Biol.Chem.* **281** 13828-13836.

Nunziante M, Gilch S & Schatzl HM 2003 Essential role of the prion protein N terminus in subcellular trafficking and half-life of cellular prion protein. *J Biol.Chem.* **278** 3726-3734.

Ochel HJ, Gademann G, Trepel J & Neckers L 2003 Modulation of prion protein structural integrity by geldanamycin. *Glycobiology* **13** 655-660.

Oesch B, Westaway D, Walchli M, McKinley MP, Kent SB, Aebersold R, Barry RA, Tempst P, Teplow DB, Hood LE & . 1985 A cellular gene encodes scrapie PrP 27-30 protein. *Cell* **40** 735-746.

Orsi A, Fioriti L, Chiesa R & Sitia R 2006 Conditions of endoplasmic reticulum stress favor the accumulation of cytosolic prion protein. *J Biol.Chem.* **281** 30431-30438.

Osherovich LZ & Weissman JS 2001 Multiple Gln/Asn-rich prion domains confer susceptibility to induction of the yeast [PSI(+)] prion. *Cell* **106** 183-194.

Pan KM, Baldwin M, Nguyen J, Gasset M, Serban A, Groth D, Mehlhorn I, Huang Z, Fletterick RJ, Cohen FE & . 1993 Conversion of alpha-helices into beta-sheets features in the formation of the scrapie prion proteins. *Proc.Natl.Acad.Sci.U.S A* **90** 10962-10966.

Parchi P, Giese A, Capellari S, Brown P, Schulz-Schaeffer W, Windl O, Zerr I, Budka H, Kopp N, Piccardo P, Poser S, Rojiani A, Streichemberger N, Julien J, Vital C, Ghetti B,

Gambetti P & Kretzschmar H 1999 Classification of sporadic Creutzfeldt-Jakob disease based on molecular and phenotypic analysis of 300 subjects. *Ann.Neurol.* **46** 224-233.

Parham SN, Resende CG & Tuite MF 2001 Oligopeptide repeats in the yeast protein Sup35p stabilize intermolecular prion interactions. *EMBO J* **20** 2111-2119.

Park KW, Hahn JS, Fan Q, Thiele DJ & Li L 2006 De novo appearance and "strain" formation of yeast prion [PSI+] are regulated by the heat-shock transcription factor. *Genetics* **173** 35-47.

Parkyn CJ, Vermeulen EG, Mootoosamy RC, Sunyach C, Jacobsen C, Oxvig C, Moestrup S, Liu Q, Bu G, Jen A & Morris RJ 2008 LRP1 controls biosynthetic and endocytic trafficking of neuronal prion protein. *J.Cell Sci.* **121** 773-783.

Patel BK & Liebman SW 2007 "Prion-proof" for [PIN(+)]: Infection with In Vitro-made Amyloid Aggregates of Rnq1p-(132-405) Induces [PIN(+)]. *J Mol Biol.* **365** 773-782.

Patino MM, Liu JJ, Glover JR & Lindquist S 1996 Support for the prion hypothesis for inheritance of a phenotypic trait in yeast. *Science* **273** 622-626.

Pattison IH 1965 Scrapie in the welsh mountain breed of sheep and its experimental transmission to goats. *Vet.Rec.* **77** 1388-1390.

Paushkin SV, Kushnirov VV, Smirnov VN & Ter Avanesyan MD 1996 Propagation of the yeast prion-like [psi+] determinant is mediated by oligomerization of the SUP35-encoded polypeptide chain release factor. *EMBO J* **15** 3127-3134.

Peden AH, Head MW, Ritchie DL, Bell JE & Ironside JW 2004 Preclinical vCJD after blood transfusion in a PRNP codon 129 heterozygous patient. *Lancet* **364** 527-529.

Pergami P, Jaffe H & Safar J 1996 Semipreparative chromatographic method to purify the normal cellular isoform of the prion protein in nondenatured form. *Anal.Biochem* **236** 63-73.

Perrett S & Jones GW 2008 Insights into the mechanism of prion propagation. *Curr.Opin.Struct.Biol.* **18** 52-59.

Perutz MF, Johnson T, Suzuki M & Finch JT 1994 Glutamine repeats as polar zippers: their possible role in inherited neurodegenerative diseases. *Proc.Natl.Acad.Sci.U.S.A* **91** 5355-5358.

Polymenidou M, Stoeck K, Glatzel M, Vey M, Bellon A & Aguzzi A 2005 Coexistence of multiple PrPSc types in individuals with Creutzfeldt-Jakob disease. *Lancet Neurol.* **4** 805-814.

Prado MA, Alves-Silva J, Magalhaes AC, Prado VF, Linden R, Martins VR & Brentani RR 2004 PrPc on the road: trafficking of the cellular prion protein. *J Neurochem.* **88** 769-781.

Priola SA & Caughey B 1994 Inhibition of scrapie-associated PrP accumulation. Probing the role of glycosaminoglycans in amyloidogenesis. *Mol Neurobiol.* **8** 113-120.

Priola SA, Chabry J & Chan K 2001 Efficient conversion of normal prion protein (PrP) by abnormal hamster PrP is determined by homology at amino acid residue 155. *J Virol.* **75** 4673-4680.

Prusiner SB 1982 Novel proteinaceous infectious particles cause scrapie. *Science* **216** 136-144.

Prusiner SB 1998a Prions. *Proc.Natl.Acad.Sci.U.S A* **95** 13363-13383.

Prusiner SB 1998b The prion diseases. *Brain Pathol.* **8** 499-513.

Prusiner SB, Groth DF, Bolton DC, Kent SB & Hood LE 1984 Purification and structural studies of a major scrapie prion protein. *Cell* **38** 127-134.

Prusiner SB & Scott MR 1997 Genetics of prions. *Annu.Rev.Genet.* **31** 139-175.

Prusiner SB, Torchia M & Westaway D 1991 Molecular biology and genetics of prions-- implications for sheep scrapie, "mad cows" and the BSE epidemic. Historical background. *Cornell Vet.* **81** 85-101.

Raasi S & Wolf DH 2007 Ubiquitin receptors and ERAD: a network of pathways to the proteasome. *Semin.Cell Dev.Biol.* **18** 780-791.

Rajan RS, Illing ME, Bence NF & Kopito RR 2001 Specificity in intracellular protein aggregation and inclusion body formation. *Proc.Natl.Acad.Sci.U.S.A* **98** 13060-13065.

Rambold AS, Miesbauer M, Rapaport D, Bartke T, Baier M, Winklhofer KF & Tatzelt J 2006 Association of Bcl-2 with misfolded prion protein is linked to the toxic potential of cytosolic PrP. *Mol Biol.Cell* **17** 3356-3368.

Rambold AS, Muller V, Ron U, Ben Tal N, Winklhofer KF & Tatzelt J 2008 Stress-protective signalling of prion protein is corrupted by scrapie prions. *EMBO J.*

Rane NS, Yonkovich JL & Hegde RS 2004 Protection from cytosolic prion protein toxicity by modulation of protein translocation. *EMBO J* **23** 4550-4559.

Resende CG, Outeiro TF, Sands L, Lindquist S & Tuite MF 2003 Prion protein gene polymorphisms in Saccharomyces cerevisiae. *Mol Microbiol* **49** 1005-1017.

Richly H, Rape M, Braun S, Rumpf S, Hoege C & Jentsch S 2005 A series of ubiquitin binding factors connects CDC48/p97 to substrate multiubiquitylation and proteasomal targeting. *Cell* **120** 73-84.

Rivera-Milla E, Stuermer CA & Malaga-Trillo E 2003 An evolutionary basis for scrapie disease: identification of a fish prion mRNA. *Trends Genet.* **19** 72-75.

Robakis NK, Devine-Gage EA, Jenkins EC, Kascsak RJ, Brown WT, Krawczun MS & Silverman WP 1986 Localization of a human gene homologous to the PrP gene on the p arm of chromosome 20 and detection of PrP-related antigens in normal human brain. *Biochem Biophys Res Commun.* **140** 758-765.

Ross ED, Minton A & Wickner RB 2005 Prion domains: sequences, structures and interactions. *Nat.Cell Biol.* **7** 1039-1044.

Rubinsztein DC 2006 The roles of intracellular protein-degradation pathways in neurodegeneration. *Nature* **443** 780-786.

Sadlish H, Rampelt H, Shorter J, Wegrzyn RD, Andreasson C, Lindquist S & Bukau B 2008 Hsp110 chaperones regulate prion formation and propagation in S. cerevisiae by two discrete activities. *PLoS.ONE.* **3** e1763.

Safar J, Wille H, Itri V, Groth D, Serban H, Torchia M, Cohen FE & Prusiner SB 1998 Eight prion strains have PrP(Sc) molecules with different conformations. *Nat.Med.* **4** 1157-1165.

Santoso A, Chien P, Osherovich LZ & Weissman JS 2000 Molecular basis of a yeast prion species barrier. *Cell* **100** 277-288.

Satpute-Krishnan P, Langseth SX & Serio TR 2007 Hsp104-Dependent Remodeling of Prion Complexes Mediates Protein-Only Inheritance. *PLoS Biol.* **5** e24.

Savistchenko J, Krzewska J, Fay N & Melki R 2008 Molecular chaperones and the assembly of the prion Ure2p in vitro. *J.Biol.Chem.* **283** 15732-15739.

Schatzl HM, Da Costa M, Taylor L, Cohen FE & Prusiner SB 1995 Prion protein gene variation among primates. *J Mol Biol.* **245** 362-374.

Scheibel T 2004 Amyloid formation of a yeast prion determinant. *J Mol Neurosci.* **23** 13-22.

Scheibel T, Bloom J & Lindquist SL 2004 The elongation of yeast prion fibers involves separable steps of association and conversion. *Proc.Natl.Acad.Sci.U.S A* **101** 2287-2292.

Scheibel T & Buchner J 2006 Protein aggregation as a cause for disease. *Handb.Exp.Pharmacol.* 199-219.

Scheibel T, Kowal AS, Bloom JD & Lindquist SL 2001 Bidirectional amyloid fiber growth for a yeast prion determinant. *Curr.Biol.* **11** 366-369.

Scheibel T & Lindquist SL 2001 The role of conformational flexibility in prion propagation and maintenance for Sup35p. *Nat.Struct.Biol.* **8** 958-962.

Scott M, Foster D, Mirenda C, Serban D, Coufal F, Walchli M, Torchia M, Groth D, Carlson G, DeArmond SJ & . 1989 Transgenic mice expressing hamster prion protein produce species-specific scrapie infectivity and amyloid plaques. *Cell* **59** 847-857.

Scott M, Groth D, Foster D, Torchia M, Yang SL, DeArmond SJ & Prusiner SB 1993 Propagation of prions with artificial properties in transgenic mice expressing chimeric PrP genes. *Cell* **73** 979-988.

Scott MR, Groth D, Tatzelt J, Torchia M, Tremblay P, DeArmond SJ & Prusiner SB 1997 Propagation of prion strains through specific conformers of the prion protein. *J Virol.* **71** 9032-9044.

Scott MR, Kohler R, Foster D & Prusiner SB 1992 Chimeric prion protein expression in cultured cells and transgenic mice. *Protein Sci.* **1** 986-997.

Scott MR, Peretz D, Nguyen HO, DeArmond SJ & Prusiner SB 2005 Transmission barriers for bovine, ovine, and human prions in transgenic mice. *J Virol.* **79** 5259-5271.

Serio TR, Cashikar AG, Kowal AS, Sawicki GJ, Moslehi JJ, Serpell L, Arnsdorf MF & Lindquist SL 2000 Nucleated conformational conversion and the replication of conformational information by a prion determinant. *Science* **289** 1317-1321.

Shewmaker F, Wickner RB & Tycko R 2006 Amyloid of the prion domain of Sup35p has an in-register parallel beta-sheet structure. *Proc.Natl.Acad.Sci.U.S A* **103** 19754-19759.

Shorter J & Lindquist S 2004 Hsp104 catalyzes formation and elimination of self-replicating Sup35 prion conformers. *Science* **304** 1793-1797.

Sigurdson C, Polymenidou M & Aguzzi A 2005 Reconstructing prions: fibril assembly from simple yeast to complex mammals. *Neurodegener.Dis.* **2** 1-5.

Sigurdson CJ & Miller MW 2003 Other animal prion diseases. *Br.Med.Bull.* **66** 199-212.

Sigurdsson 1954 A chronic encephalitis of sheep- with general remarks on infectins which develop slowly and some of their special characteristics. *Br.Vet.J.* **110** 341-354.

Silveira JR, Raymond GJ, Hughson AG, Race RE, Sim VL, Hayes SF & Caughey B 2005 The most infectious prion protein particles. *Nature* **437** 257-261.

Simoneau S, Rezaei H, Sales N, Kaiser-Schulz G, Lefebvre-Roque M, Vidal C, Fournier JG, Comte J, Wopfner F, Grosclaude J, Schatzl H & Lasmezas CI 2007 In vitro and in vivo neurotoxicity of prion protein oligomers. *PLoS.Pathog.* **3** e125.

Sittler A, Lurz R, Lueder G, Priller J, Lehrach H, Hayer-Hartl MK, Hartl FU & Wanker EE 2001 Geldanamycin activates a heat shock response and inhibits huntingtin aggregation in a cell culture model of Huntington's disease. *Hum.Mol.Genet.* **10** 1307-1315.

Sondheimer N & Lindquist S 2000 Rnq1: an epigenetic modifier of protein function in yeast. *Mol Cell* **5** 163-172.

Sondheimer N, Lopez N, Craig EA & Lindquist S 2001 The role of Sis1 in the maintenance of the [RNQ+] prion. *EMBO J* **20** 2435-2442.

Soto C, Estrada L & Castilla J 2006 Amyloids, prions and the inherent infectious nature of misfolded protein aggregates. *Trends Biochem Sci.* **31** 150-155.

Sparkes RS, Simon M, Cohn VH, Fournier RE, Lem J, Klisak I, Heinzmann C, Blatt C, Lucero M, Mohandas T & . 1986 Assignment of the human and mouse prion protein genes to homologous chromosomes. *Proc.Natl.Acad.Sci.U.S A* **83** 7358-7362.

Sparrer HE, Santoso A, Szoka FC, Jr. & Weissman JS 2000 Evidence for the prion hypothesis: induction of the yeast [PSI+] factor by in vitro- converted Sup35 protein. *Science* **289** 595-599.

Spiess C, Meyer AS, Reissmann S & Frydman J 2004 Mechanism of the eukaryotic chaperonin: protein folding in the chamber of secrets. *Trends Cell Biol.* **14** 598-604.

Spudich A, Frigg R, Kilic E, Kilic U, Oesch B, Raeber A, Bassetti CL & Hermann DM 2005 Aggravation of ischemic brain injury by prion protein deficiency: role of ERK-1/-2 and STAT-1. *Neurobiol.Dis.* **20** 442-449.

Stansfield I, Jones KM, Kushnirov VV, Dagkesamanskaya AR, Poznyakovski AI, Paushkin SV, Nierras CR, Cox BS, Ter Avanesyan MD & Tuite MF 1995 The products of the SUP45 (eRF1) and SUP35 genes interact to mediate translation termination in Saccharomyces cerevisiae. *EMBO J* **14** 4365-4373.

Steele-Mortimer O, Knodler LA & Finlay BB 2000 Poisons, ruffles and rockets: bacterial pathogens and the host cell cytoskeleton. *Traffic.* **1** 107-118.

Stefani M & Dobson CM 2003 Protein aggregation and aggregate toxicity: new insights into protein folding, misfolding diseases and biological evolution. *J Mol Med.* **81** 678-699.

Stockel J & Hartl FU 2001 Chaperonin-mediated de novo generation of prion protein aggregates. *J Mol Biol.* **313** 861-872.

Stoldt V, Rademacher F, Kehren V, Ernst JF, Pearce DA & Sherman F 1996 Review: the Cct eukaryotic chaperonin subunits of Saccharomyces cerevisiae and other yeasts. *Yeast* **12** 523-529.

Strumbo B, Ronchi S, Bolis LC & Simonic T 2001 Molecular cloning of the cDNA coding for Xenopus laevis prion protein. *FEBS Lett.* **508** 170-174.

Suggs SV, Wallace RB, Hirose T, Kawashima EH & Itakura K 1981 Use of synthetic oligonucleotides as hybridization probes: isolation of cloned cDNA sequences for human beta 2-microglobulin. *Proc.Natl.Acad.Sci.U.S.A* **78** 6613-6617.

Sunyach C, Jen A, Deng J, Fitzgerald KT, Frobert Y, Grassi J, McCaffrey MW & Morris R 2003 The mechanism of internalization of glycosylphosphatidylinositol-anchored prion protein. *EMBO J* **22** 3591-3601.

Suzuki T, Kurokawa T, Hashimoto H & Sugiyama M 2002 cDNA sequence and tissue expression of Fugu rubripes prion protein-like: a candidate for the teleost orthologue of tetrapod PrPs. *Biochem Biophys Res Commun.* **294** 912-917.

Tanaka M, Chien P, Naber N, Cooke R & Weissman JS 2004 Conformational variations in an infectious protein determine prion strain differences. *Nature* **428** 323-328.

Taraboulos A, Scott M, Semenov A, Avrahami D, Laszlo L & Prusiner SB 1995 Cholesterol depletion and modification of COOH-terminal targeting sequence of the prion protein inhibit formation of the scrapie isoform. *J Cell Biol.* **129** 121-132.

Tateishi J, Brown P, Kitamoto T, Hoque ZM, Roos R, Wollman R, Cervenakova L & Gajdusek DC 1995 First experimental transmission of fatal familial insomnia. *Nature* **376** 434-435.

Tatzelt J, Zuo J, Voellmy R, Scott M, Hartl U, Prusiner SB & Welch WJ 1995 Scrapie prions selectively modify the stress response in neuroblastoma cells. *Proc.Natl.Acad.Sci.U.S A* **92** 2944-2948.

Taylor DR & Hooper NM 2007 The low-density lipoprotein receptor-related protein 1 (LRP1) mediates the endocytosis of the cellular prion protein. *Biochem J* **402** 17-23.

Taylor JP, Hardy J & Fischbeck KH 2002 Toxic proteins in neurodegenerative disease. *Science* **296** 1991-1995.

Telling GC, Parchi P, DeArmond SJ, Cortelli P, Montagna P, Gabizon R, Mastrianni J, Lugaresi E, Gambetti P & Prusiner SB 1996 Evidence for the conformation of the pathologic isoform of the prion protein enciphering and propagating prion diversity. *Science* **274** 2079-2082.

Telling GC, Scott M, Hsiao KK, Foster D, Yang SL, Torchia M, Sidle KC, Collinge J, DeArmond SJ & Prusiner SB 1994 Transmission of Creutzfeldt-Jakob disease from humans to transgenic mice expressing chimeric human-mouse prion protein. *Proc.Natl.Acad.Sci.U.S A* **91** 9936-9940.

Ter Avanesyan MD, Dagkesamanskaya AR, Kushnirov VV & Smirnov VN 1994 The SUP35 omnipotent suppressor gene is involved in the maintenance of the non-Mendelian determinant [psi+] in the yeast Saccharomyces cerevisiae. *Genetics* **137** 671-676.

Tobler I, Gaus SE, Deboer T, Achermann P, Fischer M, Rulicke T, Moser M, Oesch B, McBride PA & Manson JC 1996 Altered circadian activity rhythms and sleep in mice devoid of prion protein. *Nature* **380** 639-642.

Tribouillard D, Bach S, Gug F, Desban N, Beringue V, Andrieu T, Dormont D, Galons H, Laude H, Vilette D & Blondel M 2006 Using budding yeast to screen for anti-prion drugs. *Biotechnol.J* **1** 58-67.

True HL 2006 The battle of the fold: chaperones take on prions. *Trends Genet.* **22** 110-117.

True HL & Lindquist SL 2000 A yeast prion provides a mechanism for genetic variation and phenotypic diversity. *Nature* **407** 477-483.

Tuite MF & Cox BS 2003 Propagation of yeast prions. *Nat.Rev.Mol Cell Biol.* **4** 878-890.

Tuite MF & Koloteva-Levin N 2004 Propagating prions in fungi and mammals. *Mol Cell* **14** 541-552.

Tuite MF, Mundy CR & Cox BS 1981 Agents that cause a high frequency of genetic change from [psi+] to [psi-] in Saccharomyces cerevisiae. *Genetics* **98** 691-711.

Vanik DL, Surewicz KA & Surewicz WK 2004 Molecular basis of barriers for interspecies transmissibility of mammalian prions. *Mol Cell* **14** 139-145.

Vella LJ, Sharples RA, Lawson VA, Masters CL, Cappai R & Hill AF 2007 Packaging of prions into exosomes is associated with a novel pathway of PrP processing. *J Pathol.* **211** 582-590.

Vey M, Pilkuhn S, Wille H, Nixon R, DeArmond SJ, Smart EJ, Anderson RG, Taraboulos A & Prusiner SB 1996 Subcellular colocalization of the cellular and scrapie prion proteins in caveolae-like membranous domains. *Proc.Natl.Acad.Sci.U.S A* **93** 14945-14949.

Vitrenko YA, Gracheva EO, Richmond JE & Liebman SW 2007 Visualization of aggregation of the Rnq1 prion domain and cross-seeding interactions with Sup35NM. *J Biol.Chem.* **282** 1779-1787.

Vorberg I, Buschmann A, Harmeyer S, Saalmuller A, Pfaff E & Groschup MH 1999 A novel epitope for the specific detection of exogenous prion proteins in transgenic mice and transfected murine cell lines. *Virology* **255** 26-31.

Wadsworth JD, Joiner S, Fox K, Linehan JM, Desbruslais M, Brandner S, Asante EA & Collinge J 2007 Prion infectivity in variant Creutzfeldt-Jakob disease rectum. *Gut* **56** 90-94.

Wadsworth JD, Joiner S, Hill AF, Campbell TA, Desbruslais M, Luthert PJ & Collinge J 2001 Tissue distribution of protease resistant prion protein in variant Creutzfeldt-Jakob disease using a highly sensitive immunoblotting assay. *Lancet* **358** 171-180.

Waelter S, Boeddrich A, Lurz R, Scherzinger E, Lueder G, Lehrach H & Wanker EE 2001 Accumulation of mutant huntingtin fragments in aggresome-like inclusion bodies as a result of insufficient protein degradation. *Mol.Biol.Cell* **12** 1393-1407.

Wandinger SK, Richter K & Buchner J 2008 The hsp90 chaperone machinery. *J.Biol.Chem.* **283** 18473-18477.

Weibezahn J, Bukau B & Mogk A 2004 Unscrambling an egg: protein disaggregation by AAA+ proteins. *Microb.Cell Fact.* **3** 1.

Weise J, Crome O, Sandau R, Schulz-Schaeffer W, Bahr M & Zerr I 2004 Upregulation of cellular prion protein (PrPc) after focal cerebral ischemia and influence of lesion severity. *Neurosci.Lett.* **372** 146-150.

Weissmann C 2004 The state of the prion. *Nat.Rev.Microbiol* **2** 861-871.

Weissmann C, Fischer M, Raeber A, Bueler H, Sailer A, Shmerling D, Rulicke T, Brandner S & Aguzzi A 1996 The use of transgenic mice in the investigation of transmissible spongiform encephalopathies. *Int.J Exp.Pathol.* **77** 283-293.

Wells GA, Scott AC, Johnson CT, Gunning RF, Hancock RD, Jeffrey M, Dawson M & Bradley R 1987 A novel progressive spongiform encephalopathy in cattle. *Vet.Rec.* **121** 419-420.

Westaway D, Cooper C, Turner S, Da Costa M, Carlson GA & Prusiner SB 1994 Structure and polymorphism of the mouse prion protein gene. *Proc.Natl.Acad.Sci.U.S A* **91** 6418-6422.

Westergard L, Christensen HM & Harris DA 2007 The cellular prion protein (PrP(C)): its physiological function and role in disease. *Biochim.Biophys.Acta* **1772** 629-644.

Wickner RB 1994 [URE3] as an altered URE2 protein: evidence for a prion analog in Saccharomyces cerevisiae. *Science* **264** 566-569.

Wickner RB, Edskes HK, Shewmaker F & Nakayashiki T 2007 Prions of fungi: inherited structures and biological roles. *Nat.Rev.Microbiol.* **5** 611-618.

Wickner RB, Taylor KL, Edskes HK, Maddelein ML, Moriyama H & Roberts BT 1999 Prions in Saccharomyces and Podospora spp.: protein-based inheritance. *Microbiol Mol Biol.Rev.* **63** 844-61, table.

Wickner RB, Taylor KL, Edskes HK, Maddelein ML, Moriyama H & Roberts BT 2000 Prions of yeast as heritable amyloidoses. *J Struct.Biol.* **130** 310-322.

Wigley WC, Fabunmi RP, Lee MG, Marino CR, Muallem S, DeMartino GN, and Thomas PJ. Dynamic association of proteasomal machinery with the centrosome. J Cell Biol. 145[2], 481-490. 1999.
Ref Type: Generic

Wilesmith JW & Wells GA 1991 Bovine spongiform encephalopathy. *Curr.Top.Microbiol.Immunol.* **172** 21-38.

Will RG, Ironside JW, Zeidler M, Cousens SN, Estibeiro K, Alperovitch A, Poser S, Pocchiari M, Hofman A & Smith PG 1996 A new variant of Creutzfeldt-Jakob disease in the UK. *Lancet* **347** 921-925.

Wille H, Michelitsch MD, Guenebaut V, Supattapone S, Serban A, Cohen FE, Agard DA & Prusiner SB 2002 Structural studies of the scrapie prion protein by electron crystallography. *Proc.Natl.Acad.Sci.U.S A* **99** 3563-3568.

Wilson PG & Culbertson MR 1988 SUF12 suppressor protein of yeast. A fusion protein related to the EF-1 family of elongation factors. *J Mol Biol.* **199** 559-573.

Winklhofer KF, Heller U, Reintjes A & Tatzelt J 2003 Inhibition of complex glycosylation increases the formation of PrPsc. *Traffic* **4** 313-322.

Winklhofer KF, Reintjes A, Hoener MC, Voellmy R & Tatzelt J 2001 Geldanamycin restores a defective heat shock response in vivo. *J.Biol.Chem.* **276** 45160-45167.

Wopfner F, Weidenhofer G, Schneider R, von Brunn A, Gilch S, Schwarz TF, Werner T & Schatzl HM 1999 Analysis of 27 mammalian and 9 avian PrPs reveals high conservation of flexible regions of the prion protein. *J Mol Biol.* **289** 1163-1178.

Wroe SJ, Pal S, Siddique D, Hyare H, Macfarlane R, Joiner S, Linehan JM, Brandner S, Wadsworth JD, Hewitt P & Collinge J 2006 Clinical presentation and pre-mortem diagnosis

of variant Creutzfeldt-Jakob disease associated with blood transfusion: a case report. *Lancet* **368** 2061-2067.

Yamanaka K, Okubo Y, Suzaki T & Ogura T 2004 Analysis of the two p97/VCP/Cdc48p proteins of Caenorhabditis elegans and their suppression of polyglutamine-induced protein aggregation. *J.Struct.Biol.* **146** 242-250.

Yang W, Dunlap JR, Andrews RB & Wetzel R 2002 Aggregated polyglutamine peptides delivered to nuclei are toxic to mammalian cells. *Hum.Mol.Genet.* **11** 2905-2917.

Yedidia Y, Horonchik L, Tzaban S, Yanai A & Taraboulos A 2001 Proteasomes and ubiquitin are involved in the turnover of the wild-type prion protein. *EMBO J* **20** 5383-5391.

Yorimitsu T & Klionsky DJ 2005 Autophagy: molecular machinery for self-eating. *Cell Death.Differ.* **12 Suppl 2** 1542-1552.

Zahn R, Liu A, Luhrs T, Riek R, von Schroetter C, Lopez GF, Billeter M, Calzolai L, Wider G & Wuthrich K 2000 NMR solution structure of the human prion protein. *Proc.Natl.Acad.Sci.U.S A* **97** 145-150.

Zanata SM, Lopes MH, Mercadante AF, Hajj GN, Chiarini LB, Nomizo R, Freitas AR, Cabral AL, Lee KS, Juliano MA, de Oliveira E, Jachieri SG, Burlingame A, Huang L, Linden R, Brentani RR & Martins VR 2002 Stress-inducible protein 1 is a cell surface ligand for cellular prion that triggers neuroprotection. *EMBO J* **21** 3307-3316.

Zanusso G, Petersen RB, Jin T, Jing Y, Kanoush R, Ferrari S, Gambetti P & Singh N 1999 Proteasomal degradation and N-terminal protease resistance of the codon 145 mutant prion protein. *J Biol.Chem.* **274** 23396-23404.

Zhou P, Derkatch IL & Liebman SW 2001 The relationship between visible intracellular aggregates that appear after overexpression of Sup35 and the yeast prion-like elements [PSI(+)] and [PIN(+)]. *Mol Microbiol* **39** 37-46.

VIII. PUBLICATIONS

Krammer C, Suhre MH, Kremmer E, Diemer C, Hess S, Schätzl HM, Scheibel T, Vorberg I. Prion protein/protein interactions: fusion with yeast Sup35p-NM modulates cytosolic PrP aggregation in mammalian cells. **FASEB J.** 2008 Mar;22(3):762-73. Epub 2007 Oct 10.

Aguib Y, Gilch S, **Krammer C**, Ertmer A, Groschup M, Schätzl HM. Neuroendocrine cultured cells resolve transient prion infection by down-regulation of PrP^c. **Mol Cell Neurosci.** 2008 May;38(1):98-109. Epub 2008 Mar 4.

Gilch S, **Krammer C**, Schätzl HM. Targeting prion proteins in neurodegenerative disease. **Expert Opin Biol Ther.** 2008 Jul;8(7):923-40.

Krammer C, Kremmer E, Schätzl HM, Vorberg I. Dynamic interactions of Sup35p and PrP prion protein domains modulate aggregate nucleation and seeding. **PRION.** 2008 Juli/August/September;2(3):1-8.

Krammer C, Kryndushkin D, Suhre MH, Kremmer E, Hofmann A, Pfeifer A, Scheibel T, Wickner R, Schätzl HM, Vorberg I. The yeast Sup35NM domain propagates as a prion in mammalian cells **Proc Natl Acad Sci U S A.** 2009 (*in press*)

Krammer C, Vorberg I, Schätzl HM, Gilch S. Therapy in prion diseases: From molecular and cellular biology to therapeutic targets. **Infect Disord Drug Targets**. 2009 (*in press*)

Gaedtke L, Lutzny G, **Krammer C**, Rost R, Vorberg I. The importance of the PrP primary sequence in prion disease transmission. 2008 Book chapter, **Research Signpost**. 2009 (*in press*)

Nunziante M, Kehler C, **Krammer C**, Maas E, Groschup M, Schätzl HM. Extended N-terminally deleted prion proteins form neurotoxic aggregates and are not recruited into lipid rafts (*in preparation*)

IX. ACKNOWLEDGEMENT

X.　CURRICULUM VITAE

Name	Carmen Krammer
Geburtstag	24. Oktober 1979
Geburtsort	Schrobenhausen
Nationalität	deutsch
Familienstand	ledig
Schulbildung	**Sept. 1886-Jul. 1990** Grundschule Langenmosen
	Sept. 1990 - Jul. 1999: Gymnasium Schrobenhausen
	Abschluss: allgemeine Hochschulreife (Abitur)
Studium	**Okt. 1999 - Apr. 2005**: Biologiestudium (Diplom) and der Technischen Universität München (TUM)
	Hauptfach: Mikrobiologie
	Nebenfächer: Biochemie, Virologie
	Apr. 2004: Diplomhauptprüfung
	Jul. 2004 - Apr. 2005: Diplomarbeit unter Anleitung von Prof. Dr. Schätzl am Institut für Virologie, TUM
	Thema: "Expression von Deletionsmutanten des murinen Prion Proteins mithilfe eines lentivirales Vektorsystems und Charakterisierung in verschiedenen Zellkultur-Modellen".
	Jul. 2005 - Dez. 2008: Promotion in der Arbeitsgruppe von Dr. Vorberg und Prof. Dr. Schätzl am Institut für Virologie, TUM (Betreuer: Prof. Dr. Buchner, Lehrstuhl für Biotechnologie, TUM)